CHALMERS

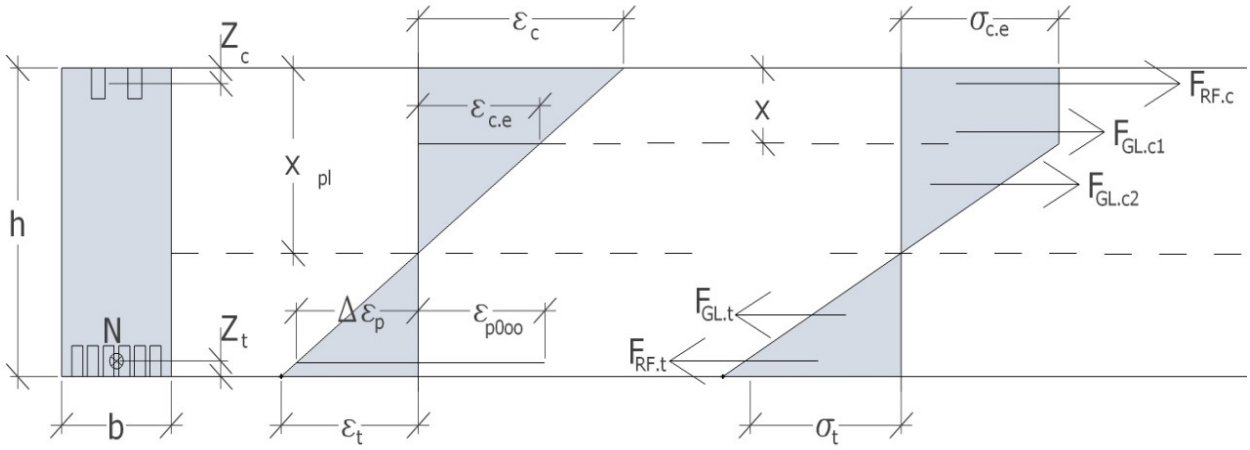

Analytical models of pre-stressed and reinforced glulam beams

A competitive analysis of strengthened glulam beams

Master of Science Thesis in the Master's Programme Structural Engineering and Building Performance Design

MARTIN PERSSON
SEBASTIAN WOGELBERG

Department of Civil and Environmental Engineering
Division of Structural Engineering
Steel and Timber Structures
CHALMERS UNIVERSITY OF TECHNOLOGY
Göteborg, Sweden 2011

Master's Thesis 2011:52

MASTER'S THESIS 2011:52

Analytical models of pre-stressed and reinforced glulam beams

A competitive analysis of strengthened glulam beams

Master of Science Thesis in the Master's Programme Structural Engineering and Building Performance Design

MARTIN PERSSON

SEBASTIAN WOGELBERG

Department of Civil and Environmental Engineering
Division of Structural Engineering
Steel and Timber Structures
CHALMERS UNIVERSITY OF TECHNOLOGY

Göteborg, Sweden 2011

Analytical models of pre-stressed and reinforced glulam beams
A competitive analysis of strengthened glulam beams

Master of Science Thesis in the Master's Programme Structural Engineering and Building Performance Design

MARTIN PERSSON
SEBASTIAN WOGELBERG

Examensarbete/Institutionen för bygg- och miljöteknik,
Chalmers tekniska högskola2011:52

Department of Civil and Environmental Engineering
Division of Structural Engineering
Steel and Timber Structures
Chalmers University of Technology
SE-412 96 Göteborg
Sweden
Telephone: + 46 (0)31-772 1000

Cover: Stress-Strain distribution for a pre-stressed beam in plastic phase, see Figure 4.8.

Chalmers Repro Service / Department of Civil and Environmental Engineering
Göteborg, Sweden 2011

Analytical models of pre-stressed and reinforced glulam beams
A competitive analysis of strengthened glulam beams

Master of Science Thesis in the Master's Programme Structural Engineering and Building Performance Design

MARTIN PERSSON
SEBASTIAN WOGELBERG

Department of Civil and Environmental Engineering
Division of Structural Engineering
Steel and Timber Structures
Chalmers University of Technology

ABSTRACT

Timber has been an important material in construction for a long period of time. Engineered timber products have enhanced their properties significantly and introducing strengthening with stiffer and stronger materials has also showed positive effects. New methods of reinforcement with improved performance from the strengthened material are now possible, since materials used for strengthening have been developed and become cheaper. This master thesis focuses on finding the effects of pre-stressing and thereby hopefully enhancing these properties further.

To investigate the different aspects of pre-stressed glulam beams a model was created. The model was created to handle unreinforced, reinforced and pre-stressed glulam beams. It was made in such way that it could handle both the linear elastic phase as well as the plastic phase and compensate for any plasticisation in the reinforcement.

To verify the design model using pre-stressing calculations, the model was compared with the test results acquired from two pre-stressed beams that were loaded until failure. The result from the two beams calculated by the created model coincided with the results from their tested counterpart quite well. But with just two test beams to compare, it is not statistically determined that the model is correct. The calculated beams reached higher ultimate values than their tested counterparts.

One of the advantages of adding reinforcement to a beam is the ability to reduce the cross-section, with a maintained flexural capacity in the beam. This was examined in the thesis and it was shown that the magnitude of the pre-stressing force was greatly influential on the strength enhancement.

An economic analysis was made to compare unreinforced glulam beams with pre-stressed beams. The comparison showed that long beams (18-25 m) with 0.5-1.5 per cent reinforcement were the most profitable.

It is obvious that the beams that were pre-stressed gain an increased flexural resistance. However, if it is more economical depends on the type, geometry and load on the beams. It is however, almost always, an economic gain for the entire construction if pre-stressed glulam beams are used.

Keywords: Pre-stressed Glulam, FRP reinforcement, Steel Reinforcement, Flexural Resistance, Modelling Glulam beams, Economical Glulam Construction

Analytisk modellering av förspända och förstärkta limträbalkar

En granskning av användningsområden för förstärkta limträbalkar

Examensarbete inom Mastersprogrammet Structural Engineering and Building Performance Design

MARTIN PERSSON
SEBASTIAN WOGELBERG
Institutionen för bygg- och miljöteknik
Avdelningen för Konstruktionsteknik
Stål- och Träbyggnad
Chalmers tekniska högskola

SAMMANFATTNING

Trä har varit ett viktigt byggnadsmaterial under en väldigt lång tid. Skapade träprodukter, som limträ, har skapats för att förbättra de bärande förmågorna som trä inne har såväl som att minska förekomsten av defekter i materialet. Eftersom materialen som används vid förstärkningar har både blivit bättre och billigare öppnar det nya möjligheter inom förstärkningsmöjligheterna för limträ. Det här examensarbetet har fokuserat på förspänningens effekter på ett förstärkt limträ tvärsnitt i en förhoppning om att kunna ytterligare öka limträbalkars bärförmåga.

För att kunna undersöka förspänningens olika fördelar skapades en modell i matlab. Med hjälp av modellen kan man studera oförstärkta, förstärkta och förspända limträtvärsnitt och jämföra dem med varandra. Modellen hanterar både den elastiska och den plastiska fasen för limträ och tar hänsyn till om förstärkningsmaterial kan flyta.

För att verifiera de förspända beräkningarna så jämfördes modellens resultat med resultaten från två förspända limträbalkar som tryckt belastats till brott på Chalmers Tekniska Högskola. Resultaten från de två testade balkarna och resultaten från modellen stämde väl överens, men med bara två balkar kan det inte fastställas med statistisk säkerhet att modell är korrekt.

En av fördelarna med att förstärka tvärsnitt är möjligen att kunna minska på dimensionerna med bibehålla den önskade kapaciteten i balken. Det visade sig att med en pålagd förspänningskraft kunde det skäras ner markant in armeringsmängden vilket gjorde det intressant att göra en ekonomisk analys huruvida besparingar kan göras med förspända förstärkningsmaterial.

En ekonomisk analys gjordes för att jämföra oförstärkta med förspända limträbalkar. Analysen visade att långa balkar (18-25m) med 0.5-1,5 % armering är de mest lönsamma.

Det har visats att förspända förstärkningsmaterial i ett limträ tvärsnitt ger en stor ökning av balkens maximala böjmotstånd. Dock beror det på balkens typ, dimensioner och laster om en förspänd balk är billigare att framställa. Det finns dock nästan alltid en kostnads besparing att hämta om hela byggnaden, med en lägre konstruktionshöjd, räknas in.

Nyckelord: Förspänt limträ, kolfiber förstärkning, stål förstärkning, böjmotstånd, Modellering av förstärkta limträbalkar, Ekonomiska limträbalkar

Contents

Preface

This master's thesis was carried out at the Division of structural Engineering, department of Civil and Environmental Engineering at Chalmers University of Technology, Sweden, during the spring of 2011.

We first want to thank our examiner and supervisor Professor Robert Kliger and our industrial supervisor Rolf Jonsson for the support and guidance throughout this whole process. We also want to thank Associate Professor Mohammad Al-Emrani for his extensive help with the large equations as well as for his great general guidance through this project.

We also would like to thank Professor Björn Engström and Associate Professor Mario Plos for their invaluable help with the pre-stressing equations and its definitions.

Further, we would like to thank Research student Alann André for sharing his model with us and for his estimation of glulam strength parameters. We also extend our thanks to Erik Gulbrandsen at Tenroc Technologies for his help with the economic aspects of our study and to our opponents and roommates, Daniel Näkne and Joakim Kvist, for their suggestive second opinions.

Finally, we want to thank Neil Townson for his excellent and greatly appreciated help with the English language in this report.

Gothenburg, July 2011

Martin Persson & Sebastian Wogelberg

Notations

Roman upper case letters

A	Cross-section area	[mm^2]
A_{GL}	Cross-section area for the glulam	[mm^2]
A_{eq}	Equivalent glulam cross-section area	[mm^2]
A_{RF}	Cross-section area for the reinforcement	[mm^2]
$A_{RF,c}$	Cross-section area for the compressive reinforcement	[mm^2]
$A_{RF,t}$	Cross-section area for the tensile reinforcement	[mm^2]
E	Young's modulus	[MPa]
E_{GL}	Young's modulus for glulam	[MPa]
E_{RF}	Young's modulus for reinforcement	[MPa]
F	Force	[N]
$F_{GL,c}$	Force from compressive zone for the glulam	[N]
$F_{GL,c1}$	Force from compressive rectangular zone for the glulam	[N]
$F_{GL,c2}$	Force from compressive triangular zone for the glulam	[N]
$F_{GL,t}$	Force from tensile zone for the glulam	[N]
$F_{RF,c}$	Force from compressive zone for the reinforcement	[N]
$F_{RF,t}$	Force from tensile zone for the reinforcement	[N]
I	Moment of inertia	[mm^4]
L	Span length	[m]
M	Moment	[Nm]
N	Pre-stressing force when in Navier's formula	[N]
N_{break}	Tensile force required for yielding	[N]
P	Pre-stressing Force	[N]
V	Shear force	[N]

Roman lower case letters

b	Width of cross-section [mm]	
e	Lever arm from the pre-stressed reinforcement	[mm]
$f_{GL,t}$	Tensile yield limit for glulam	[MPa]
$f_{RF,t}$	Tensile yield limit for reinforcement	[MPa]
f_{yd}	Reinforcement yield strength	[MPa]
h	Height of cross-section	[mm]
L	Length of the beam	[mm]

x	Height of the plasticising	[mm]
x_{pl}	Height of neutral axis in plastic phase	[mm]
z	Navier's lever arm from centre of gravity	[mm]
z_{NA}	Height of the neutral axis	[mm]
Z_c	Length from compressive reinforcement to edge	[mm]
Z_t	Length from tensile reinforcement to edge	[mm]

Greek lower case letters

α	Equivalent cross-section factor	[-]
ε	Strain	[-]
ε_c	Maximum compressive strain	[-]
ε_t	Maximum tensile strain	[-]
$\varepsilon_{c,e}$	Maximum compressive elastic strain in glulam	[-]
$\varepsilon_{t,e}$	Maximum tensile elastic strain in glulam	[-]
$\varepsilon_{RF,c}$	Tensile strain in the reinforcement	[-]
$\varepsilon_{RF,t}$	Compressive strain in the reinforcement	[-]
$\varepsilon_{p0\infty}$	The strain due to the pre-stressing force	[-]
$\Delta\varepsilon_p$	The strain due to loading, same as $\varepsilon_{RF,t}$.	[-]
φ_t	Creep factor	[-]
σ	Stress	[MPa]
τ	Shear stress	[MPa]
τ_{max}	Maximum shear stress	[MPa]

Abbreviations

Glulam	Glued Laminated Lumber
FRP	Fibre Reinforced Polymer
CFRP	Carbon Fibre Reinforced Polymer
EC5	Euro Code, Chapter 5 (EN 1995-1-1:2004(E))
SLS	Service Limit State
ULS	Ultimate Limit State

1 INTRODUCTION

Timber has been an important material in construction for a long period of time. A reason is that it is a natural material and it has been available in the surroundings of man since the dawn of civilization. Timber has however during the last centuries been replaced, in larger and more demanding structures, with “newer” and better materials, such as concrete and steel. The reason for this is that concrete and steel have been engineered to be applicable in specific structural situations, and therefore does not exhibit the same disadvantages as timber.

Glulam has inherent defects and weaknesses since it is a naturally grown material. This results in large variations in most of its properties. Steel and concrete, the two other main construction materials, are man-made. This gives them a smaller likelihood of inherent defects and weaknesses compared to timber. There has however been increased interest in timber during the last decades because of its favourable properties. Compared to concrete and steel, timber is a cheap, light-weight and an unlimited material. These favourable properties have led to research and development of new, engineered timber products, which aim to minimize variations and improve the properties compared to natural timber. One of these engineered wooden products is glued laminated timber, or glulam.

Glulam is an engineered wooden product which consists of several lamellae of building timber glued together under pressure. A positive effect of this manufacturing method is that the likelihood of defects is reduced, compared to standard building timber. This is because of the use of many smaller and independent parts, thereby increasing the strength and decreasing the spread of strength characteristics between beams, Figure 1.1.

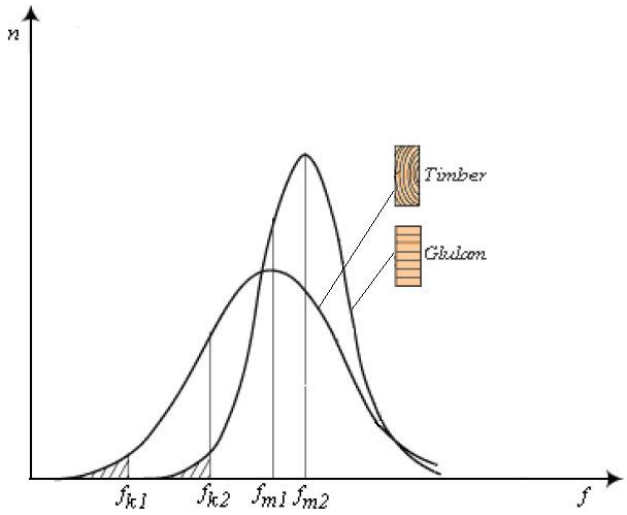

Figure 1.1 Strength properties of timber and glulam. f is the strength and n is the number of specimens. Notice the higher average strength fm, higher characteristic strength f_k (0.05 per centile) and the smaller spread of strength for glulam.

Another positive effect of manufacturing glulam is the possibility to create different types of cross-sections and shapes, thereby tailor-making them for different applications and structural systems. Today, glulam is produced as curved beams, single and double tapered beams, pitched cambered beams, regular prismatic beams with or without pre-camber and different types of cantilever beams, Figure 1.2.

Except from beams glulam is also used in columns, a variety of frames, arches, trusses and composite systems. The application of glulam is thus vast and is increasing continuously.

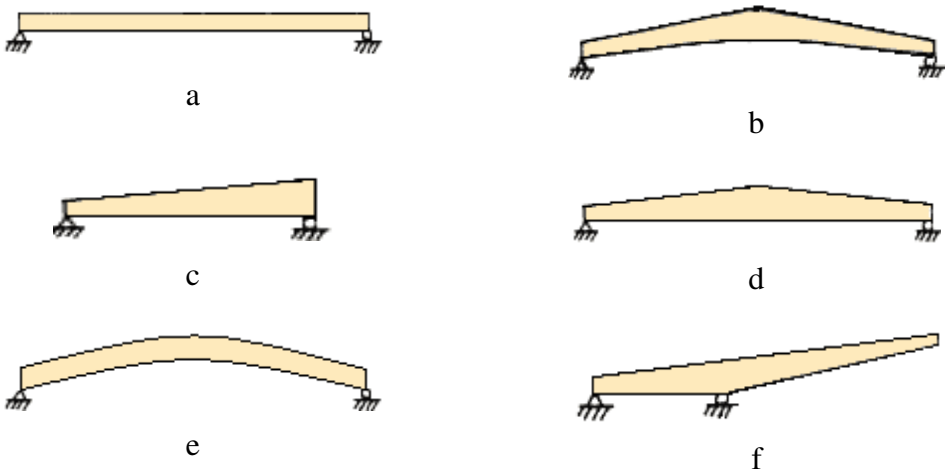

Figure 1.2 Different types of glulam beams: (a) regular prismatic beam; (b) pitched cambered beam; (c) single tapered beam; (d) double tapered beam; (e) curved beam; (f) cantilever beam on two supports.

Glulam beams are suitable for long spans since they possess a high strength to weight ratio. The prismatic beam is preferred for shorter spans while the double tapered beam is preferred for wider spans, for both material usage and economic reasons. This is an effective way of engineering glulam since the depth is larger at midspan; hence the strength is higher, where the load bearing capacity is needed to be at its highest. By constructing the beam with this shape the material costs can be reduced without having to sacrifice load bearing capacity in the process.

Even though glulam has an excellent strength and stiffness to weight ratio the governing limitation is usually deflection, which is governed by the stiffness properties of the beam. To get acceptable deflections for a long span the designer has the possibility to increase the height of the beams to get acceptable deflections. This solution increases the material usage, which is uneconomical and also non-sustainable. Another problem with timber is its failure mode, which has a brittle behaviour in tension, which is a common failure mode for beams with long spans ($L>12h$). This is an unfavourable property since the rupture of a brittle material happens more quickly and harder to predict. The increasing load bearing capacity demand of the structures, due to changes in design models and increasing imposed loads, is also a major problem that has to be dealt with.

In an effort to solve these problems, without increasing the cross-section and thereby increasing the total height of the structure/building, research has been done to find ways to enhance the stiffness and strength properties of glulam beams by means of strengthened glulam beams. This concept is not new. In the early 1960's A. Sliker, F.F. Wandgaard and E.J. Biblis proposed different ways of strengthening timber. Since then, the research has continued but the reinforcement of glulam has never become a commercial success. Some of the reasons were that the materials used as reinforcement where either too expensive or lacked a sufficient strength. It was also usual that the production method was not practically or economically viable.

The advancements made in materials, both reinforcement materials and adhesives, has now enabled a commercial competitiveness of reinforced timber products. Many of the present reinforcement methods have been created to strengthen existing structures, which has led to these methods mainly consists of reinforcing material being attached to the timber's surface. This can be done either on the sides of, or beneath the beam. These methods can increase both the shear and flexural capacity, depending on where the reinforcement is placed. There are also methods including drilled glued-in rods to strengthen the properties perpendicular to the grain and increasing the shear capacity.

When producing new strengthened glulam beams the reinforcement material is no longer restricted to the timber's surface. Recent methods that incorporate the reinforcement either horizontally between the timber lamellae or vertically in grooves have been proposed and both have proven successful in increasing the flexural capacity.

1.1 Background

Engineered timber products have enhanced these properties significantly and introducing strengthening with stiffer and stronger materials has also showed positive effects. It has been possible to create new methods of strengthening glulam, since the strengthening materials have been improved becoming both stronger and cheaper. This opens up the possibility of more advanced strengthening solutions, which previously were too expensive or lacked materials with the correct properties.

The improvement of timber is needed for it to be a competitive material, since the demands on structures have increased significantly over recent years. Today, the focus has shifted towards finding the beneficial effects when the strengthening material is subjected to pre-stressing. Some tests and research has been done, but so far no general method for either the calculation of or the production of pre-stressed glulam beams has been established.

1.2 Purpose

For timber to be a more competitive material the deviations and weaknesses needs to be reduced. This master thesis focuses on finding the effects of pre-stressing the strengthening material and thereby hopefully enhancing the beam's properties further. When the effects have been evaluated the competitiveness of pre-stressed glulam beams compared to un-strengthened beams will examined. This investigation will show which pre-stressed beams are most suitable to replace un-strengthened beams. The investigation will consider both the performance and the economic aspect to give a more complete picture of the pre-stressed beams competitiveness.

1.3 Objectives and methodology

The aim of this master thesis is to examine the performance and benefits of different strengthened glulam beams compared to un-strengthened glulam beams and which parameters govern that performance. The results should be able to be implemented in an economic analysis, to find out the competitiveness for the different strengthened beams, with the focus on pre-stressed beams.

This will be achieved by:

- Developing a method to calculate performance in terms of bending strength and deflection of pre-stressed glulam beams.
- With this method, together with existing design models for un-strengthened and strengthened beams, make a parametric study to determine which parameters that govern the load bearing capacity of the beams.
- Determine which types of beam have advantage in different applications.
- Determine which, and for what purpose, the strengthened beams can be competitive as to un-strengthened beams.

In order to complete these objectives, the following methods will be used:

- An analytical model for pre-stressed glulam beams will be established.
- A mathematical program will be created in MathCAD for the different types of beams.
- A calculation programme will be created in Matlab to perform the iterative calculations required for comparing multiple beams.
- The material and production costs determine the competitiveness of strengthened glulam beams will be included.

1.4 Limitations

Limitations that will be used in the performed study are listed below:

- The study will be adapted to a simply-supported beam.
- The study will only take creep in to consideration using modification factors.
- In SLS calculations, only deflection will be the governing criteria (based on EC5).
- The failure mode of adhesives will not be considered.
- Shear reinforcement will not be considered.
- Relaxation of the reinforcement will not be considered.
- Durability and environmental effects will only be considered using k_{mod} from EC5.
- The reinforcement will not be allowed to yield before the plastic phase for the glulam has been reached.

2 MATERIALS

2.1 Glulam

Glulam, or glued laminated timber, is an engineered wood product, which means that it has been developed and improved compared to regular sawn timber. It consists of individual strength-graded timber lamellae of regular structural timber, which are glued together under pressure and controlled conditions. This method is an effective way of utilising, and optimising, timber's natural properties. The information in this chapter is mainly taken from Svenskt Limträ AB (2007).

Glulam consist of at least two timber lamellae that are joined together with an adhesive. If there are fewer than four lamellae it is usually referred to as glued structural timber. The thickness of the laminations needs to be between 6 and 45 mm. The grains are orientated in the longitudinal direction of the structural member it represents. With this system of laminated timber it is possible to obtain larger cross-section than with solid timber. By the usage of several lamellae within one structural member, the defects of the solid timber become distributed more evenly along the structural member. This gives the glulam an increase in the overall strength classification when compared to solid timber.

The lamellae are glued together to the desired depth of the beam and the lamellae are finger-jointed to achieve the desired length. Due to this production method it is possible to create structural glulam members of large cross-section, long length and in any shape. As an example, it is easy to create a pre-camber in the beams to reduce its final deflection when it becomes loaded. The size limitation comes from the manufacturing equipment's size and the possibilities to transport large members. To get around this, when considering the length of the beam, long beams are assembled together from smaller parts by the means of finger joints at the construction site. A good quality finger joint will have inherent design strength compared to the rest of the member, thus not reducing the long beams performance. This is possible because these types of joints create a large contact surface which gives the adhesive a large area to act on.

The glulam-method was developed at the end of the ninetieth century in Germany, and in 1906 a patent was issued in the same country, which is considered as the real starting point of this technology. The technology reached Scandinavia via Norway in the beginning of the twentieth century and some of the first structures in Sweden were erected in the 1920s. Ever since the 1960s the production has increased continuously in Scandinavia, nowadays the total production is over 200 000 m^3, and about half of this is exported.

Glulam has many advantages and properties which make it a competitive material in the building sector.

- *Excellent strength to weight ratio:* This property enables glulam to be used when long spans are required. Glulam has a higher strength and stiffness than structural timber and compared to steel it is stronger when consideration to own weight is taken into account.
- *Environmental:* Glulam does not affect the environment significantly during its lifetime and when its purpose has been fulfilled it can either be reused in other structures or used for energy production. Timber is a natural material

and thereby an unlimited material. As long as the regrowth is at least the same as the harvested amount, it is considered to be a sustainable material.

- *Low weight:* This makes the structure or components cheaper to produce and transport and lighter buildings require lower foundation costs.
- *Flexible production:* Glulam can during production, be formed in to many shapes and sizes. Regular beams, tapered beams, curved beams, long beams, deep beams etc.
- *Appearance:* Timber and therefore glulam is considered an aesthetically pleasing material and compared to concrete and steel it is perceived as a warm material.
- *Easy erection:* Glulam is easily and quickly erected because of its low weight and simple joints, consisting of bolts, nails and screws. Another advantage is that the structure can take its full load directly after erection.
- *Durability:* Glulam has a high tolerance towards chemically aggressive environments.
- *Fire resistance:* Glulam has a high fire resistance because charcoal is produced at the surface and insulates the rest of the beam. It will not melt, spall, flake, buckle or explode and it burns at a steady rate and is therefore predictable.
- *Good building physics properties:* Timber has good insulating properties which reduce cold bridges.

2.1.1 Glulam manufacturing

The manufacturing process of glulam starts with the harvesting of the trees and cutting the logs in to sawn timber, which is then dried and strength graded. The timber type used in the Scandinavian countries is often Norway spruce, but if the timber is planned to be subjected to an environment with high moisture content over a long period of time, pressure treated pine is used. For the glue line between the lamellae to be optimal in strength, the moisture content should be between 8 and 15 per cent, and the difference between the two connecting lamellae no more than 5 per cent. The target moisture content within the laminate is 12 per cent.

The sawn timber is finger jointed and then cut to the desired length. After the adhesive in the finger joints has hardened, the laminates are planed and then immediately glued and placed on top of each other, until the desired depth is reached. The depths of the beams are restricted by the production machines to about two meters, but theoretically there is no restriction. The cross-section can be either homogeneous, which means that all the lamellae have the same strength, or combined, which uses a weaker timber in the inner lamellae and a stronger timber in the outer lamellae where the stresses are higher. The latter method is an economical and effective way to optimize the usage of timber.

The lamellae, which are glued and placed to the desired cross-section, are then placed in the gluing bench where the pressure of about 1 MPa is applied. This has to be done before the adhesive hardens. After the pressure is applied, the laminates are bent to the desired camber or curve, or kept straight. The adhesive then hardens under controlled moisture and temperature conditions. When the adhesive has hardened the pressure is removed and the glulam is ready for the finishing work, which consists of cutting of arises, planing and preparing holes for passages and connectors. Then, the

glulam component is visually controlled, marked, wrapped and prepared for transportation.

The production process needs to be precise and the product must be able to withstand the stresses that it is exposed to. This placed high demands on the manufacturers. To be able to guarantee an even and high product quality the manufacturers need to have an extensive and well-documented quality control. Lamellae, finger joints and adhesives must be tested regularly to check that they are up to standard.

Glulam production is a low energy-demanding process and waste in the form of, for example, sawdust is being reused in the process when drying the timber or raising the temperature during the glue hardening. The making of glulam would be an environmentally friendly process if it were not for the adhesives, which are made of non-renewable raw materials. The amount of adhesive compared to timber is very low, about one per cent, which still makes glulam a very environmentally friendly construction material.

2.1.2 Mechanical properties

Glulam hold several distinct benefits compared to other structural materials. It has one of the highest strength to weight ratio which makes it an excellent material for structural members with a long span. It is highly fire resistant, aesthetically appealing and has a good insulating property. As all wooden materials glulam has an anisotropic behaviour, which makes wooden materials strong when a force is applied parallel to its grains but much weaker if the force is aimed perpendicular to them. Also its flexural resistance is still low compared to other structural materials with the same dimensions, Dolan (1997).

2.1.2.1 Failure modes

There are numerous ways a structural member can fail. The failure modes and strength characteristics depend on many things such as material parameters, material composition, load variation and duration, moisture content, craftsmanship and cross-sectional appearance to mention but a few. All possible failure modes are important to consider when the members are being designed.

Which failure mode becomes the governing one, often depends on the different defects that the glulam beam might have inherent. This will not however be considered in this report. The material for this section is taken from Jacob and Garzon (2007).

Tensile failure

The tensile failure, usually appearing at the bottom of a beam, is the most common failure mode for un-reinforced glulam beams loaded in bending, due to the fact that the tensile resistance of glulam is lower than its compressive counterpart. The tensile failure is a brittle one and there is no, unlike for compressive failure, plastic deformation possible. This fact also further enhances the chance of a tensile failure since there is no increase in the possible maximum possible strain through plastic deformation.

A tensile failure is said to occur when any point in the beam reaches the maximum tensile capacity.

There are two main types of tensile failure. Firstly, while still being in the linear elastic phase, the beam fails at the tension side. This happens primarily to un-strengthened beams where the lower tensile capacity becomes the governing factor for the failure.

Then there is the tensile failure while the compressive zone has entered the plastic phase. This happens mainly to beams that have been strengthened. Due to the plastic behaviour in the compressive zone the beam behaves somewhat more ductile. The failure in itself is still brittle since it is a tensile failure.

Compressive failure

For this failure mode to become governing one, is requires a large amount of over-strengthening on the tensile side because of glulam's plastic deformation capabilities in compression. It is assumed that a compressive failure has occurred when any point in the beam has reached the compressive plastic stress capacity of the beam. The compressive failure is, due to the plastic deformation, a ductile failure.

Shear failure

Short beams or beams that have been over-strengthened on both the tensile and compressive side will instead experience a shear failure. Shear failure is induced when the shear force from the load exceeds the beam shear capacity. A shear failure occurs at the supports of the beam and very quickly propagates in the direction of the fibres, effectively splitting the beam in two. The shear failure is governed to a high extent by the size of the cross-section.

Buckling - Lateral-torsional buckling

Buckling is a failure mode which is caused by an axial compression of a structural component. The force does not have to be a purely axial compression force, it could be bending where a part of the cross-section is subjected to compression stress and the other to tension or both bending and pure axial compression force. The stresses cause a stability problem which results in a lateral deformation of the component. The amount of compression stress needed to cause buckling is lower than the ultimate stress capacity of the component. If the component is subjected to flexure a twisting deformation will occur together with the lateral deformation, this is called lateral-torsional buckling.

2.1.2.2 Stress/strain – Creep and stress relaxation

There are different types of deformation, the instantaneous are divided into elastic and plastic deformations, the long term are considered as either creep or stress relaxation. The difference between the elastic and plastic deformation is that the elastic is reversible whereas the plastic is irreversible. This means that the elastic deformation does not have a permanent effect on the component/structure and it will disappear when the load is removed. The plastic deformation will have a permanent effect on

the component/structure even after the load is removed. Creep and stress relaxation are two different ways to describe the phenomenon that occurs when a stress is imposed on a structural member for a long period of time (Burström, 2007).

Creep

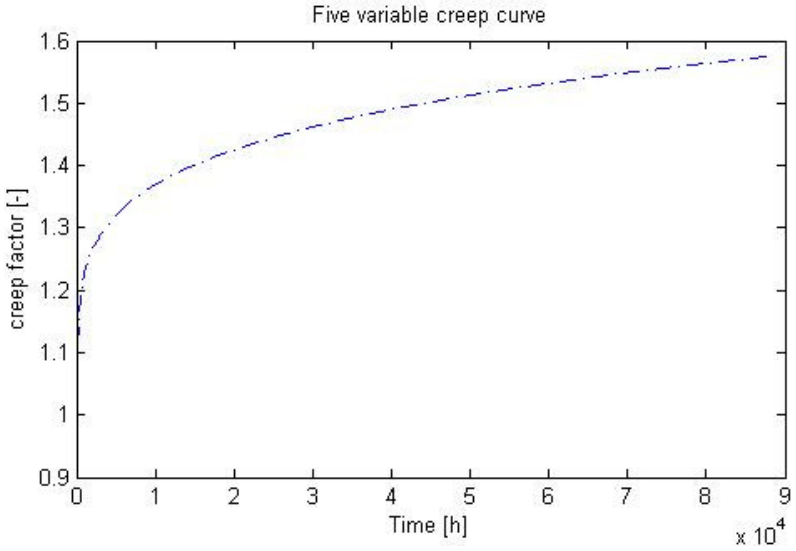

Figure 2.1 A five variable creep curve. The deformation is normally greater in the beginning and reduces with time.

The deformation increases when a member is permanently loaded. The definition of creep is the part of the deformation that increases with time if a load is imposed for over a long period of time, which makes the strain increase further over that specific period of time. The creeps deformation is normally greater in the beginning and later it reduces with time, see Figure 2.1, when the load is kept constant. Creep also has a reversible and an irreversible effect. The reversible effect doesn't disappear instantaneously when the stress is withdrawn; it reduces with time similar to the increase of strain. The creep effect can be described with the creep factor φ, which generally can be calculated using the following equation

$$\varphi_t = \frac{Creep\ deformation\ at\ time\ t}{Elastic\ deformation} \qquad (2.1)$$

This factor is very useful because the creep deformation can be calculated when the elastic deformation is known (Burström, 2007)

Stress relaxation

The definition of stress relaxation is that when the strain level is kept constant, the stress level in the material will reduce with time Burström (2007). This phenomenon is important to consider with pre-stressed construction components because the pre-stressing force will decrease with time, which leads to a reduced positive effect from the pre-stressing method.

2.2 Reinforcement materials

The material chosen for the strengthening has to have superior mechanical properties compared to the base material. As it also should have a much higher Young's modulus and, assuming perfect bond between the glulam then the strengthening material, therefore carries more stress then the glulam at equal strain. This implies that the strengthening material needs to have a higher yield limit then the base material to be able to take care of the additional stress it is exposed to without yielding.

2.2.1 Steel

Steel is a widely used material in the building sector. It is used both as a strengthening material, for example in concrete, and individually in structural components such as beams, columns, frames and suspension cables to mention but a few. Steel has proven to be a very useful material with many positive properties, for example high strength to weight ratio, bending resistance and ductility. Steel has some disadvantages, for example it is prone to chemical corrosion and has poor fire resistance. The material for this section is mainly taken from Owens (1992).

A big advantage of steel is its versatility. It can be manufactured in different strengths, material properties, shapes and product forms. Steel can be produced with yield limits from about 250 to about 2000 MPa, for common structural applications, and product forms spanning from thin plates/sheets to large beams. This versatility also makes steel an economically sound material since it can be tailored to any given situation.

Steel is today one of the most used materials for strengthening purposes. Due to its strength and ductile behaviour it is used in most concrete structures to strengthen its rather poor tensile cracking limit (Engström, 2010A).

2.2.1.1 Mechanical properties

Steel is normally a ductile material, which is an advantage in construction components since failure can be predicted because of large deformations before the member collapses. It also inhabits good fracture toughness and it behaves as an elastic material, with a high elastic modulus, until the yield limit is reached. After the yield limit is reached it can withstand large plastic deformations, due to its ductile behaviour. However steel can break in a brittle failure mode if the structural component has been exposed to fatigue, where cyclically variable stresses cause defects and cracks.

Steel can be considered to be an isotropic material, i.e it has the same properties in all directions, as opposed to timber. Thereby steel has about the same strength in tension as in compression. The shear strength however, is somewhat lower.

The steel used for strengthening is usually hot rolled steel with a high tensile strength, since it is the tensile properties that predominantly need to be strengthened in the base material. The hot rolling process increases the steels' strength and at the same time keeps large portions of the original ductility, which are favourable effects for reinforcing steel (Engström, 2010A).

Steel that is used for pre-stressed members is instead cold-worked steel, which is a very high strength steel. This procedure comes with some drawbacks. The steel gets a reduced plastic zone and becomes more vulnerable to corrosion and high temperatures

(Engström, 2010A). The higher yield limit acquired from cold-worked steel is needed to reduce the effects of relaxation in the steel after it has been pre-stressed.

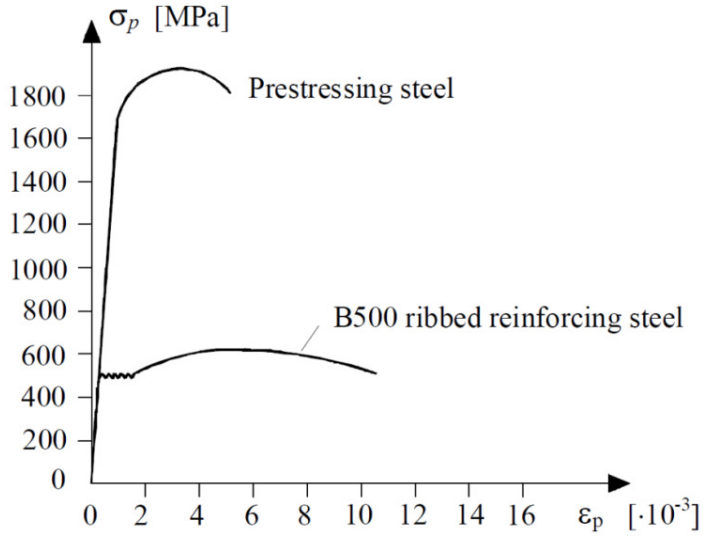

Figure 2.2 The difference between pre-stressing and reinforcing steel (Engström, 2010A))

2.2.2 Fibre Reinforced Polymers (FRP)

Fibre reinforced polymers, further referred to as FRPs, are engineered materials where strengthened fibres are placed in a resin matrix to create a material with extraordinary properties. The FRPs were most commonly used in the aerospace and military applications, but an increased choice in raw materials, which is better, cheaper and with simpler manufacturing methods have enabled FRPs to be competitive in more areas. FRP is today already used on structures like bridges, mainly to strengthen weakening structural parts. But there is a lot of research going on in to finding new applications for FRP in structural design. The material for this section is mainly taken from Peters (1998).

2.2.2.1 FRP manufacturing

Structural composites like FRPs are a mixture of two or more components. One of them being a long (compared to the diameter) and stiff fibre and the other an adhesive, resin or matrix, between the fibres. The fibres are generally stronger and stiffer than the matrices. The fibres also show anisotropic behaviour, which means that they have different properties in different directions.

In the composite the fibres and matrices will keep their individual properties and thereby directly influence the properties of the final product. The composites are designed to acquire the properties demanded for the given usage. The fibres can be oriented in different directions in different lamellae to achieve an isotropic behaviour of the composite. The composites can also be tailored to specific properties, for example temperature-resistance and electrical conductivity, by a correct choice of fibres and matrices.

The production process itself varies depending on the final product. There is a general production method which is the same for all composites. The difference is in how each step of the process is performed for different composites.

The first step of the manufacturing process is wetting (or mixing) of the fibres with the resins, which are in a liquid state. Thereafter the structure/design of the composites is built up, both in micro- (fibre orientation) and macrostructure (for example shaping of a reinforcement bar). The third step is compaction of the mix to decrease the voids between fibres and thereby decrease the amount of defects. The final step is curing or hardening of the composite.

To ensure the quality and properties of the composites a three-level testing method is applied. The method consists of testing the raw materials before production, testing the composite during the process and testing of the final product.

2.2.2.2 Mechanical properties

The mechanical properties of FRPs are determined by the raw materials in the composite and the structure of them and thereby general properties are hard to distinguish. However, all FRPs show high strength and stiffness-to-weight ratio. There are several fibres and resins with different properties to choose from which affect the final product in different ways. Some commonly used fibres are fibreglass, graphite/carbon fibres and aramids. While the fibres' function is to carry the load the matrices' main functions are to keep the fibre in place, transfer the loads, protect the fibres and carry inter-laminar shear. Some commonly used matrices/resins are polyester and vinyl esters and epoxy resins. The mechanical properties of these fibres and resins are briefly stated below.

2.2.2.3 Matrices

Polyester is the most commonly used matrix in combination with glass fibres. Vinyl ester is a related plastic with higher and better mechanical properties then polyester. Epoxy is the unquestionable strongest matrix material. It is commonly used together with carbon fibres or aramid fibres to create materials with extremely high strength (Jacob and Garzon, 2007).

2.2.2.4 Fibres

Glass fibre is made by creating long fibres from melted glass. It exists in a large variety and is electrically insulating. It is cheap to produce, which makes it a well-used material. It has a relatively low Young's modulus, which makes it less interesting as a strengthening material (Jacob and Garzon, 2007).

FRP made with carbon fibre in combination with either epoxy or vinyl ester resins creates one of the strongest FRPs there is. It has a high Young's modulus and generally has an equal compressive and tensile strength. It also has a high resistance to fatigue. It is however sensitive to impact and has a sudden and brittle failure. It is very conductive material and can create galvanic cells when it comes in to contact with metals (Jacob and Garzon, 2007).

Aramid fibres are in a FRP matrix better known as Kevlar. Kevlar is just a product name that DuPont have for their products which contain aramid fibres. Being an

organic polymer it has a distinct golden colour and compared to carbon fibre has a very high impact resistance. It is also very resistant to heat and chemicals. It has a somewhat lower Young's modulus and strength properties than carbon fibre and it deteriorates in sunlight, which makes is less desirable for beam strengthening purposes (Jacob and Garzon, 2007).

2.2.3 Adhesives

Adhesives have an important part in both glulam and strengthened glulam products. They are used both between the lamellae in glulam and between the strengthening material and glulam. The adhesives used for these purposes have high demands on them in strength, stiffness and how they are affected by temperature and moisture changes. Further demands are put on adhesives used in strengthened beams, since they need to have good bond strength to two different materials.

The idea of strengthening is to introduce a material with higher stiffness and thereby make it receive higher stress at a given strain. It is imperative that the adhesives used can transfer the stress between the two components. The ability to do so requires high strength (shear strength in this application) and stiffness. It also has to be able to be deformed and elongated without failing, since large deformations can be expected before either the timber or the reinforcement fails. These two properties, stiffness and elongation, are however generally opposites as can be seen in Figure 2.3. The solution of this problem requires a good design and selection of the adhesive.

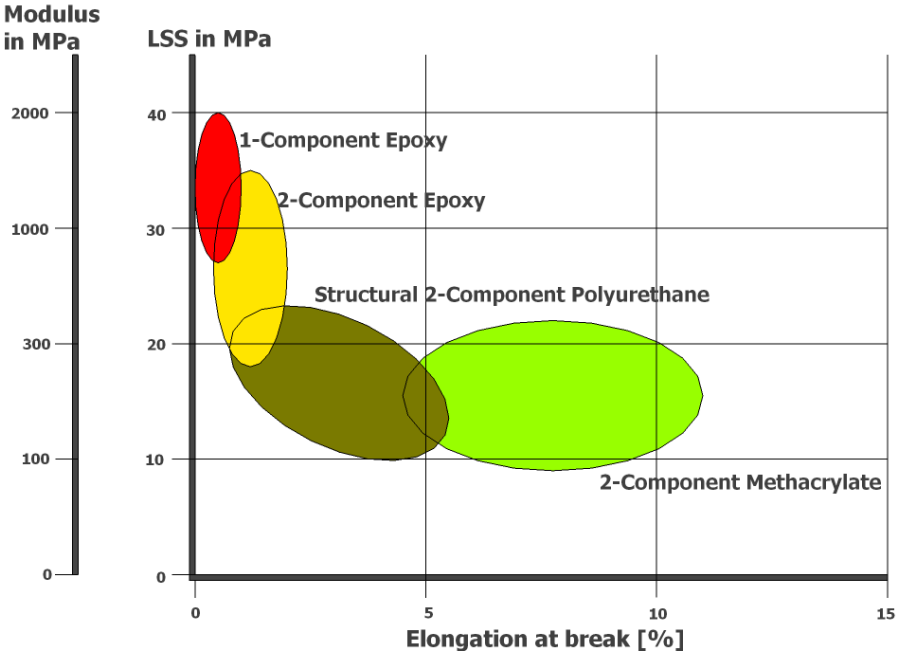

Figure 2.3 Relation between stiffness and elongation for some commonly used adhesives

3 REINFORCEMENT METHODS

There are several different ways a beam can be strengthened. In this thesis the glulam beam will be strengthened with rectangular plates where spaces have been sawn out in advance, see Figure 4.3. The strengthening material can be chosen to be either steel or FRP. The glulam beam can be un-strengthened, reinforced or pre-stressed. In this chapter these methods will be briefly demonstrated. This will be done by having a homogenous glulam beam subjected to a tensile force until failure occurs. This way of presenting these strengthening methods have been acquired from Engström (2010A). There will be a summary of the work done so far on each method included at the end of each sub-chapter.

3.1 Unreinforced beam

A plain glulam beam, seen in Figure 3.1, subjected to a tensile force will be able to resist a tensile force N equal to its tensile capacity. If more force is applied the beam will break in a tensile failure. The failure load can be calculated through (3.1).

$$N_{break} = f_{t,GL} A_{GL} \tag{3.1}$$

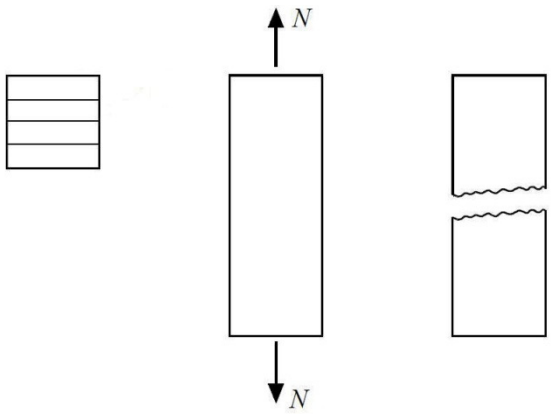

Figure 3.1 A glulam member subjected to a tensile force N (Engström, 2010A).

3.2 Reinforced beam

A glulam beam that has been symmetrically reinforced will behave differently from a plain glulam beam. The reinforcement increases the overall resistance by making the beam stiffer, since a material with a higher Young's modulus will carry more stress at equal strain. When the glulam, at a higher load, yields the strengthening material will carry the entire applied load by itself, see Figure 3.2. This assumes there is sufficient strengthening material placed in the beam to withstand the stress increase applied when the glulam fails. If there is not enough reinforcement, the entire beam, i.e. the glulam and the reinforcement, will yield when the glulam fails in tension.

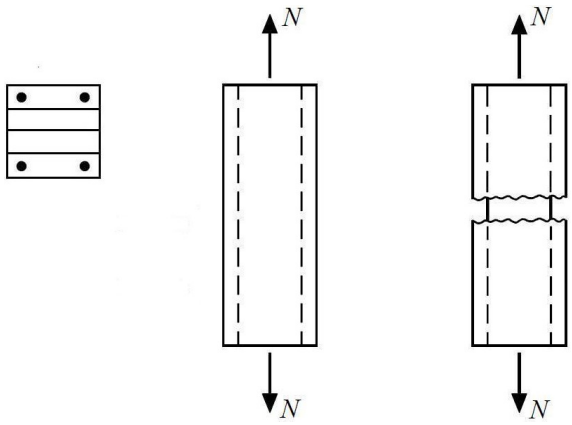

Figure 3.2 Reinforced glulam member loaded by an axial tensile force N (Engström, 2010A).

To calculate a reinforced cross-section the section is recalculated as an equivalent glulam cross-section. The cross-section is thereby transformed by the following formula.

$$A_{eq} = A_{GL} + (\alpha - 1)A_{RF} \tag{3.2}$$

$$where\ \alpha = \frac{E_{RF}}{E_{GL}} \tag{3.3}$$

The reinforced cross-section's ultimate load carrying capacity depends on whether the reinforcement yields together with the glulam or if it can keep carrying the applied load after the glulam fails. As seen in (3.4) the lower of these two capacities becomes the governing one.

$$N_{break} = min\begin{cases} f_{t,GL}A_{eq} \\ f_{t,RF}A_{RF} \end{cases} \tag{3.4}$$

3.2.1 Strengthening of glulam

"Conventional glued-laminated (glulam) beams often fail in bending-induced tension" (Silva-Henriquez, 2009). Glulam beams with long spans ($L>12h$) loaded in bending commonly fail in a tension failure, since a glulam beam can plasticise in its compressive zone. If this failure mode can be delayed the glulam beam can utilise its plasticising ability to a higher extent. This will give a higher maximum flexural resistance in the ultimate limit state. If there can be achieved a method to increase this material property in glulam, a lot more constructions will be able to incorporate glulam into their structural design.

There have been a large number of experiments, FEM models and trials made to try to reinforce glulam beams. The aim has been to be able to either reduce the height of the beams or to improve the flexural resistance. "Fibre reinforcement may also allow lower grades of lumber to be used effectively in advanced structural members." (Dolan, 1997). But also "to enhance further the strength of beams made

from good quality timber" (Guan, 2005). The beams have been reinforced in numerous different ways. There are beams that have been reinforced on the tension side only (Silva-Henriquez, 2009), (Dolan, 1997). Both are with reinforcing steel rods, the same way concrete is being reinforced today. Sheets of FRP being glued to the bottom of the cross-section is another method. This method is also applicable to existing structures in need of strengthening, since there is no altering of the existing cross-section of the beam.

Then there have been trials where both the tension and compressive side have been reinforced. According to Jacob and Garzon (2007), the choice of using 25% of the overall amount of reinforcement on the compressive side yields the best results. Both the flexural resistance and the overall stiffness were increased when the reinforcement was added in this way. With the compressive reinforcement additional stiffness is added, but the beam is forced to a brittle failure on the tensile side. This due to the fact that the compression strength of the beam is enhanced with compressive reinforcement and thereby far exceeds the tensile capacity. When examining the different material used as reinforcement Jacob and Garzon (2007) showed that CFRP was the strengthening material which made the glulam beams the stiffest. The reinforcing steel also increases the stiffness, to a slightly lesser extent, and it decreases with added loading due to yielding of the steel. The beam reinforced with steel showed an overall more ductile behaviour due to the plastic yielding capacity of the reinforcing steel.

It was not possible for Jacob and Garzon (2007) to determine which reinforcing material increased the ultimate load capacity the most, because all failure modes where governed by the defects of the timber. Despite this Jacob and Garzon (2007) could show that the tested beams did experience an increase in ultimate load capacity of between 57-95.8%. It is also important, according to Jacob and Garzon (2007), to not over reinforce the beams since the reinforcement will then not be fully utilized before a shear failure occurs.

3.3 Pre-stressed beam

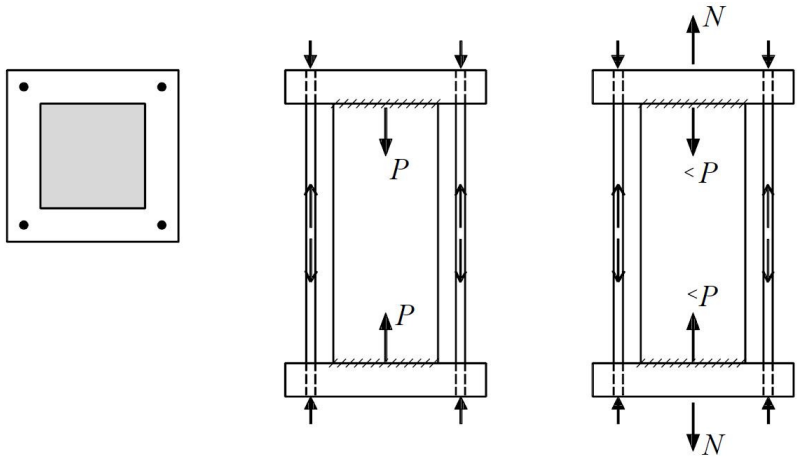

Figure 3.3 Principal model of a pre-stressed member, before loading and when subjected to a tensile load N (Engström, 2010A).

The beam has four external rods as reinforcement, as seen in Figure 3.3.This does not represent a realistic case for a pre-stressed beam, but is an arrangement made to more

easily visualise the pre-stressed effect. These rods are given an initial tensile force, a pre-stressing force, and are then fastened to the object. This creates a uniformly compressive force that applies to the glulam. The tensile force N is then applied and increased until a failure of the beam occurs.

The transformed cross-section in this example is defined slightly different than (3.2), as can be seen in (3.5).

$$A_{eq} = A_{GL} + \alpha A_{RF} \tag{3.5}$$

As with the reinforced beam, the failure occurs either when the glulam fail and the reinforcement cannot take the added stress created by the glulam´s failure, or at that time when the reinforcement yields after the glulam has yielded. The lower of these two forces becomes the governing one according to (3.4).

3.3.1 Pre-stressed strengthened glulam

The concept of pre-stressing glulam is not a new idea, in 1991 Thanasis, Triantafillou and Deskovic presented a report of an innovative method of pre-stressing glulam. Some studies have followed and even though all studies have presented positive results, pre-stressed glulam has failed to have an impact on the production market and even in research, which the amount of material that can be found on the subject bears witness to.

The concept of pre-stressing a beam, no matter what material is being used is that an axial compressive force is applied to the cross-section. This compression force is applied using a reinforcing material that has been subjected to a tensile force before it is introduced and bonded to the beam. The compression force from the tendon shifts the stress distribution in the cross-section and places the compression side of the beam in tension and vice versa. The application of load must now first exceed the subjected pre-stressing stress and then the capacity of the beam for the beam to reach its maximum flexural resistance.

The studies made have included different types and different placements of the strengthening material. The results from the experimental and analytical methods have varied because of this. A common denominator is that all results have shown an improvement compared to both regular glulam and reinforced glulam. Both the reinforced and the pre-stressed show an increase in modulus of elasticity and modulus of rupture compared to a regular glulam beam. All studies shows that the pre-stressed beam has a higher modulus of rupture than the reinforced beams, but the studies vary in the results of modulus of elasticity. Some studies show higher modulus of elasticity in pre-stressed and some show approximately equal values (Dolan, 1997); (Silva-Henriquez, 2009); (Triantafillou, 1992); (Yahyaei-Moayyed, 2010A).

A difficulty in pre-stressing timber is the placement of the tendon. In some studies the tendon is glued to the outside of the outmost lamella on the tension side. This leaves the tendon unprotected against, for example mechanical damage and fire. A solution to this problem is to cover the tendon with an additional wood-lamella, a so-called “bumper”. This solution protects the tendon, but the beams load-carrying capacity drops considerably after the initial failure of the bumper (Yahyaei-Moayyed, 2010A).

4 THE MODEL

To investigate the different aspects of strengthened glulam beams an analytical model was established. By predefining the highest compressive strain ε_c other strains of interest could be obtained in the cross-section through strain compatibility. The entire sequence of events during the beam's loading was analysed. This became possible to do since the ε_c was step-wise increased from zero strain until a failure criterion for the beam became fulfilled. There where however some cases where the general shape of the strain distribution were varying. For these cases a direct application of Navier's formula was needed instead, see Chapter 4.3.1.

The model was created to handle unreinforced, reinforced and pre-stressed glulam beams and to be able to compare different properties between them, given a complete set of geometrical and material input data. It was established in such way that it could handle the linear elastic phase as well as the plastic phase for glulam and compensate for any yielding in the reinforcement. The model could handle any chosen configuration of compressive and tensile reinforcement. The full calculations are presented as a number of MathCAD-, found in Appendix A, and Matlab codes, found in Appendix B.

4.1 Unreinforced beam

4.1.1 Elastic phase

If a homogenous and even-sided beam is subjected to a bending moment imposed by a distributed load the centre of gravity and the neutral axis both becomes located in the centre of the beam's cross-section. When the neutral axis is situated in the middle of the beam the outermost tensile strain and compressive strain become equal, since strain compatibility is assumed in a linear elastic analysis. An un-strengthened glulam beam with sufficient cross-section will, in linear elastic calculations, fail in bending induced tension, since in most cases glulam's tensile yield limit is lower than its compressive yield limit.

For a real beam there are many different failure modes that can be expected to occur depending on what defects the particular beam has inherent and where they are located.

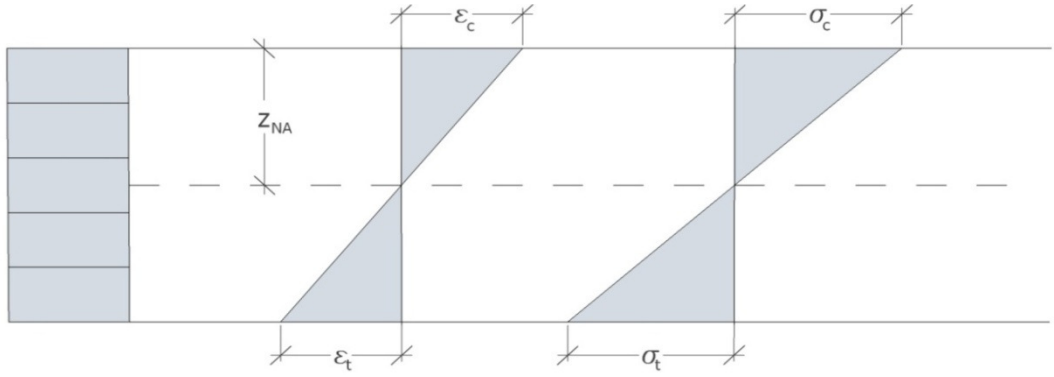

Figure 4.1 The stress and strain distribution of an ordinary glulam beam subjected to a uniform flexural moment, elastic phase.

$$\varepsilon_c = \varepsilon_t \tag{4.1}$$

With these assumptions there is a geometric problem left to calculate the resisting bending moment. The geometry, seen in Figure 4.1, for the bending moment can be retrieved as defined in (4.2). From this resisting bending moment, different loads for load cases can be calculated.

$$M = \frac{\varepsilon_c \, E \, b \, h^2}{12} + \frac{\varepsilon_t \, E \, b \, h^2}{12} \tag{4.2}$$

4.1.2 Plastic phase

Unreinforced glulam beams rarely starts to plasticise since the compression yield limit in most beams exceeds the tensile yield limit.

If the plasticisation phase for an unreinforced beam is to be considered, it occurs when the glulam has reached its elastic compressive strain limit and thus no longer will carry any further stress at that point in the cross-section. The strain will continue to increase until a failure occurs in the beam. This results in a stress distribution with a rectangular shaped plasticisation zone seen in Figure 4.2. To calculate the resisting bending moment for this beam, the force equilibrium seen in (4.3) must first be defined from Figure 4.2.When the force equilibrium is defined the individual forces can be derived from Figure 4.2, as can be seen in (4.4).

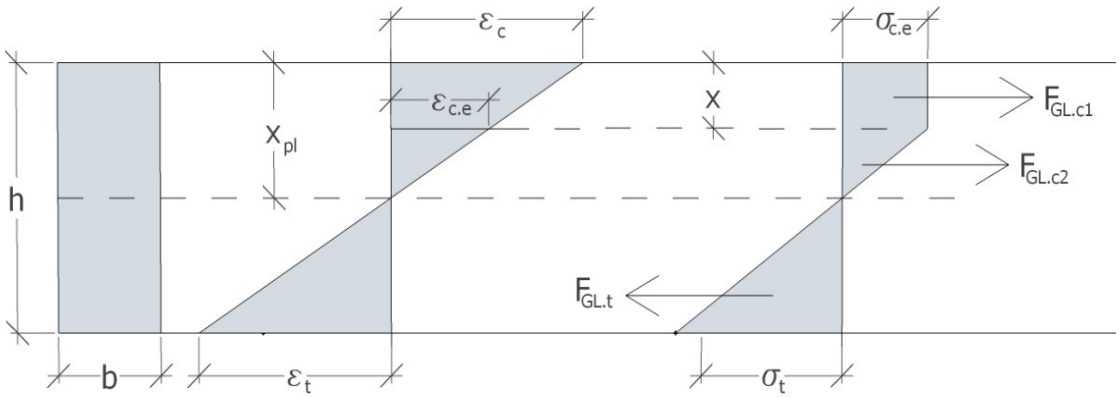

Figure 4.2 The stress and strain distribution of an unreinforced beam subjected to a uniform flexural moment, plastic phase.

$$F_{GL,c1} + F_{GL,c2} = F_{GL,t} \tag{4.3}$$

$$\begin{aligned} F_{GL,c1} &= A_{c1} b E_{GL} \varepsilon_{c,e} \\ F_{GL,c2} &= A_{c2} b E_{GL} \varepsilon_{c,e} \\ F_{GL,t} &= A_{GL,t} b E_{GL} \varepsilon_t \end{aligned} \tag{4.4}$$

With the plasticisation in the glulam the new shape in the form of a rectangle emerges. The height of this rectangle, denoted x in Figure 4.2, is dependent on how much of the cross-section has started to plasticise. x can be derived from (4.13) which defines the difference between the present step of ε_c and the present level of $\varepsilon_{c,e}$.

$$x = \frac{\varepsilon_c - \varepsilon_{c,e}}{\varepsilon_c} x_{pl} \tag{4.5}$$

With x defined the only unknown parameter in the cross-section is x_{pl}. x_{pl} is derived from the force equilibrium. For that to be possible all forces in the force equilibrium need their associated strains calculated. As ε_c is initially the only known strain, since it is predefined as the chosen strain to stepwise increase, all other strains must be redefined to reflect its relationship with ε_c through strain compatibility. The strains, seen in (4.6), become redefined by means of ε_c and x_{pl} and known cross-sectional geometry.

$$\begin{aligned} \varepsilon_t &= \frac{h - x_{pl}}{x_{pl}} \varepsilon_c \\ \varepsilon_{c,e} &= \frac{x_{pl} - x}{x_{pl}} \varepsilon_c \end{aligned} \tag{4.6}$$

x_{pl} can then be extracted through the force equilibrium equation, by inserting (4.6) into (4.4). With x_{pl} calculated the resisting bending moment is found by calculating moment equilibrium around x_{pl}, as seen in (4.7).

$$\begin{aligned} M = F_{GL,c1}\left(x_{pl} - \frac{x}{2}\right) + \frac{2}{3} F_{GL,c2}\left(x_{pl} - x\right) \\ + \frac{2}{3} F_{GL,t}\left(h - x_{pl}\right) \end{aligned} \tag{4.7}$$

4.2 Reinforced beam

To strengthen the glulam beam a chosen amount of strengthening material is be added to the beam. This adds maximum flexural resistance, stiffness and deflection resistance to the beam.

4.2.1 Elastic phase

The calculations for a reinforced beam get several additions due to the reinforcement, compared to the un-strengthened beam. First the cross-section will be recalculated into an equivalent cross-section to account for the superior material properties the reinforcement has inherent. With the equivalent cross-section the reinforcement will be recalculated into an equivalent amount of glulam. The centre of gravity no longer resides at the centre of the beam due to this. It has instead been relocated toward the point where the highest concentration of reinforcement resides, as can be seen in

Figure 4.3. The highest compressive strain will always be higher than the highest tensile strain due to this relocation, assuming the largest amount of reinforcement resides on the tensile side.

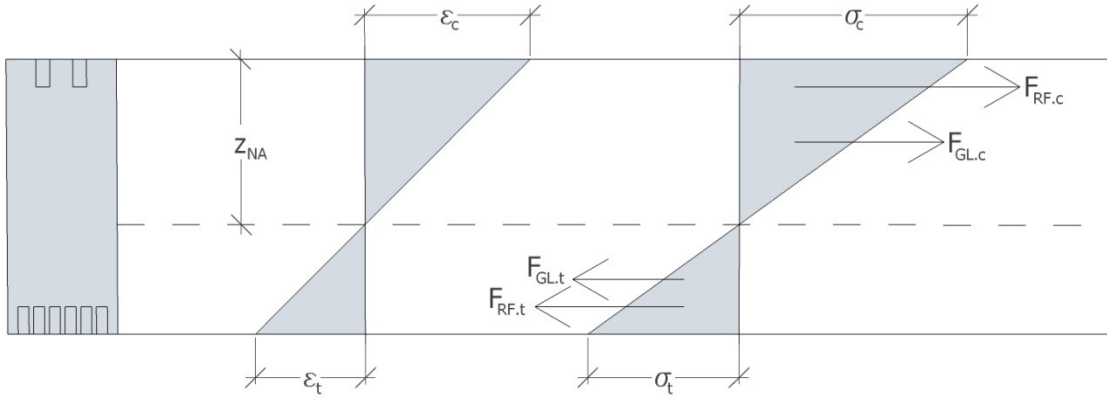

Figure 4.3 The stress and strain distribution of a reinforced glulam beam subjected to a uniform flexural moment, elastic phase.

With an asymmetrical equivalent cross-section, a new centre of gravity (and for reinforced beams) the same as the neutral axis can be calculated according to (4.8). Note that the centre of gravity and the neutral axis only can be assumed to be at the same height in the cross-section if no axial force is acting on the beam.

$$z_{NA} = \frac{\sum_{i=1}^{i=n}(A_i E_i z_i)}{\sum_{i=1}^{i=n}(A_i E_i)} \tag{4.8}$$

The *EI* is calculated for each individual part of the equivalent cross-section, seen in (4.9). Then all the different parts are added together to establish the global stiffness of the cross-section. In total *EI* consists of three parts, one for the entire glulam body and one for each of the two concentrations of reinforcement.

$$EI = \sum E \left[\frac{b\ h^3}{12} + A\ (z_{leverarm})^2\right] \tag{4.9}$$

With a variable amount of reinforcement, it can no longer be assumed that the beam will fail in bending induced tension. Depending on the amount of compressive and tensile reinforcement a shear or even a compressive failure become likely failure modes for a beam that un-strengthened would fail in bending induced tension. To find which failure mode that will become the governing one, for each specific reinforcement configuration, a mathematical loop is established. The loop, seen as (4.10) and (4.11), will start with an assumption that there occurs a tensile failure. If the maximum compressive strain, on the other side of the beam, at the point in time is higher than its ultimate capacity value, it is a compressive failure that instead governs the failure for that specific bream. The strains then become recalculated based on the compressive failure strain instead to give the correct maximum strain distribution for that beam.

$$\begin{cases} \varepsilon_t = \varepsilon_{t,e} \\ \varepsilon_c = \dfrac{\varepsilon_t}{h_{GL} - z_{NA}} z_{NA} \end{cases} \tag{4.10}$$

$$\begin{cases} \varepsilon_t = \begin{cases} \frac{\varepsilon_{c,e}}{z_{NA}}(h_{GL} - z_{NA}) & if \ \ \varepsilon_c > \varepsilon_{c,e} \\ \varepsilon_t & otherwise \end{cases} \\ \varepsilon_c = \begin{cases} \varepsilon_{c,e} & if \ \ \varepsilon_c > \varepsilon_{c,e} \\ \varepsilon_c & otherwise \end{cases} \end{cases} \tag{4.11}$$

Two more forces have appeared in the force equilibrium equation due to the reinforcement, see Figure 4.4 and (4.12). They are located at the centre of the concentrations of reinforcement and are defined by the strengthening material's parameters, as can be seen in (4.13).

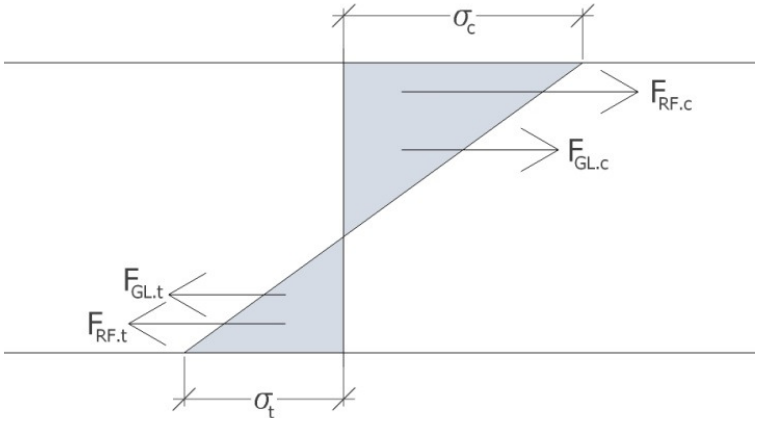

Figure 4.4 The stress and force distribution for the moment created by the applied load.

$$F_{RF,c} + F_{GL,c} = F_{GL,t} + F_{RF,t} \tag{4.12}$$

$$\begin{gathered} F_{RF,c} = A_{RF,c}\, E_{RF} \varepsilon_{RF,c} \\ F_{GL,c} = A_{c1} b E_{GL} \varepsilon_c \\ F_{GL,t} = A_{GL,t} b E_{GL} \varepsilon_t \\ F_{RF,t} = A_{RF,t} E_{RF} \varepsilon_{RF,t} \end{gathered} \tag{4.13}$$

$$\begin{gathered} \varepsilon_{RF,c} = \frac{Z_{na} - Z_c}{Z_{na}} \varepsilon_c \\ \varepsilon_{RF,t} = \frac{h - Z_{na} - Z_t}{Z_{na}} \varepsilon_c \\ \varepsilon_t = \frac{h - Z_{na}}{Z_{na}} \varepsilon_c \end{gathered} \tag{4.14}$$

With these forces defined the resisting moment can be calculated through moment equilibrium around z_{na}, as seen in (4.15)

$$M_{max} = \frac{1}{3}\varepsilon_c E_{GL} b {z_{NA}}^2 + \varepsilon_{Rc} E_{RF} A_{Rc}\left(z_{NA} - \frac{h_{GL}}{2}\right) + \frac{1}{3}\varepsilon_t E_{GL} b (h - z_{NA})^2 + \varepsilon_{Rt} E_{RF} A_{Rt}\left(h - z_{NA} - \frac{h_{GL}}{2}\right) \quad (4.15)$$

4.2.2 Plastic phase

For further calculations for a reinforced beam in the plastic phase it is recommend to look at Jacob and Garzon (2007), since one of their objects is to establish this as an analytical model.

As for the unreinforced beam the plastic phase occurs when ε_c reaches $\varepsilon_{c,e}$. When this condition is met, the glulam can no longer carry more stress as the strain increases further. When this occurs, the constitutive relationship between the strain and stress distribution through Young's modulus ceases to be valid and distribution gets a new appearance, as seen in Figure 4.5

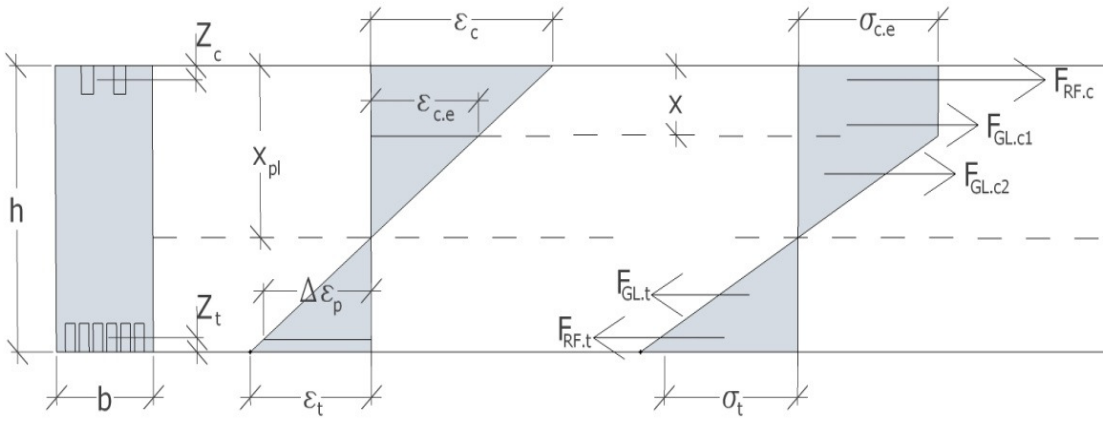

Figure 4.5 Stress and strain distribution of a reinforced beam subjected to a uniform flexural moment, plastic phase.

The constitutive relationship can no longer be directly applied, but the force and moment equilibrium conditions must still be fulfilled. The maximum stress the glulam can tolerate is known; hence the rectangular stress block created by the increasing plasticisation of the glulam can be calculated. It should be noted that the reinforcement does not have to cease carrying more stress when the glulam does. Although the top reinforcement lies within the rectangular compressive zone that is not able to carry any additional stress, this reinforcement will continue to carry an increasing amount of stress until its yielding limit is reached. The force equilibrium from Figure 4.5 becomes defined as shown in (4.16) and its associated forces are defined in (4.17).

$$F_{RF,c} + F_{GL,c1} + F_{GL,c2} = F_{GL,t} + F_{RF,t} \quad (4.16)$$

$$F_{RF,c} = A_{RF,c}\, E_{RF}\varepsilon_{RF,c}$$

$$F_{GL,c1} = A_{c1} b E_{GL}\varepsilon_{c,e}$$

$$F_{GL,c2} = A_{c2} b E_{GL}\varepsilon_{c,e} \qquad (4.17)$$

$$F_{GL,t} = A_{GL,t} b E_{GL}\varepsilon_{t}$$

$$F_{RF,t} = A_{FR,t} E_{RF}\varepsilon_{RF,t}$$

F_{GLc1} and $F_{GL,c2}$ are defined by the maximum elastic strain for glulam and the $F_{RF,c}$ instead has its strain derived from ε_c at that chosen step, which can be much larger then $\varepsilon_{c,e}$ when the plastic phase goes on. The strains needed for (4.16) are defined as displayed in (4.18).

$$\varepsilon_{RF,c} = \frac{x_{pl} - Z_c}{x_{pl}}\varepsilon_c$$

$$\varepsilon_{RF,t} = \frac{h - x_{pl} - Z_t}{x_{pl}}\varepsilon_c \qquad (4.18)$$

$$\varepsilon_{t} = \frac{h - x_{pl}}{x_{pl}}\varepsilon_c$$

$$\varepsilon_{c,e} = \frac{x_{pl} - x}{x_{pl}}\varepsilon_c$$

$$x = \frac{\varepsilon_c - \varepsilon_{c,e}}{\varepsilon_c} x_{pl} \qquad (4.19)$$

With the addition of the height x in (4.19), the height of the plastic zone, the remaining unknown parameter x_{pl} can now be extracted from the force equilibrium as it is now the only unknown parameter left. The extraction is identical to that described in Chapter 4.1.2.

The solution of x_{pl} is preferably done with the Matlab command "*solve*" as it changes appearance depending on the glulam having a plastic zone or if any part of the reinforcement reaching its yielding strength.

When the plastic neural axis x_{pl} has been found, the resisting bending moment can be calculated by moment equilibrium around x_{pl}, as seen in (4.20).

$$M = F_{GL,c1}\left(x_{pl} - \frac{x}{2}\right) + \frac{2}{3}F_{GL,c2}(x_{pl} - x)$$
$$+F_{RF,c}(x_{pl} - Z_c) + \frac{2}{3}F_{GL,t}(h - x_{pl}) \quad (4.20)$$
$$+F_{RF,t}(h - x_{pl} - Z_t)$$

4.3 Pre-stressed beam

A pre-stressing force can be seen as an axial force acting on the cross-section. This force will act as a compressive force and be applied at the middle of the tensile reinforcement. If this force would have been applied at the centre of gravity it will only add a uniformly spread compressive stress across the beam. When this force does not act in the centre of gravity an additional moment will be applied to the cross-section which depends on the lever arm *e*, see Figure 4.6. Together, these two stress distribution produce the total stress distribution imposed on the cross-section by the pre-stressing force.

The pre-stressing force has several positive effects. The compressive force of the pre-stressing increases the load bearing capacity in the ultimate limit state. This is only valid if a tension failure occurs, since the added compression does not increase any other yield limits. The second part of the pre-stressing force, the bending moment that occurs due to the lever arm *e*, creates an upward directed deflection of the beam. This reduces the overall deflection of the beam, which is the most common service limit state requirement. With this pre-camber additional load can be applied before the service limit state requirements are met.

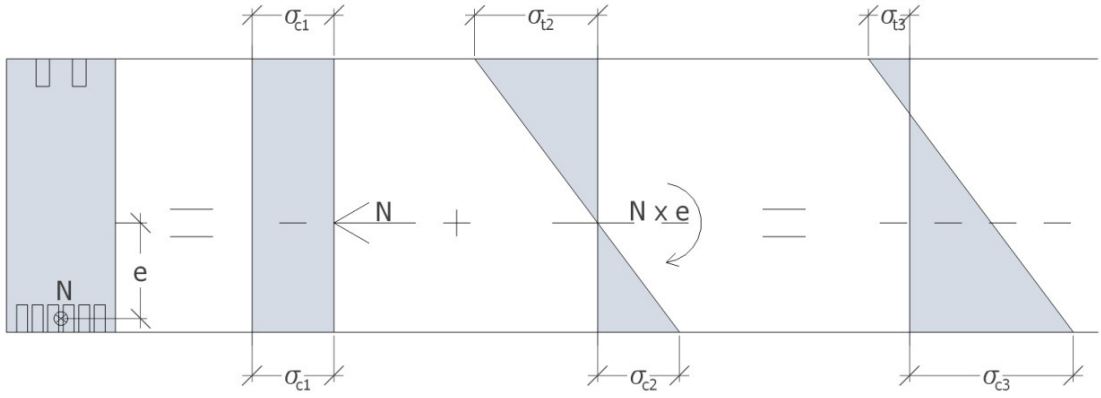

Figure 4.6 The stress distributions created by a pre-stressing force

4.3.1 Elastic phase

For this thesis, the pre-stressing force cannot be greater than the maximum axial force than what EC5 allows for. If a greater pre-stressing force is applied the beam, according to EC5, will experience a lateral torsional buckling. This has been chosen because the beam at full compression should still be able to be handled and moved.

The beam would be able to sustain sometimes several hundred percent more before yielding, but without constant bracing this would not be able to be sustained.

With the initial stress distribution from the pre-stressing load, an increasing additional moment is applied to the cross-section. This moment represents the pure bending moment created by the load after the pre-stressing force is applied. The stresses at the top and at the bottom of the beam can assume both compressive and tensile stresses during the elastic phase, as can be seen in Figure 4.7. A sign convention must therefore be upheld during the elastic phase. In this thesis the sign convention from Al-Emrani (2008) is used.

- Axial - force-positive if in tension
- Moment - positive if there is tension at the bottom side.
- Coordinate z is measured from the equivalent cross-sections centre of gravity – positive downwards
- The eccentricity of the axial force is measured from the equivalent cross-sections centre of gravity – positive downwards.
- Calculated stress – positive if tension

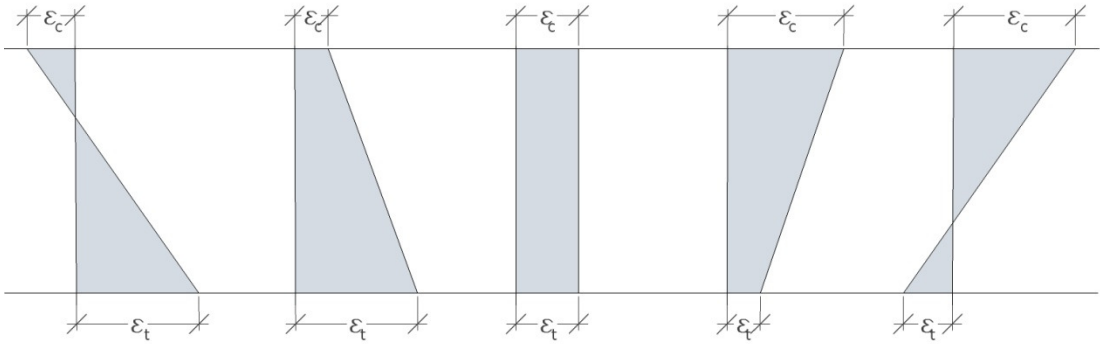

Figure 4.7 All different strain distributions a pre-stressed glulam beam can experience in the elastic phase.

To calculate the elastic phase Navier's formula has been used. This is the least complicated way to calculate the elastic phase, since there is no way in advance to know what shape the stress distribution will assume when the load increases. Navier's formula is valid for all linear elastic distribution forms, thus making it the most efficient way to calculate the resisting moment.

Through Navier's formula we can, for each increased strain, extract the moment that the load applied by changing (4.21) into (4.22).

$$\varepsilon_c E_{GL} = \frac{N}{A} + \frac{N\,e + M}{I} z \tag{4.21}$$

Then since the strain ε_c gets prescribed each time, it together with its representative z makes it possible to extract M, the moment imposed by the load.

$$M = \frac{(E\,\varepsilon_c\,A\, - N\,)I}{Az} - N\,e \tag{4.22}$$

$$\varepsilon_t = \frac{M}{E_{GL}I} z_t$$

$$\varepsilon_{RF,t} = \frac{M}{E_{GL}I} z_{RF,t}$$

$$\varepsilon_{RF,c} = \frac{M}{E_{GL}I} z_{RF,c} \qquad (4.23)$$

$$\varepsilon_c = \frac{M}{E_{GL}I} z_c$$

When this moment is calculated it is used to extract its associated strains seen in (4.23). With these strains the load resisting moment can be calculated by (4.15). It should be noted that if N=0 the same resisting moment calculated in Chapter 4.2.1 will be obtained. This ability will be used later in the computer program to minimise computer calculations.

4.3.2 Plastic phase

The elastic model ends when the compressive strain reaches the elastic strain limits. After that has occurred, the glulam in the compressive zone starts to plasticise and gain the stress distribution seen in Figure 4.8.

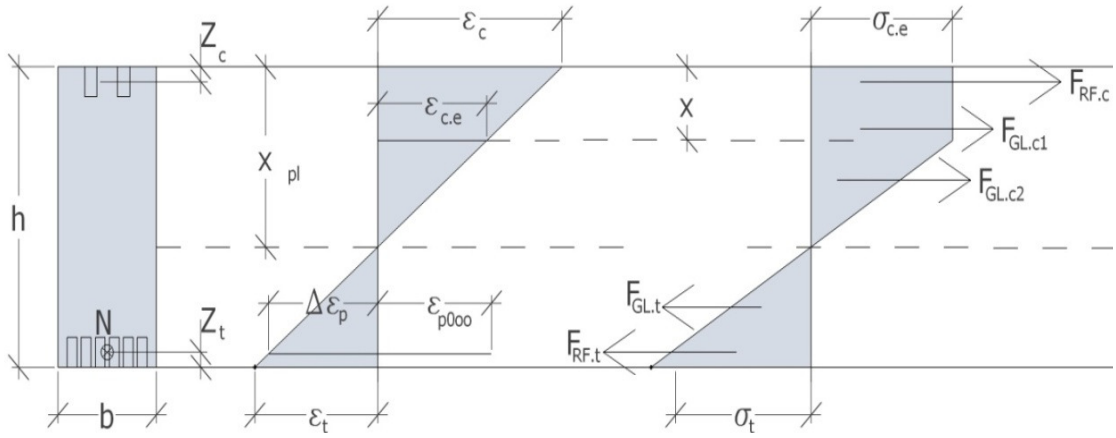

Figure 4.8 Stress and strain distribution for a pre-stressed beam subjected to a uniform flexural moment, plastic phase.

The pre-stressed beam has an addition to the strain distribution, when compared to (4.18). This strain $\varepsilon_{p0\infty}$, as it is called in an equivalent pre-stressed concrete cross-section (Engström, 2010A), is the pre-existing strain in the pre-stressed reinforcement due to the pre-stressing force. With this addition to account for the pre-stressing force, x_{pl} can now be calculated through the force equilibrium.

$$F_{RF,c} + F_{GL,c1} + F_{GL,c2} = F_{GL,t} + F_{RF,t} \qquad (4.24)$$

The force equilibrium has the same definition as in Chapter 4.2.2, hence the definitions of the different forces become the same.

$$F_{RF,c} = A_{FR,c}\, E_{RF}\varepsilon_{RF,c}$$

$$F_{GL,c1} = A_{c1} b E_{GL}\varepsilon_{c,e}$$

$$F_{GL,c2} = A_{c2} b E_{GL}\varepsilon_{c,e} \tag{4.25}$$

$$F_{GL,t} = A_{GL,t} b E_{GL}\varepsilon_t$$

$$F_{RF,t} = A_{FR,t} E_{RF}\varepsilon_{RF,t}$$

From this equilibrium condition and the fact that ε_c is always known the x_{pl} will be able to be calculated if the strains are expressed with ε_c. In (4.26) the difference should be noted in $\varepsilon_{RF,t}$ where the $\varepsilon_{p0\infty}$ is present, compared to (4.18).

$$\varepsilon_{FR,c} = \frac{x_{pl} - Z_c}{x_{pl}}\varepsilon_c$$

$$\varepsilon_{RF,t} = \frac{h - x_{pl} - Z_t}{x_{pl}}\varepsilon_c + \varepsilon_{p0\infty} \tag{4.26}$$

$$\varepsilon_t = \frac{h - x_{pl}}{x_{pl}}\varepsilon_c$$

$$\varepsilon_{c,e} = \frac{x_{pl} - x}{x_{pl}}\varepsilon_c$$

$$x = \frac{\varepsilon_c - \varepsilon_{c,e}}{\varepsilon_c} x_{pl} \tag{4.27}$$

With these functions defined and ε_c as the stepping parameter x_{pl} can be extracted through the force equilibrium. The resisting moment can be calculated by moment equilibrium around x_{pl}, as seen in (4.28).

$$M = F_{GL,c1}\left(x_{pl} - \frac{x}{2}\right) + \frac{2}{3}F_{GL,c2}\left(x_{pl} - x\right)$$

$$+F_{RF,c}\left(x_{pl} - x\right) + \frac{2}{3}F_{GL,t}\left(h_g - x_{pl}\right) \tag{4.28}$$

$$+F_{RF,t}(h - x_{pl} - Z_t)$$

4.4 Yielding of the reinforcement

The reinforcement can reach its yield point before the beam fails in ultimate limit state. In this case the reinforcement, if it has a plastic capability like for example steel, is assumed to have a bilinear stress-strain curve, cf. Figure 4.9. With the bilinear assumption, the reinforcement can experience an infinite amount of additional strain

after reaching the yield limit, without being able to carry any more stress above this limit.

4.4.1 Elastic phase

If the reinforcement should start to yield during the elastic phase the Navier's formula no longer remains valid. When that happens the case must be viewed by the means of the force equilibrium from the stress distribution.

If the beam is reinforced the force equilibrium is obtained from Figure 4.4. It will become as (4.29), where depending on which reinforcement is yielding (4.30), (4.31) or (4.32) should become inserted.

$$F_{RF,c} + F_{GL,c} = F_{GL,t} + F_{RF,t} \tag{4.29}$$

If the beam is pre-stressed, several cases exist. The different cases of stress distribution in the elastic phase due to the pre-stressing force are showed in Figure 4.7. The more cases that are permitted into the calculations the more general the calculations can be considered to be.

When any part of the reinforcement starts to yield the present stress distribution must first be determined. When the stress distribution has been determined the force equilibrium can be found as (4.29) with (4.30), (4.31) or (4.32) inserted depending on which part of the reinforcement is yielding.

4.4.2 Plastic phase

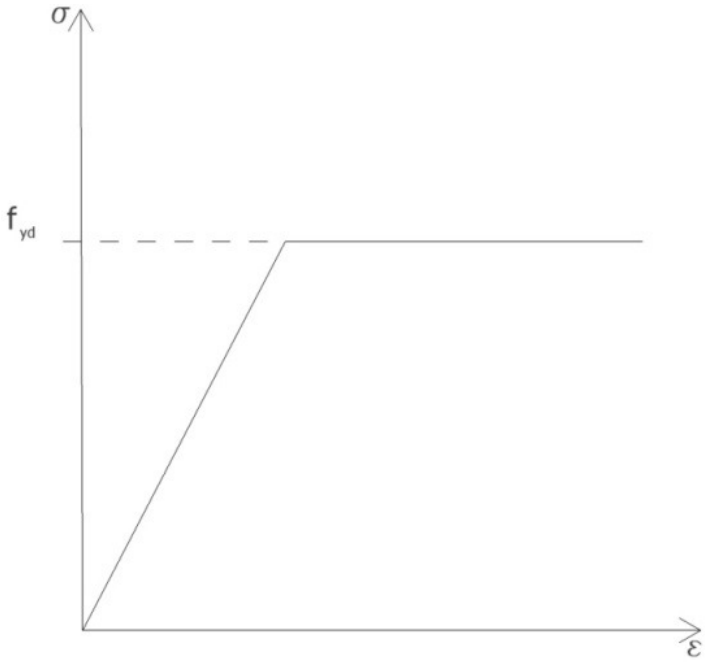

Figure 4.9 A bilinear work curve for steel

When the reinforcement reaches its maximum stress level it will either start to plasticise or get a brittle failure. If the reinforcement has the ability to plasticise it will, after reaching its maximum stress level, not take any more stress with the

increasing strain. When this occurs the x_{pl} must be recalculated with the condition stated in (4.30), (4.31) or (4.32) depending on which part of the reinforcement has reached its yielding point.

If the compressive reinforcement has reached its yielding strength, then (4.29) is only valid if (4.30) is used to replace the force for the compressive reinforcement.

$$F_{RF,c} = \frac{f_{yd}}{A_{RF,c}} \tag{4.30}$$

If instead the tensile reinforcement has reached its yielding strength, then inserting (4.31) into (4.29) for the tensile reinforcement makes the equation valid.

$$F_{RF,t} = \frac{f_{yd}}{A_{RF,t}} \tag{4.31}$$

If both the compressive and the tensile reinforcement have reached the yielding strength equation (4.32) makes (4.29) valid.

$$\begin{cases} F_{RF,c} = \dfrac{f_{yd}}{A_{RF,c}} \\ F_{RF,t} = \dfrac{f_{yd}}{A_{RF,t}} \end{cases} \tag{4.32}$$

4.5 Shear failure

Disregarding the various types and amount of reinforcement, the shear failure appears at the same load, since the size of the cross-section and the length of the beam determine the shear failure. In this thesis, either evenly distributed loads or the four point bending test has been used. For the cases with a uniformly-distributed load, the equation (4.33) can be used to define the maximum shear force before shear failure occurs. Equation (4.34) represents the counterpart for the concentrated point load combination.

$$\tau = \frac{3V}{2bh} \qquad \tau \leq \tau_{max} \tag{4.33}$$

$$\tau = \frac{3P}{4bh} \qquad \tau \leq \tau_{max} \tag{4.34}$$

5 VERIFICATION OF THE MODEL

To make an initial verification, the pre-stressing force in the model was set to zero. When the pre-stressing force in the model is set to zero the beam being calculated should behave as a reinforced beam instead. By comparing these results with the results provided in Jacob and Garzon (2007) for reinforced beams, an initial verification could be done.

To calibrate the model with pre-stressed reinforcement, the model results were compared with the test results acquired from two tested pre-stressed beams. These beams were loaded until failure with a four point bending test. The dimensions of the tested beams can be found in Table 5.1 and further information about these tests can be found in Haghani (2010)

The pre-stressed beams were tested by the same machine and with the same test method as the reinforced beams were in Jacob and Garzon (2007); since the description of the test procedure comes from their thesis. The tested beams were strengthened with pre-stressed CFRP, therefore plasticisation of reinforcement was prohibited in the models calculations for the duration of this verification.

5.1 The four point bending test

The two beams were tested with a four point bending configuration. The four point bending test is designed to create a constant bending moment between the applied loads, as can be seen in Figure 5.1. To accomplish this, the beam was loaded at two locations. The load is applied at one third of the beams length from either side of the beam. The beams were simply supported on roller bearings.

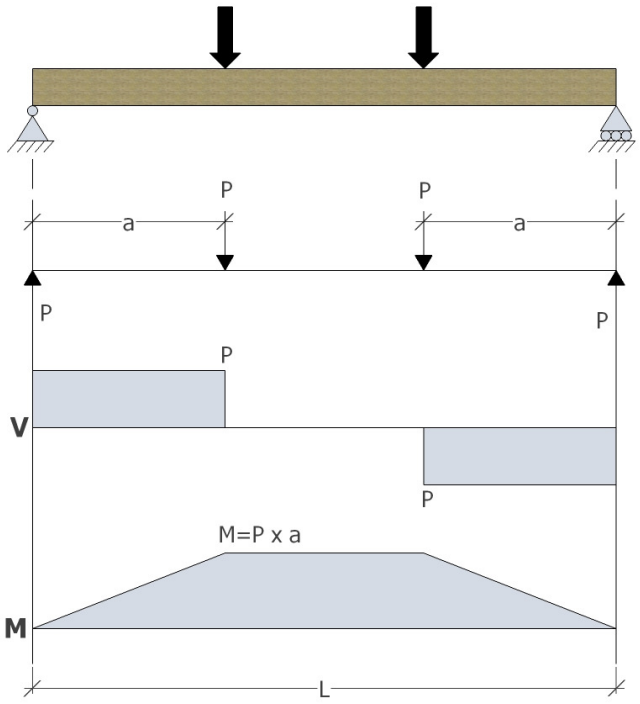

Figure 5.1 The four point bending test. From top to bottom: a sketch of the test; simplified model; shear force distribution; moment distribution.

The two upper loading cells slowly increases their applied force, thus creating two reaction forces, in opposite direction, in static roller supports. It is these four forces the name "four point bending test" is intended to reflect. For each load increment from the loading cells the deflections at chosen points were measured and recorded.

5.2 Adjustments to the model

The final applied pre-stressing force to the reinforcement in the two tested beams far exceeded the highest allowed force for equivalent beams calculated in the model. To compensate for this the definition of the pre-stressing force in the model was overridden and replaced by the fixed value given in Haghani (2010) for each of the beams, see Table 5.1.

Table 5.1 Material parameters for the tested and the calculated beams.

	Test beam 1	Test beam 2	Calculated beam 1 Figure 5.2	Calculated beam 2 Figure 5.3
Height	200 mm	200 mm	200 mm	200 mm
Width	115 mm	115 mm	115 mm	115 mm
Length	3600 mm	3600 mm	3600 mm	3600 mm
Pre-stressing force	50 kN	70 kN	50 kN	70 kN
FRP plate reinforcement	30x1.2 mm	30x2.4 mm	30x1.2 mm	30x2.4 mm

The calculated beams were given the same strength parameters as supplied to Jacob and Garzon (2007), since these beams were from the same set of glulam beams delivered to Chalmers. Jacob and Garzon (2007) had tested the beams and shown that the modulus of elasticity was lower than the values supplied, but since these specific beams had not been tested the originally supplied values were chosen.

Table 5.2 Strength parameters for the tested glulam beams, from Jacob and Garzon (2007). These values are most likely mean, not characteristic, values.

$f_{t,0,k}$	$f_{c,0,k}$	$f_{v,k}$	E	G_{mean}	ρ_k
44MPa	46MPa	7MPa	13.5GPa	760MPa	400kg/m^3

The reinforced and unreinforced reference beams in Figure 5.2 and Figure 5.3 are created from the reinforced model, the same as in Jacob and Garzon (2007), where if the reinforcement is set to zero an unreinforced beam can be calculated.

5.3 Results

The result from the model agreed well with the results from their tested counterpart, as can be seen in Figure 5.2 and Figure 5.3. There were however some tangible differences that are going to be addressed in this chapter.

The two beams that were tested by Haghani (2010) both ended up with a tension induced bending failure just as the beams that where calculated by the model did. But as can be seen in Table 5.3 as well as in Figure 5.2 and Figure 5.3, the calculated beams reached a higher maximum load then their tested counterparts.

The calculated beams have a higher load bearing capacity because the values in Table 5.2 are too high. If characteristic values would be used instead, the load bearing capacity would become lower. The load bearing capacity for the calculated beams would then be considered to be on the "safe side".

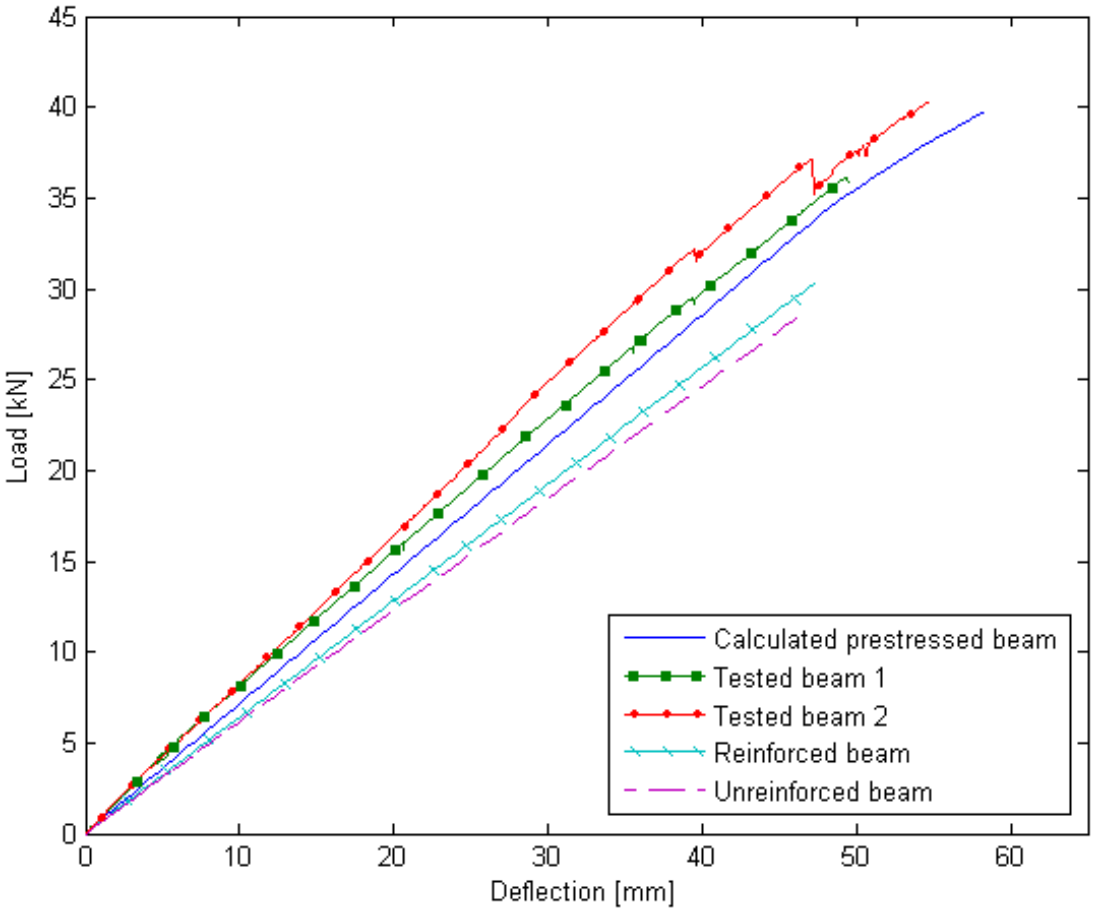

Figure 5.2 Tested beam together with calculated beam with identical settings as test beam 1. Test beam 2, reinforced and unreinforced beams are added for visualization.

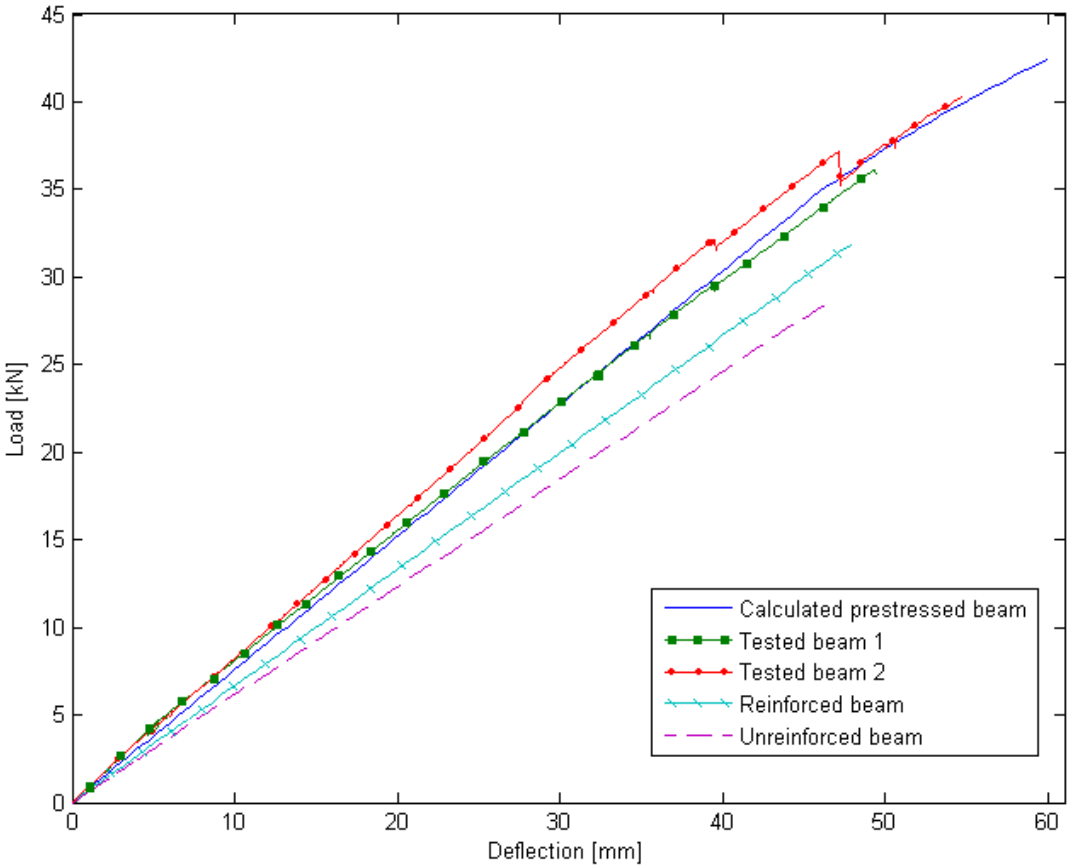

Figure 5.3 *Tested beam together with calculated beam with identical settings as test beam 2. Test beam 1, reinforced and unreinforced beams are added for visualization.*

The pre-stressed beams have not, though they may appear to in Figure 5.2 and Figure 5.3, gained stiffness due to the pre-stressing force. The deformations are lower due to the fact that the beams with an applied pre-stressing force gain a pre-camber.

Table 5.3 *The beams ultimate load and deflection when the beam experienced failure.*

	Test Beam 1	Test beam 2	Calculated beam 1 Figure 5.2	Calculated beam 2 Figure 5.3
Ultimate Load	35.77 kN	40.32 kN	39.79 kN	42.43 kN
Ultimate deflection	49.46 mm	54.75 mm	58.40 mm	60.03 mm

It is apparent that the model overestimates the deflection when compared to the test beams, as can be seen in Figure 5.2 and Figure 5.3. If the deflection would be derived from the definition for the curvature instead of the more approximated formula used, see (5.1), a more correct result would most likely be obtained. A different calculation

program than Matlab should then be chosen, since Matlab does not possess a built-in function to handle integrals.

$$\delta = \frac{P_{load}\frac{L}{3}\left(3L^2 - 4\left(\frac{L}{3}\right)^2\right)}{24EI} \qquad (5.1)$$

$$P_{load} = \frac{3M}{L}$$

The calculated beams have, as mentioned before, gained their strength parameters from the Table 5.2, which are mean values for these types of glulam beams. With just two beams to compare with, it does not statistically prove that these values are the correct ones for these beams. It is, because of this, not possible to conclude that the model can predict all pre-stressed beams' behaviour when loaded until failure. It does however provide a strong indication that the model created for this master thesis is able to quite accurately predict a real beam's behaviour strengthened with pre-stressed reinforcement.

6 HEIGHT REDUCTION WITH MAINTAINED FLEXURAL RESISTANCE (ULS)

One of the advantages of adding reinforcement to a beam is the ability to reduce the cross-section but maintain the flexural capacity in the ultimate limit state. Reducing the cross-section of the beam can give a lower cost for manufacturing that particular beam, thus becoming a more appealing choice. There would also be an economical cost reduction for the whole construction, since the entire wall can be shortened due to the lower height of the beams.

To produce a calculation that would give these values, the model was slightly rewritten. A new start program was created that originated from a chosen un-strengthened beam's height. The start program then calculated the reinforced beam and the pre-stressed beam with a chosen reduced height. The reinforcement in these beams was gradually increased until the same resisting moment was achieved in the strengthened beams as in the original un-strengthened beam. The beams where then given a further height reduction and the corresponding reinforcement amount was found to achieve an equivalent flexural capacity. This iteration continued until the strengthened beams could not reach the original un-strengthened beam's strength with less than 3% reinforcement. The 3% level was chosen since above this value is no economic gain to be made from strengthening due to the vast amount of reinforcement required.

The beams were given strength parameters according to Table 6.1 or Table 6.2 depending on what was examined. Table 6.1 contains the strength parameters for a standard beam. Table 6.2 shows the same parameters but for a glulam beam constructed out of lower quality timer.

Table 6.1 Characteristic value for the calculated GL40c beams.

$f_{m,k}$	$f_{t,0,k}$	$f_{c,0,k}$	$f_{v,k}$	$E_{0.05}$	G_{mean}	ρ_k
30,8MPa	17,6MPa	25,4MPa	2,7MPa	10.5GPa	760MPa	400kg/m^3

Table 6.2 Characteristic value for the calculated GL24h beams.

$f_{m,k}$	$f_{t,0,k}$	$f_{c,0,k}$	$f_{v,k}$	$E_{0.05}$	G_{mean}	ρ_k
24MPa	16.5MPa	24MPa	2.7MPa	9400GPa	720MPa	380kg/m^3

Figure 6.1 and Figure 6.2 are created from this program and are presenting calculations for a slightly enlarged verification sized beam and a large in practice used beam. The verification beam needed to be enlarged to a height of 500 mm since its original size had too few lamellae to create good results for the analysis. With an increased height the width and length were also enlarged so the beam proportions remained unchanged.

The reinforcement percentages shown in all these type of graphs are relative to its corresponding cross-sectional size. This means that one percent reinforcement for a

smaller size is a lesser amount of reinforcement than one percent for a greater cross-section.

6.1 Results

All the pre-stressed beams with a reduced height needed a lesser amount of reinforcement than a reinforced beam with the same reduction to gain the original un-strengthened beam's maximum flexural resistance in ultimate limit state.

When comparing these two beams curves it can be seen that the smaller and shorter beam from Figure 6.1 has an increasing difference between what the reinforced and pre-stressed beams need for reinforcement. When comparing this to the more constant difference in Figure 6.2 there are some conclusions to be drawn. For the larger beam, due to its length, it has a low and fairly constant maximum pre-stressing force capability for all the tested heights.

When the pre-stressing force remains constant the difference between the reinforced and the pre-stressed beam also seems to remain constant. This is due to that most other parameters are kept the same, such as location and geometry of the reinforcement. The smaller beam gets, with increased amount of reinforcement, a possibility to increase its pre-stressing force without having to sacrifice significant amounts of its tensile strength. This would explain the increased difference in reinforcement needed as the general reinforcement amount in the beams increases.

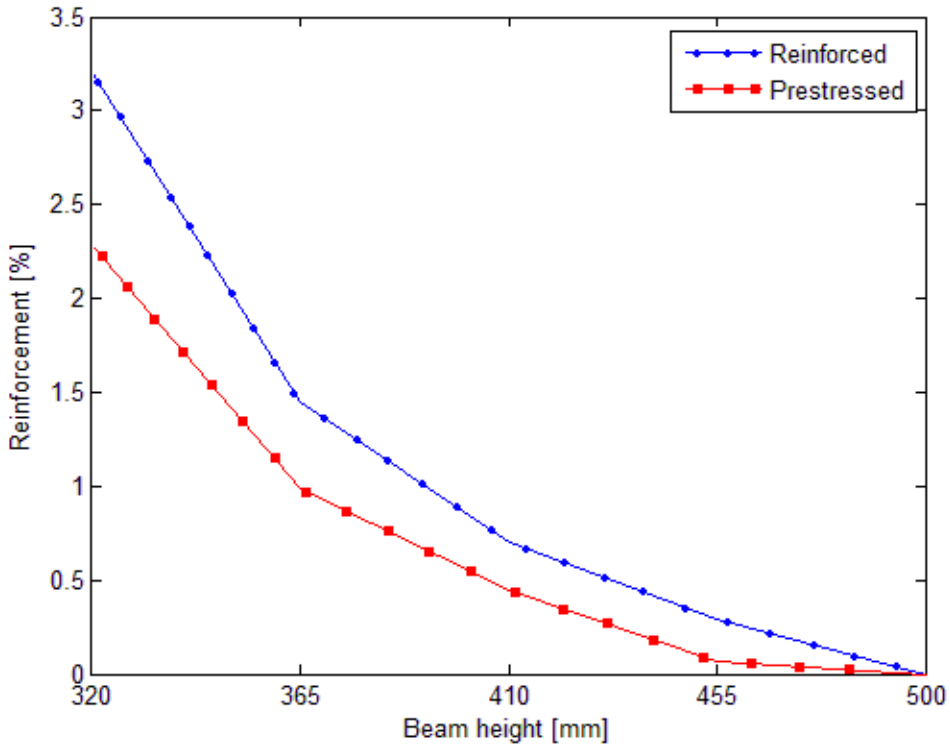

Figure 6.1 *Reinforcement needed to obtain the same resisting moment in ULS with reducing beam height. The original beam had the starting height of 500 [mm] and a length of 5 meters.*

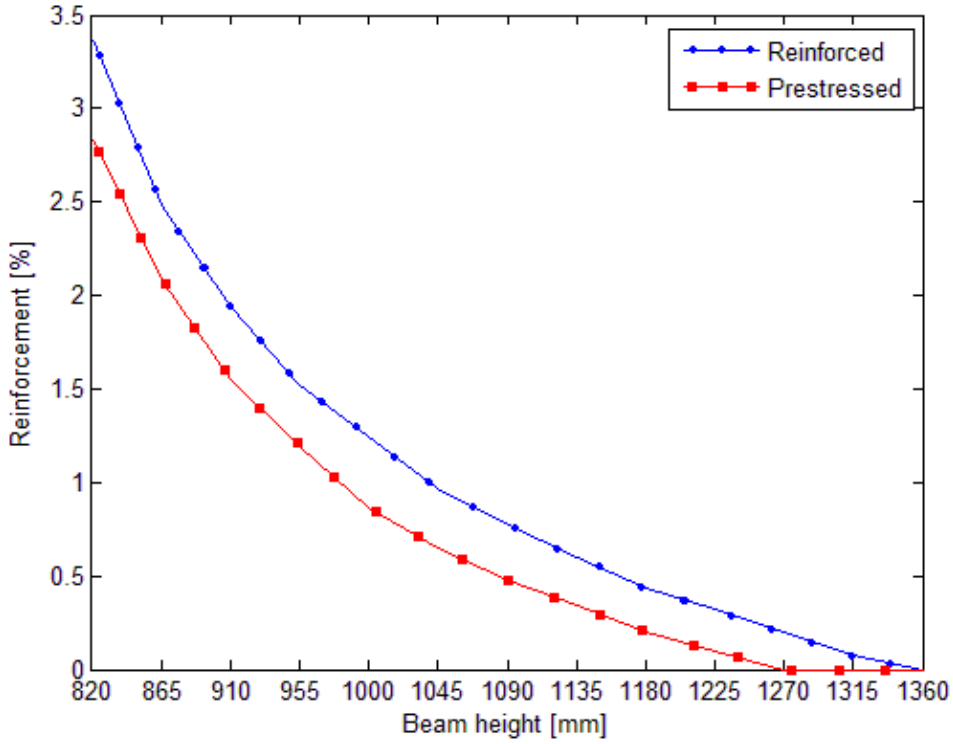

Figure 6.2 *Reinforcement needed to obtain the same maximum resisting moment in ULS with reducing beam height. The original beam had a starting height of 1360 [mm] and a length of 18 meters.*

Another notable effect can be seen in the very first height reduction steps in these figures. The reinforced beam needs a certain amount of reinforcement when the first glulam lamella is removed. The pre-stressed beam however needs almost no reinforcement at all to compensate for the removal of the first lamellae. The maximum allowed pre-stressing force comes from the beams lateral torsional demands, which is a fixed value that is completely unrelated, at least for the amount of reinforcement present in these beams. When a very small amount of reinforcement is added to the beam, this reinforcement will be tensioned to a very high stress level. Although it loses its ability to add tension strength to the beam its contributing pre-stressing effect is enough to allow the beam to reach the same maximum resisting bending moment as the original unreinforced beam.

The pre-stressed beam is, in these calculations, a duplicate of the reinforced beam. A further increased reduction in the need for reinforcement would be achieved by an optimisation of the reinforcement geometry and location within the beam for the pre-stressed beam. This, due to the effects from the pre-stressing force, is dependent on a number of geometry parameters, such as for example the lever arm e. If optimised for each beam configuration, it would create an even bigger gap between the two curves. Hence a more positive result for the pre-stressed beam would be obtained.

6.2 Increased pre-stressing force

The pre-stressing force applied by Haghani (2010) exceeds the maximum allowed pre-stressing force generated by the model. It is possible that the requirement that was set on the pre-stressing force in the model is too strict. For this reason the effects of an increased pre-stressing force above the pre-allowed limit was examined.

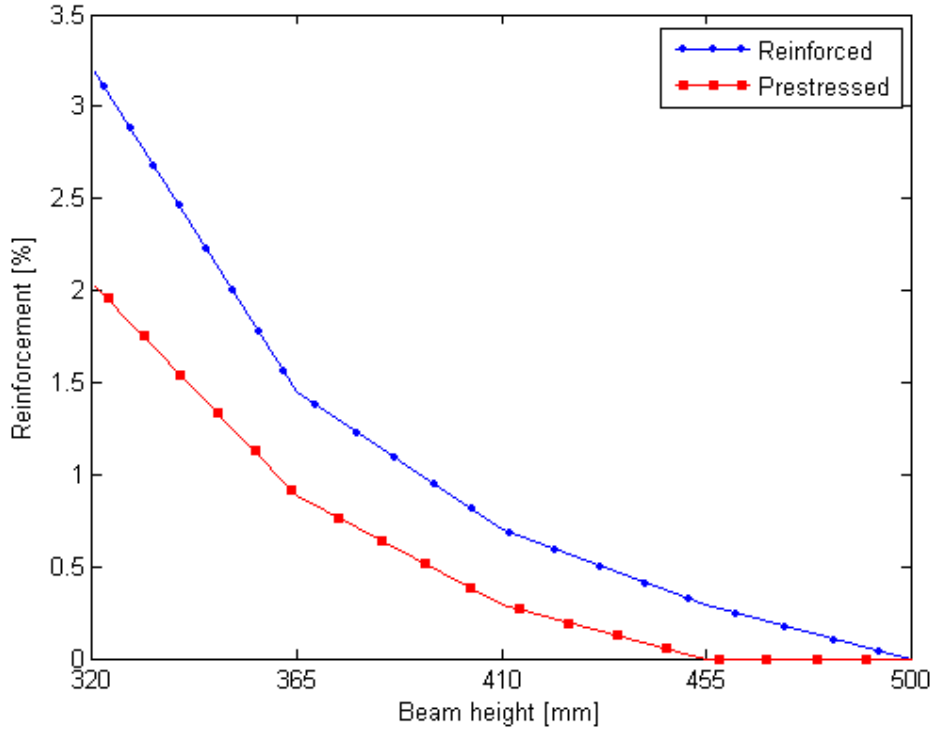

Figure 6.3 *Reinforcement needed to obtain the same maximum resisting moment in ULS with reducing beam height. The original beam had the starting height of 500 [mm] and a length of 5 meters. 1.5 times the pre-stressing force is applied.*

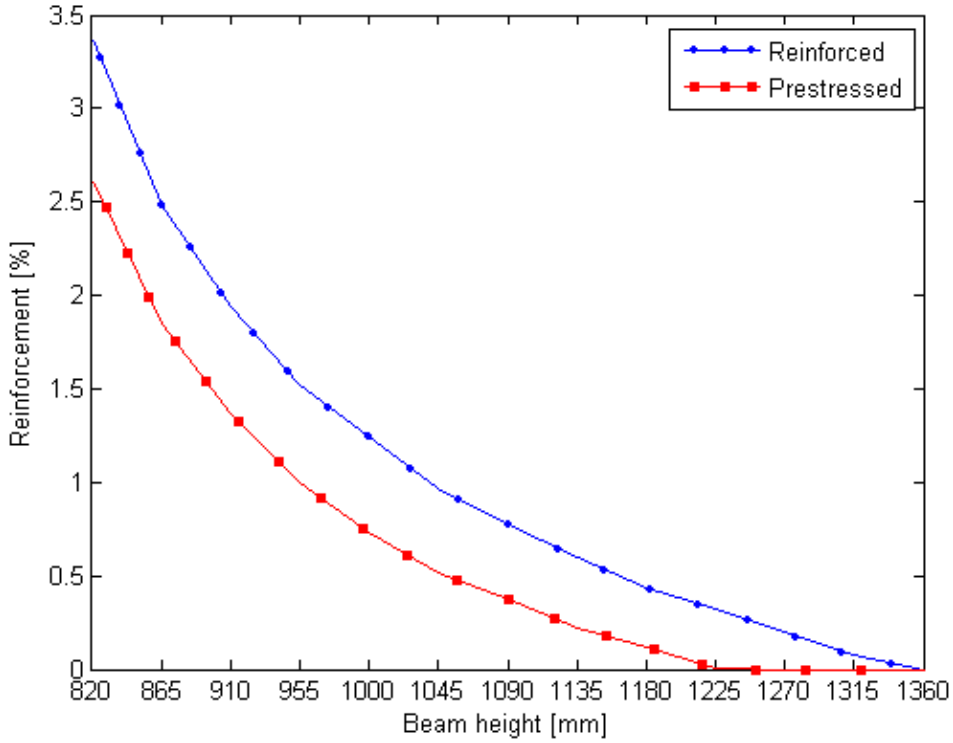

Figure 6.4 *Reinforcement needed to obtain the same maximum resisting moment in ULS with reducing beam height. The original beam had the starting height of 1360 [mm] and a length of 18 meters. 1.5 times the pre-stressing force is applied.*

If the pre-stressing force was allowed to be 1.5 times larger, the difference between the reinforced and the pre-stressed beam increases with an almost identical amount, see Table 6.3. The precision of the calculated values are limited to entire lamellae' being removed which is 45 mm at a time. A reference point at one per cent of reinforcement amount was set to create Table 6.3. The heights were then interpolated between the height results closest to one per cent, thus being less accurate. An increase in the difference of height between the reinforced and pre-stressed beam are shown in Table 6.3. The difference is clearly visible if the numbers of removed lamellae with zero per cent needed reinforcement is compared between Figure 6.4 and Figure 6.2.

Table 6.3 The difference in height reductions with 1,5 times the pre-stressing force and amount of reinforcement corresponding to 1 percent of the beam's cross-section.

	1360x215 1,0*P	1360x215 1,5*P	500x200 1,0*P	500x200 1,5*P
Reinforced	1040mm	1040mm	392mm	392mm
Pre-stressed	982mm	955mm	365mm	360mm

6.3 Reduced glulam quality

With the reduced strength parameters, seen in Table 6.2, the glulam has been given the strength properties equivalent to a glulam beam produced of lower quality timber.

Using lower quality timber in the glulam beam cuts productions cost, thus becoming a competitive choice if the difference in maximum flexural resistance in ultimate limit state is low compared to a stronger beam made from graded timber.

The difference between the higher and lower quality beam are relative small in comparison to the difference between the pre-stressed and reinforced beam, as can be seen in Figure 6.5 and Figure 6.6

The difference for the two main factors governing for failure of the beam, the tensile limit for the glulam and the difference between the compressive and the tensile limits are quite low. This contributes to the low difference between the beams. The compressive limit in itself plays only a subordinate role since the plasticisation possibility of the compressive side makes it almost impossible to reach a compressive failure, unless the beam is extremely over-reinforced on the tensile side. This low difference can be viewed in Table 6.1 and Table 6.2.

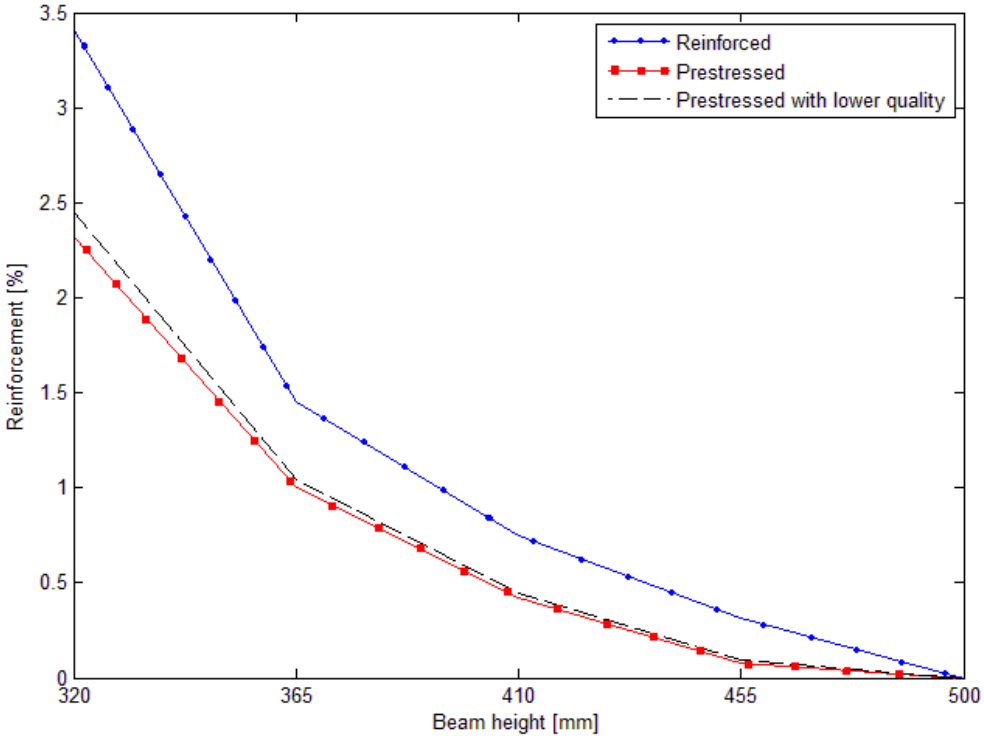

Figure 6.5 *Reinforcement needed to obtain the same maximum resisting moment in ULS with reducing beam height, with an added comparison of different glulam qualities. The original beam had a starting height of 500 [mm] and a length of 5 meters.*

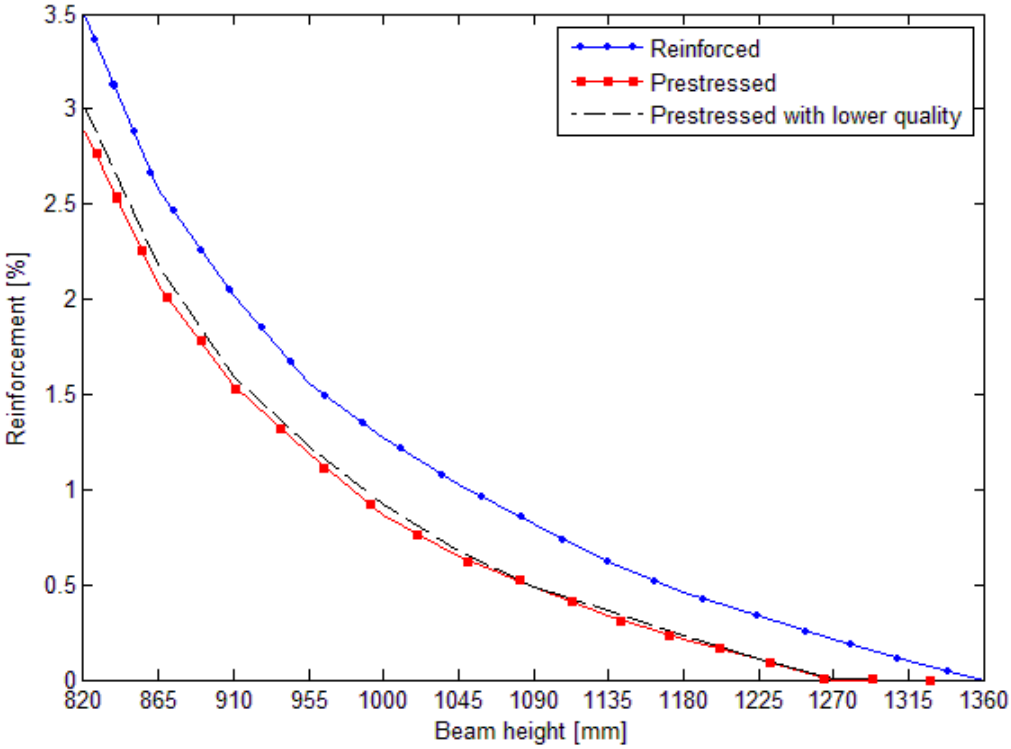

Figure 6.6 *Reinforcement needed to obtain the same maximum resisting moment in ULS with reducing beam height, with an added comparison of different glulam qualities. The original beam had a starting height of 1360 [mm] and a length of 18 meters.*

With the most common failure mode for these beams being bending induced tension failure, the glulam fails at almost identical loading. The glulam with the lower quality gains a larger compressive strain due to the pre-stressing force. This increase in compressive strain reduces the difference in the different glulam's tensile yield limit. This causes the beams to gain similar maximum flexural resistance in the ultimate limit state.

With lower quality timber in the pre-stressed beam a small amount of flexural resistance is sacrificed. This makes it a less attractive choice as seen from its structural behaviour. With the lower production cost of lower quality glulam, this beam might still prove be an economically viable choice, if a deeper investigation is conducted.

7 ECONOMICAL COMPARISON

When glulam is strengthened many of the member's properties becomes enhanced. Raised stiffness properties of the beam, higher maximum capacity and a more predictable failure mode are some of them. But for the method to have a real impact in the building sector it must also be economically viable and profitable. For this to be achieved, the savings in timber and construction materials must be bigger than the additional costs for reinforcement.

For this economical comparison the height reduction method, used in Chapter 6, is utilized to obtain the material savings for different chosen scenarios. From this model the difference in cross-section is also gathered and compared. With the different cross-sections analysed, the costs for the pre-stressed beams are added together and compared with the cost for an un-strengthened beam, thus giving the economical difference for the different beams with the same flexural resistance.

To be able to perform this analysis, costs and savings values for the different parameters is needed. Erik Gulbrandsen (2011) at Tenroc Technologies has supplied these values, see Table 7.1. With the given values, the comparison could only be made with steel as the strengthening material and only pre-stressed and not regular reinforced beams could be compared to an un-strengthened beam. The price of glulam varies with supply and demand and therefore no fixed cost can be assumed. In this comparison the minimum and the maximum values for GL40c, as this quality was used for the two tested beams, will be considered.

There are two scenarios that have to be considered when doing this comparison. The first is to compare the costs for one un-strengthened glulam beam with the cost of one pre-stressed beam, where the two beams have the same maximum flexural resistance in the ultimate limit state. There is also an interest in finding out which economic effects pre-stressed beams would have on a building. A simple structure with four roof beams and a length of 30 m has, for this case, been analysed. The savings that can be made for this building, except for the reduction in cost per beam, is the reduction in wall material, since the total height of the building is reduced due to the smaller cross-section of the pre-stressed beam. In the building or project comparison transportation, is also being considered as an economic factor.

All comparisons have been made for five fixed beam heights; 1620, 1350, 1260, 990 and 720 mm. This generates many results and for visual reasons, some will not be shown in the report. The full diagrams can be found in Appendix D and the calculation sheets for these diagrams in Appendix C. All beams have been calculated with 0.5, 1.0, 1.5, 2.0, 2.5 and 3.0 per cent of reinforcement. For some beams the results ends before the reinforcement reaches 3.0 per cent. In these beams the higher amounts of reinforcement could not be utilized fully due to shear failure.

It should also be noted that savings are negative values, which means that a negative value is a positive result for the pre-stressed beam. The y-axes were inverted in the diagrams to make it easier to visualize the positive or negative effect of pre-stressing.

Table 7.1 Cost values, supplied by Erik Gulbrandsen (2011) at Tenroc Technologies

Cost category	**Description**	**Value**
Glulam	Material cost	3000-5000 SEK/m^3
Steel	Material cost	9 SEK/kg
Adhesive	Material cost	34 SEK/kg
Production, unreinforced	Is included in the material cost for glulam.	0 SEK/m^3
Production, pre-stressed	Salaries, machines	185 SEK/m^3
Factory	Loans and other costs tied to the property	105 SEK/m^3
Operation and maintenance	Electricity etc. to machines and service	34 SEK/m^3
Wall material	Savings caused by reduced wall area	750 SEK/m^2
Transport	Considers a truck with capacity to carry 28 tons between Gothenburg and Stockholm.	12000 SEK

7.1 Comparison of various beam lengths

This analysis purpose is to examine whether the pre-stressing method is suited for long or short beams. Un-strengthened glulam beams have practically no fixed maximum length since they can be finger jointed during construction. Pre-stressed beams manufactured in factories do have practical restraints concerning their length, since they have to be transported as one unit and cannot be finger-jointed after the reinforcement has been put in place. Therefore the longest beam analysed is 25 metres. All beams compared have a width of 215 mm.

7.1.1 Single beam comparison

The price of glulam influences the results drastically, as seen in Figure 7.1 and Figure 7.2. When glulam is at its most expensive, the pre-stressed beams are profitable when using 0.5-1.5 per cent reinforcement. At higher reinforcement amounts the cost for reinforcement outweighs the gain in glulam reduction. Even though all lengths show profitable results, when glulam is the most expensive and are within the recommended reinforcement span, it is the longer and higher beams that produces the best results. When the price of glulam is low all beams show poor results.

The comparison shows that when considering the cost per beam, longer beams are more profitable. With the requirement that glulam must be at its most expensive level and that the reinforcement amount does not exceed approximately 1.5 per cent. The best reinforcement configuration is at 1.0 per cent.

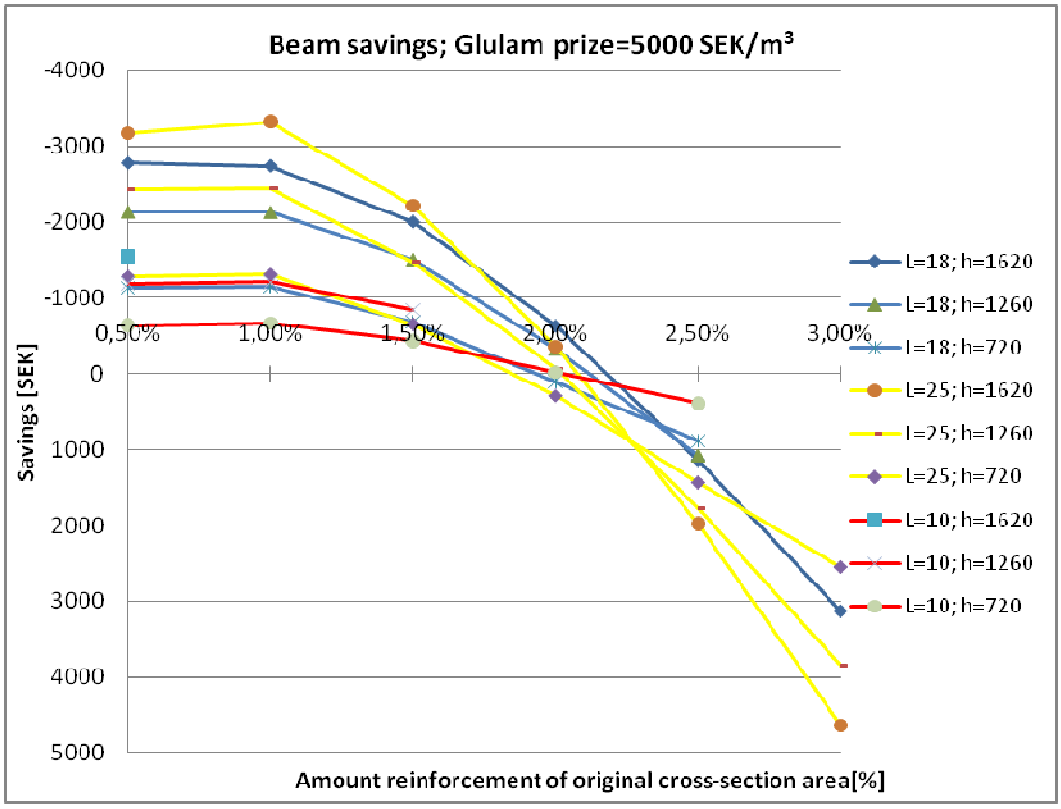

Figure 7.1 Beam length comparison; width = 215mm, L=length [m], h=height [mm]

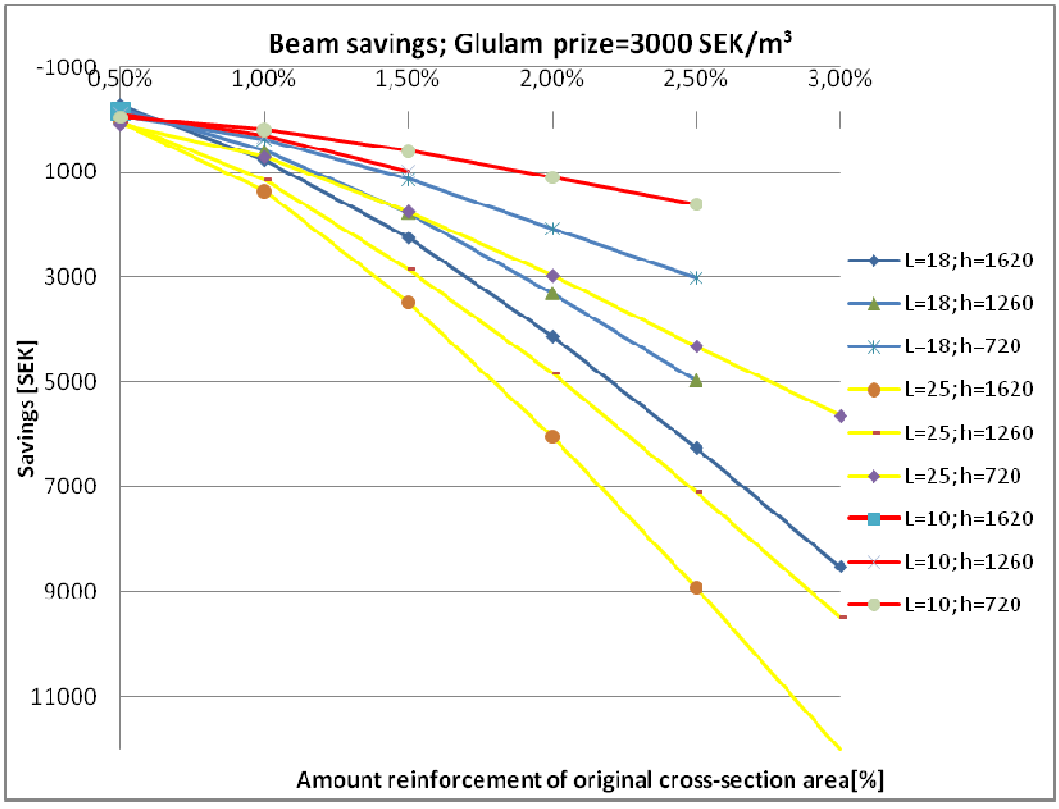

Figure 7.2 Beam length comparison; width = 215mm, L=length [m], h=height [mm]

7.1.2 Project comparison

Compared to the cost per beam analysis the project savings show very promising results, which can be seen in Figure 7.3 and Figure 7.4. Even though the glulam price has a large influence, all beams show profitable results, except for one when the beam is highly reinforced. As for the single beam analysis the longer and higher beams show best results when the glulam price is higher and the best reinforcement configuration is at 1.5 per cent.

When the glulam price is set to the lowest price the best reinforcement configuration for the longer beams are at 1.0 per cent. After this amount the 25 metre long beam becomes less profitable then the 18 metre, which depends on the fact that the beams' cost compared to project saving is higher for the longer beams

The project analysis showed good results regardless of which price the glulam has. It is the longer and higher beams that show the highest profit but the results from the shorter and lower beams are positive as well. The results are optimized when the reinforcement amount is 1.0-1.5 per cent of the original cross-section area.

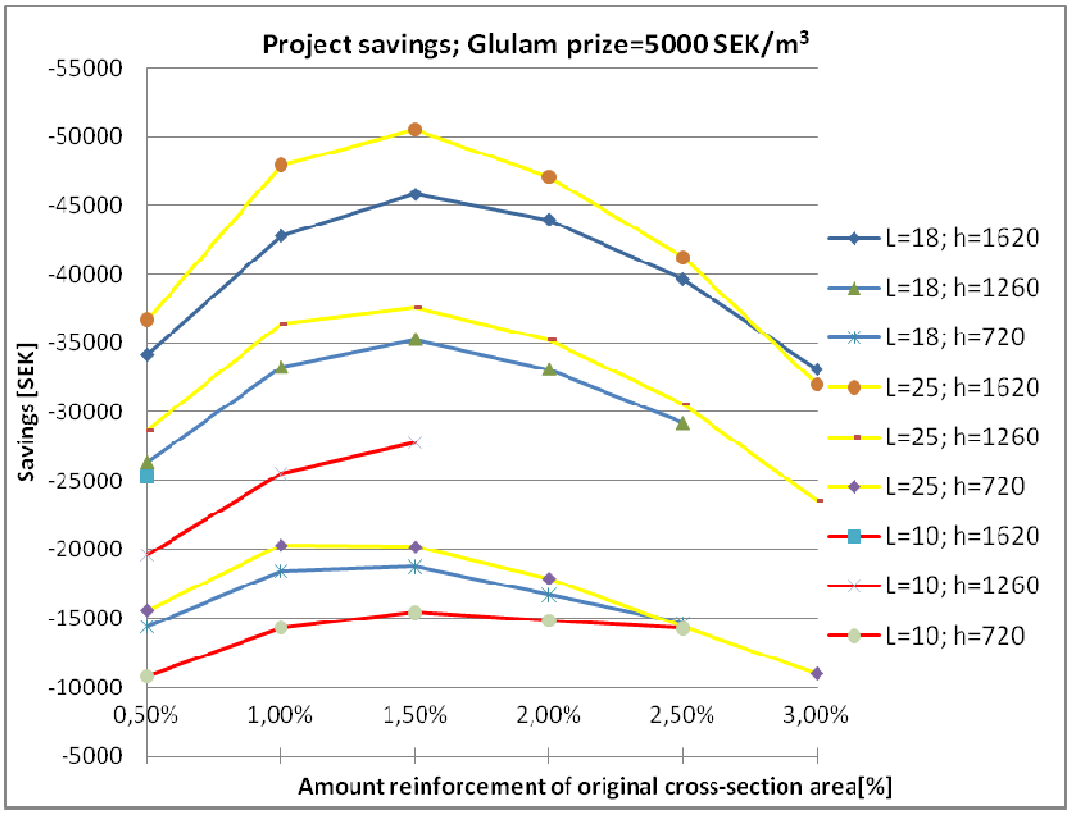

Figure 7.3 Beam length comparison; width = 215mm, L=length [m], h=height [mm]

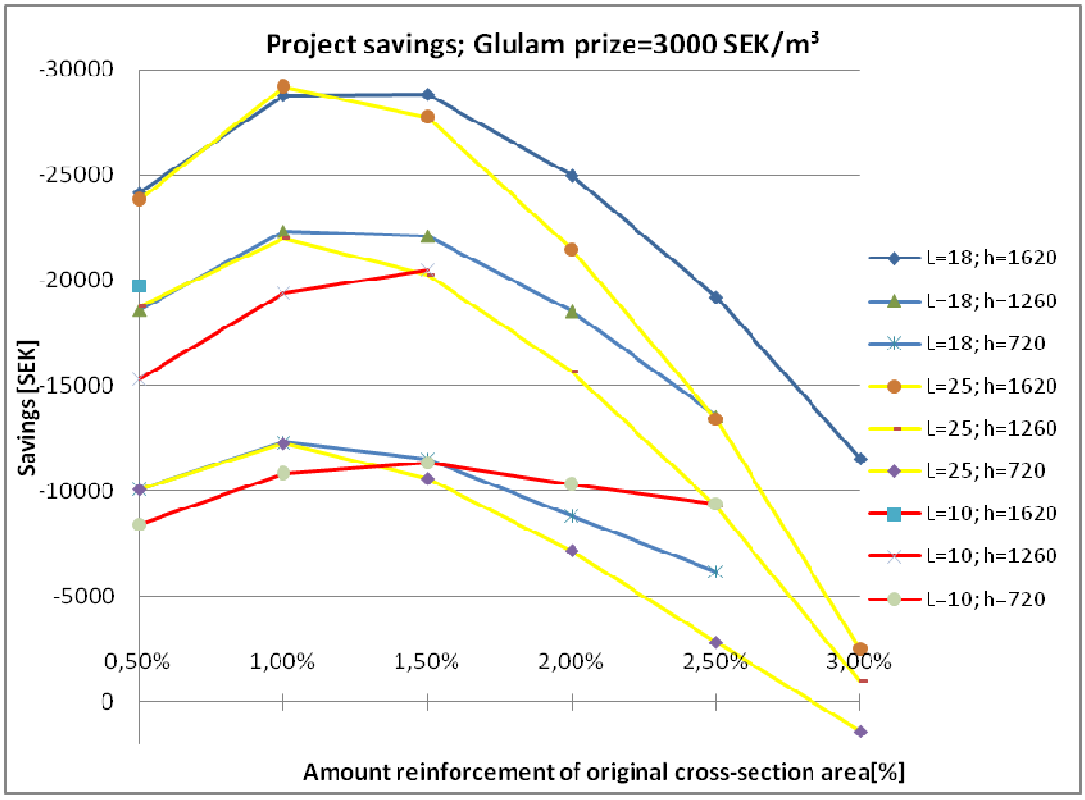

Figure 7.4 Beam length comparison; width = 215mm, L=length [m], h=height [mm]

7.2 Comparison of various beam widths

This comparison is made to find out whether the pre-stressing method is more suitable for wider or narrower beams. The lengths of the beams are 18 metres. It has to be noted that this analysis still uses the height reduction method, but with different widths.

7.2.1 Single beam comparison

The results for this comparison are highly affected by the price of glulam. This analysis also shows that the largest beams are the most profitable, when the glulam price is high and when there is between 0.5 and 1.5 percent reinforcement, which is shown in Figure 7.5. As before, when the glulam has its lowest price the larger beams are the most expensive and no beam is profitable, as can be seen in Figure 7.6.

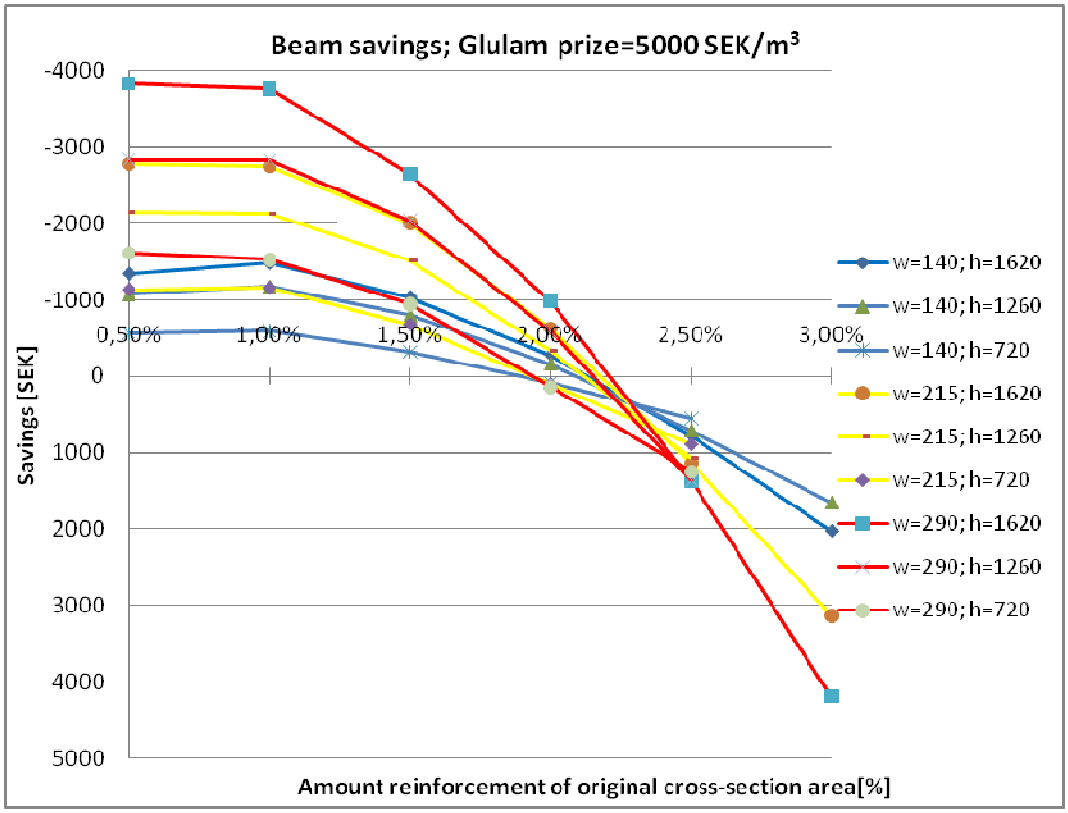

Figure 7.5 Beam width comparison; length = 18m, w=width [mm], h=height [mm]

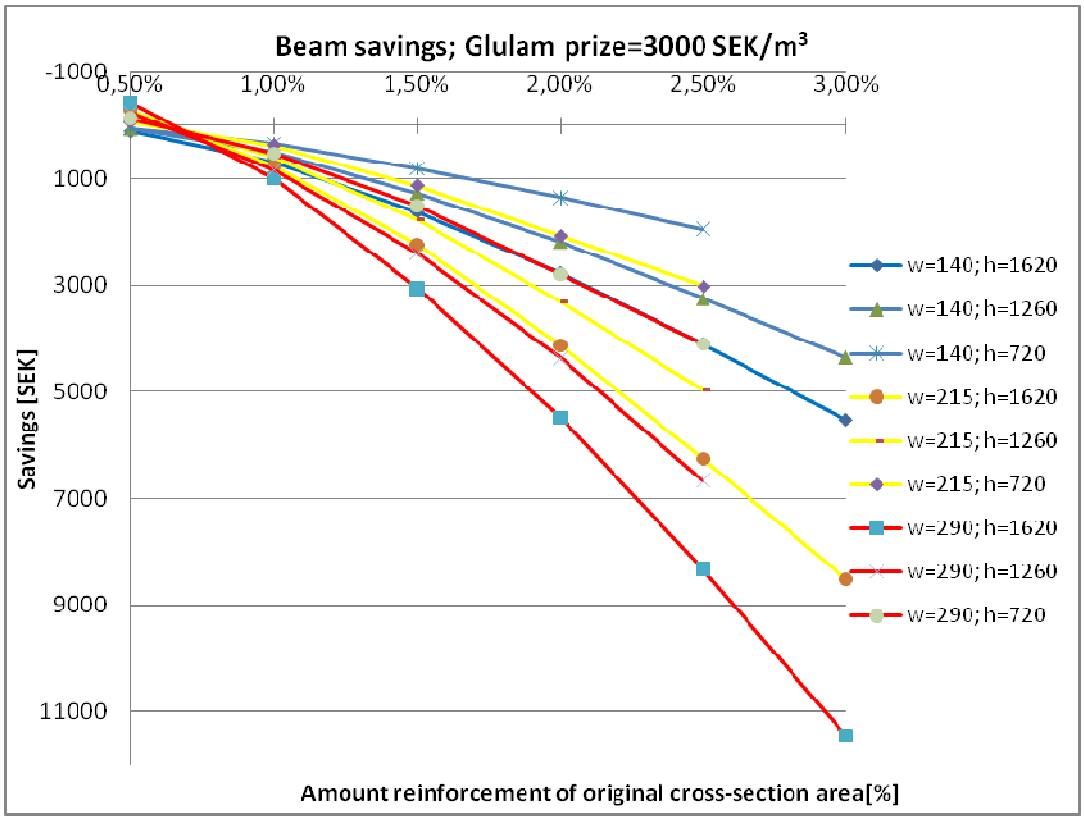

Figure 7.6 Beam width comparison; length = 18m, w=width [mm], h=height [mm]

7.2.2 Project comparison

The project savings comparison show similar results as for the beam length comparison. The best reinforcement configuration, when glulam is at its most expensive level, as seen in Figure 7.7, is at 1.5 percent for the wider beams. For the narrower beam the best configuration is at 2.0 per cent. Once again the larger beams show the best result, when glulam is at its most expensive level. If the larger and the smaller beams reduce their cross-section with the same percentage the savings will be greater for the larger beams than for the smaller ones. The fact that all beams show positive results is of most importance for the competitiveness for the pre-stressed beam, since this gives the pre-stressed beams a large section of market to be competitive in.

When the glulam is at its lowest price the profits at 1.0 percent reinforcement are similar. At higher amounts of reinforcement the narrowest beam is the most profitable, shown in Figure 7.8, but also that the higher the beam is, the better the results become.

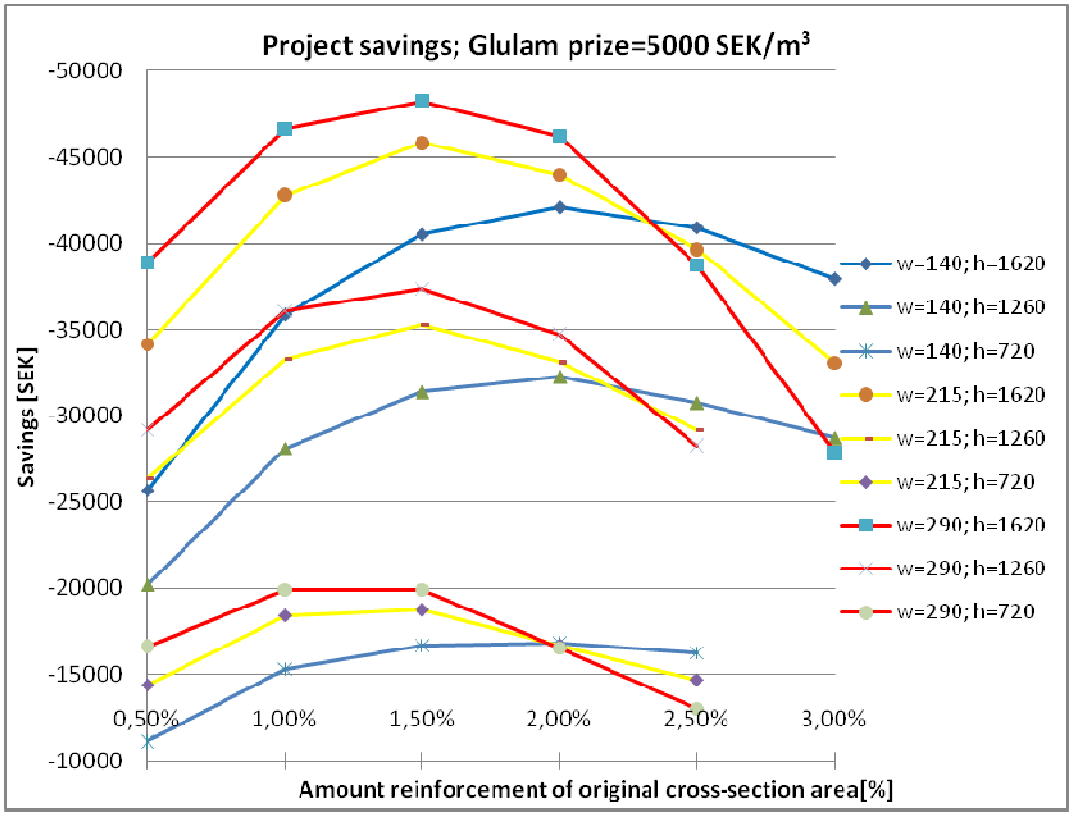

Figure 7.7 Beam width comparison; length = 18m, w=width [mm], h=height [mm]

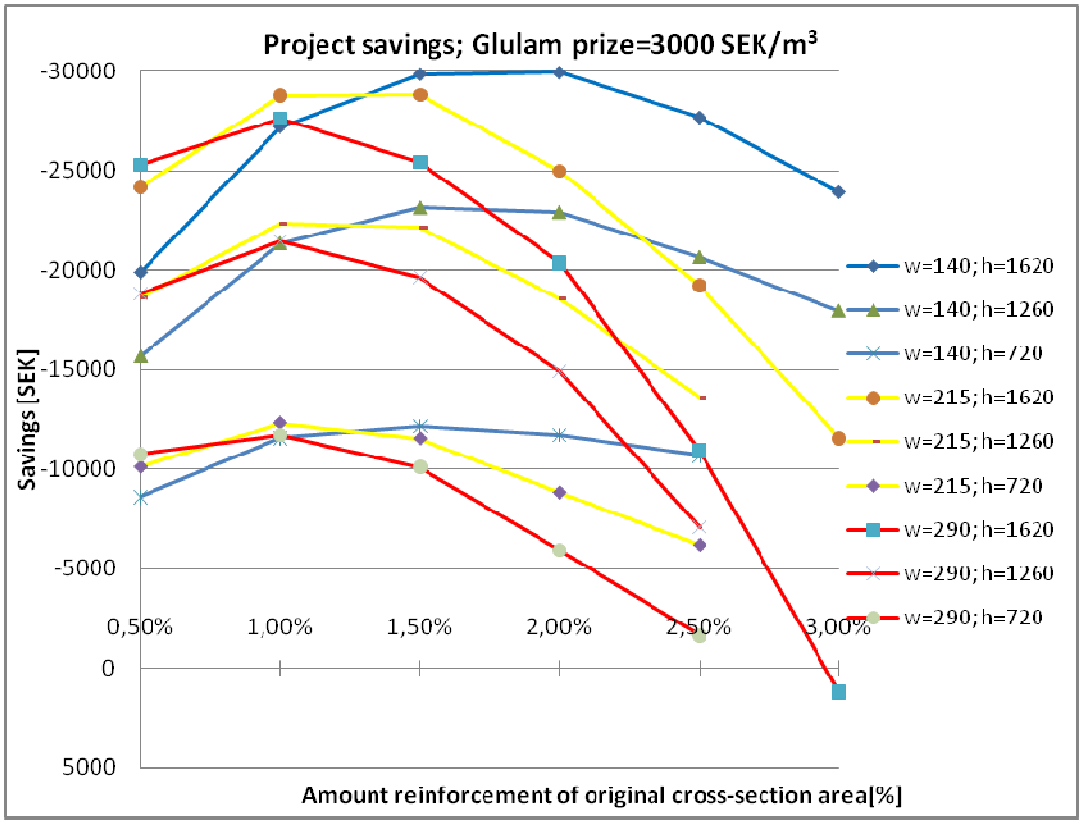

Figure 7.8 Beam width comparison; length = 18m, w=width [mm], h=height [mm]

7.3 Comparison with various grades on the pre-stressing force

The method established in this thesis allows for quite small amount of pre-stressing force, compared to the force applied to the beams that were used to verify the model. The verification beams had approximately 200% of the pre-stressing force applied in the model, without any buckling problems. The in practice used pre-stressing force can therefore be higher. How much higher and what economic consequences it results in is examined in this sub-chapter.

In this part the analysis was made with 100%, 200% and 300% of the calculated pre-stressing force the model showed as the maximum pre-stressing force.

7.4 Single beam comparison

The results from the cost per beam analysis are shown in Figure 7.9 and Figure 7.10. The results show an expected behaviour pattern. The higher the pre-stressing force becomes the greater the profits become. Compared to earlier results the reinforcement configuration that generates best results, for the beams with increased force, is at 0.5 per cent. The important part in this comparison is that when the glulam price is low the results are positive, unlike the seen results in the previous analysis.

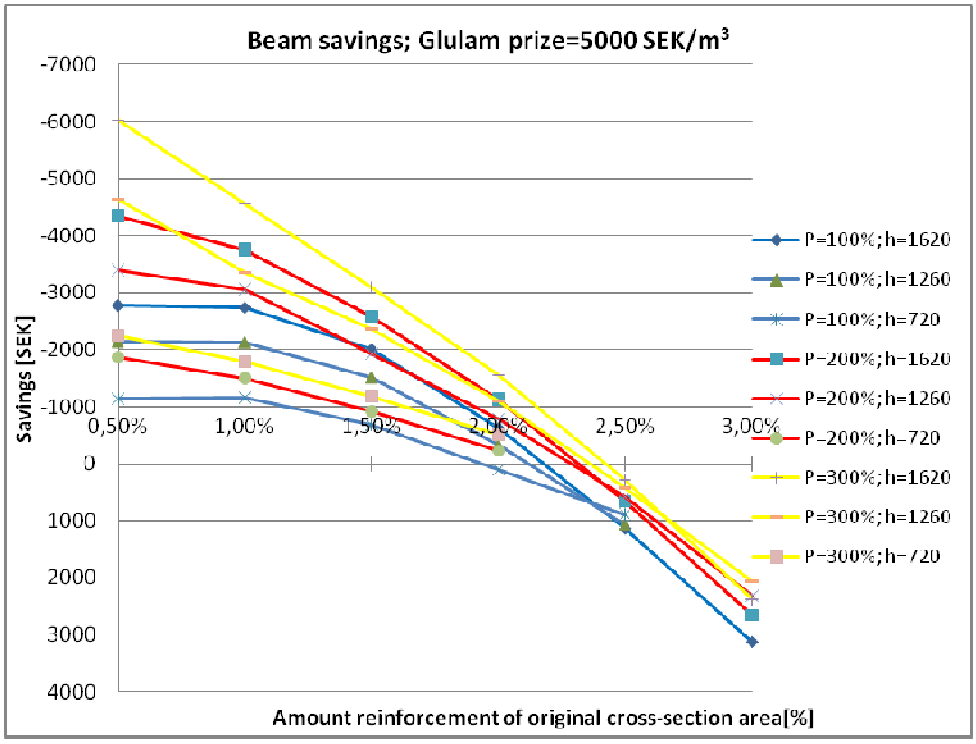

Figure 7.9 Various pre-stressing force; length=18 m, width=215 mm, P= amount of calculated acceptable pre-stressing force, h=height [mm]

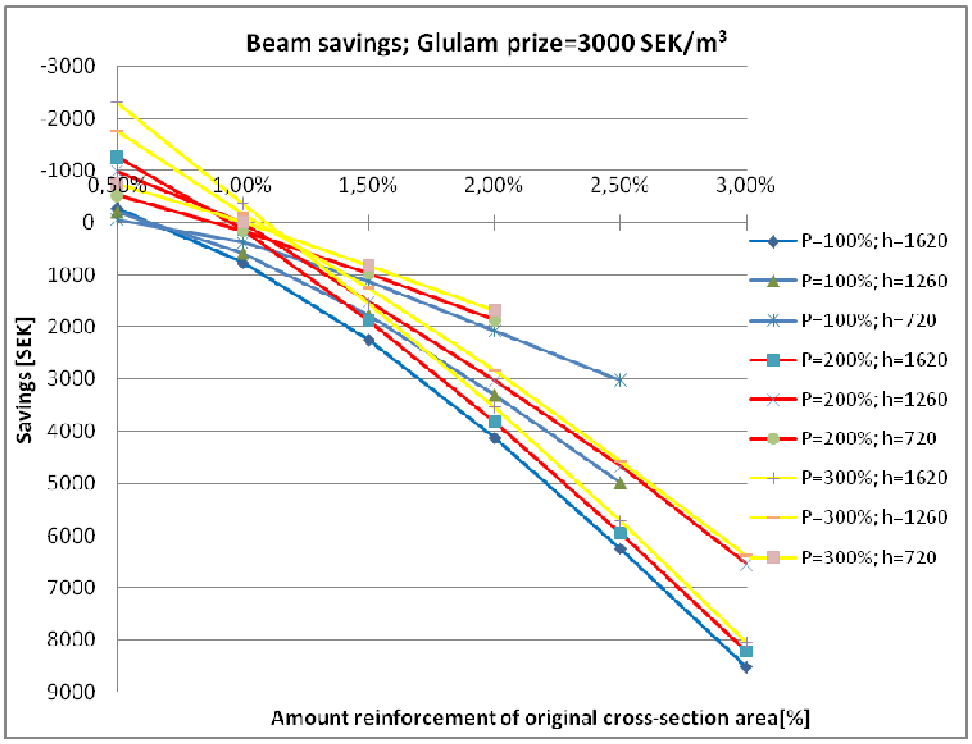

Figure 7.10 Various pre-stressing force; length=18 m, width=215 mm, P= amount of calculated acceptable pre-stressing force, h=height [mm]

7.5 Project comparison

In Figure 7.11 and Figure 7.12 the project savings are displayed. All beams show good results. The thing to be noted is the reinforcement configuration. For the best

result the configuration varies between the different levels of force applied. When the force is 300% of the calculated value the best reinforcement configuration is at 0.5%, for 200% it is at 1.0 % and for 100% it is at 1.5 %.

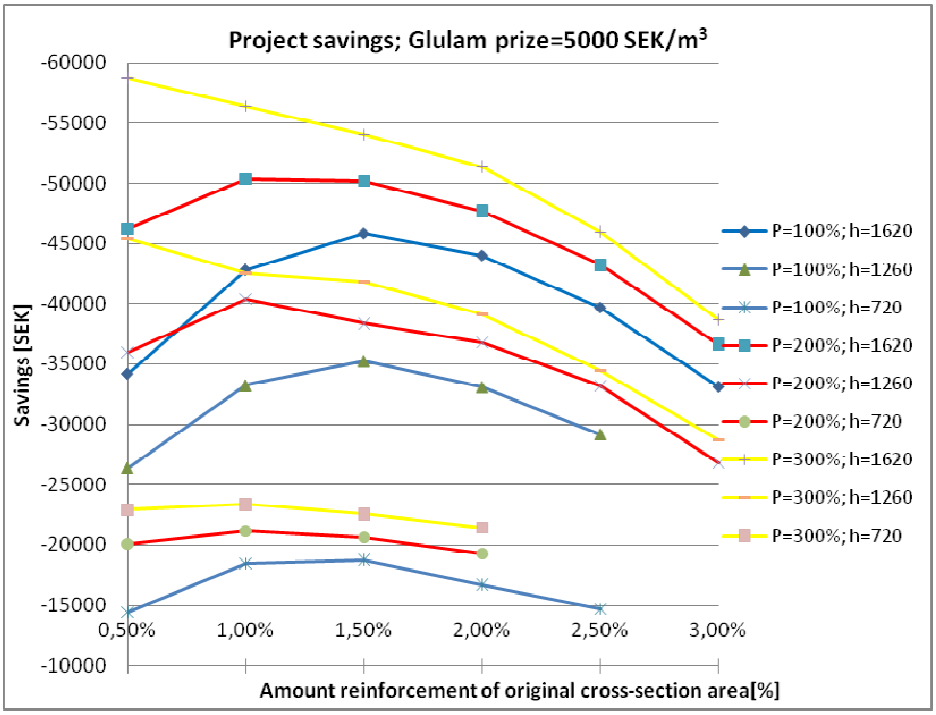

Figure 7.11 Various pre-stressing force; length=18 m, width=215 mm, P= amount of calculated acceptable pre-stressing force, h=height [mm]

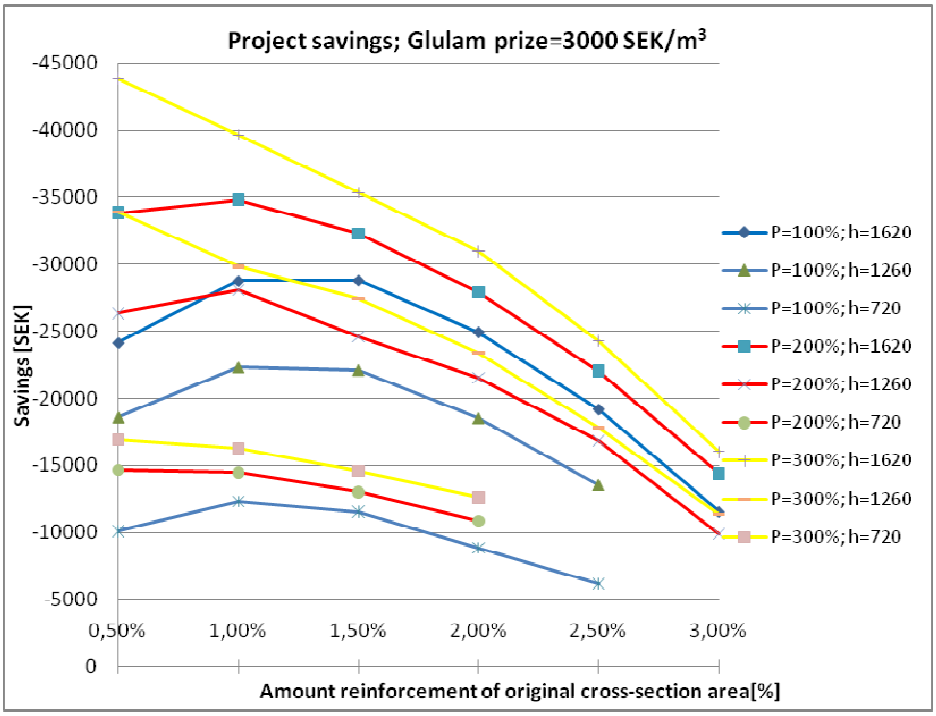

Figure 7.12 Various pre-stressing force; length=18 m, width=215 mm, P= amount of calculated acceptable pre-stressing force, h=height [mm]

8 CONCLUSION AND RECOMMENDATION FOR FURTHER RESEARCH

8.1 Conclusion

The created model for pre-stressed glulam beams gain in the end a large span of functions and can handle many different types of settings for the glulam beams. It can calculate unreinforced, reinforced and pre-stressed beams given the beam's geometry and reinforcement amount and placement. The model can also handle both the elastic and plastic phases which the glulam can experience, as well as detect and counter for yielding in the reinforcement. This gave a very flexible base model to conduct the different analyses that were chosen to be done.

The base model was verified through the results of two empirically-tested pre-stressed glulam beams. When the results from the tested beams were compared to the results from the model, with identical input parameters, the results were very much alike. The model was seen as verified for this thesis although only two beams are not enough to statistically prove the verification, but do however produce a satisfactory indication. The model gave however a higher maximum deflection than both of the tested beams.

From the model it has been shown that pre-stressed reinforcement increases the flexural resistance for the strengthened beam. The exact amount of increased maximum flexural resistance in ultimate limit state varies depending on the beams geometry and the amount of pre-stressing force allowed to be applied to the beam. As can be seen in Chapter 6, the amount of pre-stressing force greatly influences the amount of gained flexural resistance.

To more easily show the improved behaviour from the pre-stressing force and at the same time to provide a numerical basis for the economic analyses, the height reduction addition to the model was created. The height reduction calculation show that compared with an unreinforced beam, a pre-stressed beam of lower height required a lesser amount of reinforcement then a reinforced beam needed for the same height. This model also showed that the difference in maximal flexural resistance between pre-stressed beams with different quality glulam is very low.

In the economic analysis a comparison of costs and savings was made between a regular glulam beam and a pre-stressed glulam beam. With the given input parameters the pre-stressed beams showed good profitability. The pre-stressed beams generally showed their strongest competitiveness when the glulam was expensive, they had long spans and large cross-sections. The results showed that no more than 1.5 percent of reinforcement should be used, when considering the economical aspect.

The economic analysis considered two cases, one with cost per beam and one case were the beams were integrated in a project or building. Generally the pre-stressed beams showed negative results when only considering the cost per beam of the same quality and when the glulam was least expensive. However when introducing a higher pre-stressing force, than the limitation according to EC5 sets, the pre-stressed beams were economical competitive to regular glulam beams. The analysis showed that, for almost all beams analysed, pre-stressed beams were more economical than unreinforced beams when integrated into a building project. It might however be hard to influence the producers and the users if the cost per beam is not more competitive then we were hoping for.

8.2 Recommendation for further research

Adding the reinforcement on the compressive side of the beam, should have an additional positive effect for the beam. The distribution recommended by Jacob and Garzon (2007) assigns too much of the reinforcement to the compressive side. A similar study to that made by Jacob and Garzon (2007) but for pre-stressed glulam beams would perhaps give a better indication, though the number will most likely not be fixed as was the case for the reinforced beam.

In the pre-stressed beams, the reinforcement was placed in the same position as the reinforced beams. This however might not be the most beneficial position due to the lever arm *e*. Studies to find a better location for the reinforcement might also improve the beam's performance.

As discussed in Chapter 5.3, a more advanced calculation method for the deflection would most likely improve the deflection results from the model.

In the model the limitations for the magnitude of the pre-stressing force are probably too rigid, at least compared to other work done in this field. A further analysis of the beam´s behaviour, when pre-stressed, might give a possibility to reduce these limitations and thereby increase the maximum allowable pre-stressing force.

Taking creep and relaxation into account would give the model a possibility to calculate long term loads and deflections, which it cannot now do.

In the economic analysis different widths of the beams were compared. However theses were made using our height-reduction model. The cost per beam might be more competitive if an analysis was made with a determined height and a reduction of the width instead. An analysis of different glulam classes is also of interest. The performance analysis showed that the pre-stressing effect varied little with different glulam properties. Therefore a low-grade glulam with a small material cost would be highly competitive.

The cost of GL24h and the difference in price to GL40c should be examined. Since it was shown that the difference in maximum flexural resistance in ULS was very low when the beams were pre-stressed, there might be further savings to be made by using lower quality timber.

If the price for GL40c becomes very high, it might also be cost efficient to instead strengthen a lower quality beam with pre-stressed reinforcement to take the GL40c's place.

9 REFERENCE

Al-Emrani, M., Engström, B., Johansson, M., Johansson, P.,(2008): *Bärande Konstruktioner,del 2*{Load bearing Constructions, part 2. In Swedish} Department of Civil and Environmental Engineering, Chalmers University of Technology, Göteborg, Sweden, 2008, B232pp

Brunner, M., Schnueriger, M., (2005): *Timber beams strengthened by attaching prestressed carbon FRP laminates with a gradiented anchoring device.* Internationel Institute for FRP in Counstruction, Hong Kong, 2005

Burström, P G. (2007): *Byggnadsmaterial – Uppbyggnad, tillverkning och egenskaper*{(*Building materials* – In Swedish)}. Studentlitteratur, Lund, {Sweden}, {2007}, 562 pp

Dolan, C.W., Galloway, T.L., Tsunemori, A. (1997): *Pre-stressed Glued-Laminated Timber Beam – Pilot Study*.ASCE Journal of Composites for Construction, Vol. 1, No. 1, February 1997, pp. 10-16

Engström, B. (2010A): *Design and analysis of pre-stressed concrete structures.*Department of Civil and Environmental Engineering, Chalmers University of Technology,Göteborg, Sweden, 2010, 191pp

Engström, B. (2010B): *Design and analysis of continuous beams and columns.*Department of Civil and Environmental Engineering, Chalmers University of Technology,Göteborg, Sweden, 2010, 131pp

Gulbrandsen, E (2011) Tenroc Technologies; oral information during consecutive meetings

Guan, Z.W., Rodd, P.D., Pope, D.J. (2005): Study of glulam beams pre-stressed with pultruded GRP. *Computers and Structures*, Vol. 83, 2005, pp. 2476-2487

Haghani, R, (2010): *Anchorage of pre-stressed FRP laminates used to strengthen structural members*. Department of Civil and Environmental Engineering, Chalmers University of Technology, Göteborg, Sweden. (2010)

Illston, J.M., Domone, P.L.J. (2001): *Construction materials – their nature and behavior*. Spon Press, London and New York, {England and USA}, {2001}, 554 pp

Jacob, J., Garzon, O.L. (2007): *Flexural Strengthening of Glued Laminated Timber Beams with Steel and Carbon Fiber Reinforced Polymers*. Master´s Thesis. Department of Civil and Environmental Engineering, Chalmers University of Technology, Publication no. 2007:28, Göteborg, Sweden, 2007, 152 pp.

Peters, S.T., (1998): *Handbook of composites – Second edition*, Chapman & Hall, {ISBN: 0-412-54020-7}, London, {United Kingdom}, {1998}, 1118 pp

Porteous, J., Kermani A. (2007):*Structural Timber Design to Eurocode 5,* Blackwell Publishing Ltd, Oxford, UK, (2009), 542pp

Ritter, M.A., Wacker, J.P., Duwadi, S.R. (1995): *Field Performance of Stress-Laminated Timber Bridges on Low-Volume Roads*. Proceeding of 6th International Conference of Low-Volume Roads, Vol. 2, {June} 1995, pp. 347-356

Silva-Henriquez, R., Gray, H., Dagher, H.J., Davids, W.G., Nader, J. (2009): Strength Performance of Pre-stressed Glass Fiber-Reinforced Polymer, Glued-Laminated Beams. *Forest Products Journal*, Vol. 60, No. 1, June 2009, pp. 33-39

Svenskt Limträ AB (2007): *Limträguide* {Guide toglulam. In Swedish}, Svenskt Limträ AB, {ISBN: 91-630-3868-4}, Stockholm,{Sweden}, {2007}, 66 pp

The steel construction institute (1992): *Steel Designer's Manual – Fifth Edition*, Blackwell Science Ltd, {ISBN:0-632-03877-2}, London, {United Kingdom}, {1992}, 1266 pp.

Triantafillou, T.C., Deskovic, N (1992): Pre-stressed FRP Sheets as External Reinforcement of Wood Members. *ASCE Journal of Structural Engineering*, Vol. 118, No. 5, May 1992, pp. 1270-1284

Yahyaei-Moayyed, M., Taheri, F. (2010A): Creep response of glued-laminated beam reinforced with pre-stressed sub-laminated composite. *Construction and Building Materials* (2010), doi:10.1016/j.conbuildmat.2010.11.078, 12 pp.

10 APPENDICES

10.1 Appendix A: The MathCAD for the model

1. Input

1.1 Load and service class

Load

$G_{perm} := 0\frac{N}{m}$ Loads considered to be permanent, such as roof joists and cladding

$Loadcase := 1$

Loadcases
1 = Uniformly distributed load
2 = Concentrated load at mid span
3 = Triangular load (load Q at one end and zero load at the other end)

$Load\_type := 8$

Type of imposed load
1 = Domestic, residential areas
2 = Office areas
3 = Congregation areas
4 = Shopping areas
5 = Storage areas
6 = Traffic area, vehicle weight < 30kN
7 = Traffic area, 30kN < vehicle weight < 160kN
8 = Snow loads on buildings, Finland, Iceland, Norway, Sweden

$Load\_duration := 3$

Load duration class
1 = Permanent action (self-weight)
2 = Long term action (storage)
3 = Medium term action (imposed floor load, snow)
4 = Short term action (wind)
5 = Instantaneous action (accidental load)

Service class

$Service\_class := 2$

Service class
1 = 20*C and RH<65%
2 = 20*C and RH<85%
3 = Worse than class 2

1.2 Material data

Glulam

$\rho_{GL} := 380\frac{kg}{m^3}$ $\gamma_{M.GL} := 1.25$

$f_{m.k.GL} := 28MPa$ $f_{v.0.k.GL} := 2.7MPa$ $f_{c.90.k.GL} := 2.7MPa$

$f_{c.0.k.GL} := 24MPa$ $f_{t.0.k.GL} := 36.5MPa$

$E_{0.k.GL.mean} := 11.6GPa$ $E_{0.k.GL.0.05} := 9.4GPa$ $G_{k.GL.mean} := 0.72GPa$

Reinforcement

$\rho_{RF} := 1400\frac{kg}{m^3}$ $\gamma_{M.RF} := 1.15$

$E_{0.k.RF} := 165GPa$ $f_{t.0.k.RF} := 2800MPa$ $f_{y.RF.d} := 500MPa$

1.3 Geometry and cross-section properties

General beam dimensions

$h := 0.7m$ $w := 0.215m$ $L_s := 10m$

Slack-reinforced glulam beam

Number of reinforcement rods in compression and tension side

$n_{c.RF.s} := 1$ $n_{t.RF.s} := 2$

Dimensions of reinforcement rods

$h_{RF.s} := 70mm$ $w_{RF.s} := 10mm$ $\%A_{RF.slack} := \frac{(n_{c.RF.s} + n_{t.RF.s})\cdot h_{RF.s}\cdot w_{RF.s}}{h\cdot w} = 1.395\,\%$

Pre-stressed glulam beam

Number of reinforcement rods in compression and tension side

$n_{c.RF.p} := 1$ $n_{t.RF.p} := 2$

Dimensions of reinforcement rods

$h_{RF.p} := 70mm$ $w_{RF.p} := 10mm$ $\%A_{RF.pre} := \frac{(n_{c.RF.p} + n_{t.RF.p})\cdot h_{RF.p}\cdot w_{RF.p}}{h\cdot w} = 1.395\,\%$

1.4 SLS limits

Accepted deflections

Instantaneous Final Final with consideration to pre-camber

$\delta_{lim.inst} := \frac{L_s}{400}$ $\delta_{lim.fin} := \frac{L_s}{250}$ $\delta_{lim.net.fin} := \frac{L_s}{250}$

2. Material and geometry properties

2.1 Load and service class

$k_{mod} = 0.8$ $k_{def} = 0.8$ $\psi_0 = 0.7$ $\psi_1 = 0.5$ $\psi_2 = 0.2$

2.2 Material data

Glulam

$$k_h := \begin{cases} 1.0 & \text{if } h \geq 0.6m \\ \min\left[\left(\frac{0.6m}{h}\right)^{0.1}, 1.1\right] & \text{otherwise} \end{cases}$$

$k_h = 1$ (EN 1995-1-1:2004 (3.2))

$$G_{0.k.GL.0.05} := \frac{E_{0.k.GL.0.05}}{16} = 0.588\,GPa$$

$$f_{m.d.GL} := \frac{f_{m.k.GL}}{\gamma_{M.GL}} \cdot k_h \cdot k_{mod} = 17.92\,MPa$$

$$f_{v.0.d.GL} := \frac{f_{v.0.k.GL}}{\gamma_{M.GL}} \cdot k_{mod} = 1.728\,MPa$$

$$f_{c.0.d.GL} := \frac{f_{c.0.k.GL}}{\gamma_{M.GL}} \cdot k_{mod} = 15.36\,MPa$$

$$f_{t.0.d.GL} := \frac{f_{t.0.k.GL}}{\gamma_{M.GL}} \cdot k_h \cdot k_{mod} = 23.36\,MPa$$

$$f_{c.90.d.GL} := \frac{f_{c.90.k.GL}}{\gamma_{M.GL}} \cdot k_{mod} = 1.728\,MPa$$

$$E_{0.d.GL.mean} := \frac{E_{0.k.GL.mean}}{\gamma_{M.GL}} = 9.28\,GPa$$

$$G_{d.GL.mean} := \frac{G_{k.GL.mean}}{\gamma_{M.GL}} = 0.576\,GPa$$

$$\varepsilon_{c.k.ult} := \frac{f_{c.0.k.GL}}{E_{0.k.GL.mean}} = 2.069 \times 10^{-3}$$

$$\varepsilon_{t.k.ult} := \frac{f_{t.0.k.GL}}{E_{0.k.GL.mean}} = 3.147 \times 10^{-3}$$

$$\varepsilon_{c.d.ult} := \frac{f_{c.0.d.GL}}{E_{0.d.GL.mean}} = 1.655 \times 10^{-3}$$

$$\varepsilon_{t.d.ult} := \frac{f_{t.0.d.GL}}{E_{0.d.GL.mean}} = 2.517 \times 10^{-3}$$

Reinforcement

$$E_{0.d.RF} := \frac{E_{0.k.RF}}{\gamma_{M.RF}} = 143.478\,GPa$$

$$f_{t.0.d.RF} := \frac{f_{t.0.k.RF}}{\gamma_{M.RF}} = 2.435 \times 10^{9}\,Pa$$

$$\alpha_k := \frac{E_{0.k.RF}}{E_{0.k.GL.mean}} = 14.224$$

$$\alpha_d := \frac{E_{0.d.RF}}{E_{0.d.GL.mean}} = 15.461$$

2.3 Geometry and cross-section properties

General

$$A_{beam} := h \cdot w = 0.15\,m^2$$

Regular glulam beam

$$A_{reg} := A_{beam} = 0.15\,m^2$$

$$W_{y.reg} := \frac{w \cdot h^2}{6} = 0.018\,m^3$$

$$I_{y.reg} := \frac{w \cdot h^3}{12} = 6.145 \times 10^{-3}\,m^4$$

$$I_{z.reg} := \frac{h \cdot w^3}{12} = 5.797 \times 10^{-4}\,m^4$$

$$z_{NA.d.reg} := \frac{h}{2} = 0.35\,m$$

Slack-reinforced glulam beam

$$A_{slack.RF} := \left(n_{c.RF.s} + n_{t.RF.s}\right)\cdot h_{RF.s}\cdot w_{RF.s} = 2.1\times 10^{-3}\,m^2$$

$$A_{c.RF.s} := h_{RF.s}\cdot w_{RF.s}\cdot n_{c.RF.s} \qquad A_{t.RF.s} := h_{RF.s}\cdot w_{RF.s}\cdot n_{t.RF.s}$$

$$A_{slack.GL} := A_{beam} - A_{slack.RF} = 0.148m^2$$

Transformation of the section with reinforcement

$$A_{d.trans.s} := h\cdot w + \left(\alpha_d - 1\right)\cdot\left(n_{c.RF.s}\cdot h_{RF.s}\cdot w_{RF.s} + n_{t.RF.s}\cdot h_{RF.s}\cdot w_{RF.s}\right) = 0.181m^2$$

Creating the ekvalent section for the beam

$$Z_{c.s} := \frac{h_{RF.s}}{2} = 0.035m \qquad Z_{t.s} := \frac{h_{RF.s}}{2} = 0.035m$$

Calculating neutral axies (from top fiber and down)

$$z_{NA.d.slack} := \frac{A_{c.RF.s}\cdot E_{0.d.RF}\cdot\frac{h_{RF.s}}{2} + A_{t.RF.s}\cdot E_{0.d.RF}\cdot\left(h - \frac{h_{RF.s}}{2}\right) + \frac{1}{2}\cdot w\cdot h^2\cdot E_{0.d.GL.mean}}{E_{0.d.RF}A_{c.RF.s} + E_{0.d.RF}A_{t.RF.s} + w\cdot h\cdot E_{0.d.GL.mean}} = 0.369m$$

Calculating Iy, Iz and Wy, design values

$$I_{y.d.slack} := \left[\frac{w\cdot h^3}{12} + h\cdot w\cdot\left(z_{NA.d.slack} - \frac{h}{2}\right)^2\right] \ldots + \left(\alpha_d - 1\right)\cdot\left[\begin{array}{l}\left(\frac{n_{c.RF.s}\cdot w_{RF.s}\cdot h_{RF.s}^3}{12}\right) + A_{c.RF.s}\cdot\left(z_{NA.d.slack} - \frac{h_{RF.s}}{2}\right)^2 \ldots \\ + \frac{n_{t.RF.s}\cdot w_{RF.s}\cdot h_{RF.s}^3}{12} + A_{t.RF.s}\cdot\left(h - z_{NA.d.slack} - \frac{h_{RF.s}}{2}\right)^2\end{array}\right]$$

$$I_{z.c.d.slack} := \begin{cases}\left(\alpha_d - 1\right)\cdot\frac{h_{RF.s}\cdot w_{RF.s}^3}{12} & \text{if } n_{c.RF.s} = 1 \\ \left(\alpha_d - 1\right)\left[\sum_{n=1}^{\frac{n_{c.RF.s}}{2}}\left[2\left[\left(\frac{h_{RF.s}\cdot w_{RF.s}^3}{12}\right) \ldots + h_{RF.s}\cdot w_{RF.s}\cdot\left[\frac{w}{2\cdot\left(n_{c.RF.s}+1\right)}\cdot(2n-1)\right]^2\right]\right]\right] & \text{if } \left(\frac{n_{c.RF.s}}{2}\right) \in Z \\ \left(\alpha_d - 1\right)\left[\frac{h_{RF.s}\cdot w_{RF.s}^3}{12} \ldots + \sum_{n=2}^{\frac{n_{c.RF.s}+1}{2}}\left[2\left[\left(\frac{h_{RF.s}\cdot w_{RF.s}^3}{12}\right) + h_{RF.s}\cdot w_{RF.s}\cdot\left[\frac{w}{\left(n_{c.RF.s}+1\right)}\cdot(n-1)\right]^2\right]\right]\right] & \text{otherwise}\end{cases}$$

$$I_{z.t.d.slack} := \begin{cases} (\alpha_d - 1)\cdot\frac{h_{RF.s}\cdot w_{RF.s}^{3}}{12} & \text{if } n_{t.RF.s} = 1 \\ (\alpha_d - 1)\left[\sum_{n=1}^{\frac{n_{t.RF.s}}{2}}\left[2\left[\left(\frac{h_{RF.s}\cdot w_{RF.s}^{3}}{12}\right)\ldots + h_{RF.s}\cdot w_{RF.s}\cdot\left[\frac{w}{2\cdot(n_{t.RF.s}+1)}\cdot(2n-1)\right]^2\right]\right]\right] & \text{if } \left(\frac{n_{t.RF.s}}{2}\right)\in Z \\ (\alpha_d - 1)\left[\frac{h_{RF.s}\cdot w_{RF.s}^{3}}{12}\ldots + \sum_{n=2}^{\frac{n_{t.RF.s}+1}{2}}\left[2\left[\left(\frac{h_{RF.s}\cdot w_{RF.s}^{3}}{12}\right) + h_{RF.s}\cdot w_{RF.s}\cdot\left[\frac{w}{(n_{t.RF.s}+1)}\cdot(n-1)\right]^2\right]\right]\right] & \text{otherwise} \end{cases}$$

$$I_{z.d.slack} := \frac{h\cdot w^{3}}{12} + I_{z.c.d.slack} + I_{z.t.d.slack}$$

$$z_{max.d.slack} := \max\left(z_{NA.d.slack}, h - z_{NA.d.slack}\right) = 0.369\,m \qquad W_{y.d.slack} := \frac{I_{y.d.slack}}{z_{max.d.slack}} = 0.025\,m^3$$

$$S_{top.d.slack} := z_{NA.d.slack}\cdot w\cdot\frac{z_{NA.d.slack}}{2} = 0.015\,m^3$$

$$S_{bot.d.slack} := \left(h - z_{NA.d.slack}\right)\cdot w\cdot\frac{h - z_{NA.d.slack}}{2} = 0.012\,m^3$$

$$S_{d.slack} := \max\left(S_{top.d.slack}, S_{bot.d.slack}\right) = 0.015\,m^3$$

$I_{y.d.slack} = 9.115\times 10^{-3}\cdot m^4$ $I_{z.d.slack} = 6.06\times 10^{-4}\,m^4$ $W_{y.d.slack} = 0.025\,m^3$

$S_{d.slack} = 0.015\,m^3$

Pre-stressed glulam beam

$$A_{pre.RF} := \left(n_{c.RF.p} + n_{t.RF.p}\right)\cdot h_{RF.p}\cdot w_{RF.p} = 2.1\times 10^{-3}\,m^2$$

$$A_{c.RF.p} := h_{RF.p}\cdot w_{RF.p}\cdot n_{c.RF.p} \qquad A_{t.RF.p} := h_{RF.p}\cdot w_{RF.p}\cdot n_{t.RF.p}$$

$$A_{pre.GL} := A_{beam} - A_{pre.RF} = 0.148\,m^2$$

Transformation of the section with reinforcement

$$A_{d.trans.p} := h\cdot w + \left(\alpha_d - 1\right)\cdot\left(n_{c.RF.p}\cdot h_{RF.p}\cdot w_{RF.p} + n_{t.RF.p}\cdot h_{RF.p}\cdot w_{RF.p}\right) = 0.181\,m^2$$

Creating the ekvalent section for the beam

$$Z_{c.p} := \frac{h_{RF.p}}{2} = 0.035\text{m} \qquad Z_{t.p} := \frac{h_{RF.p}}{2} = 0.035\text{m}$$

Calculating neutral axies (from top fiber and down)

$$z_{NA.d.pre} := \frac{A_{c.RF.p} \cdot E_{0.d.RF} \frac{h_{RF.p}}{2} + A_{t.RF.p} \cdot E_{0.d.RF} \left(h - \frac{h_{RF.p}}{2} \right) + \frac{1}{2} \cdot w \cdot h^2 \cdot E_{0.d.GL.mean}}{E_{0.d.RF} A_{c.RF.p} + E_{0.d.RF} A_{t.RF.p} + w \cdot h \cdot E_{0.d.GL.mean}} = 0.369\text{m}$$

Calculating Iy, Iz and Wy, design values

$$I_{y.d.pre} := \left[\frac{w \cdot h^3}{12} + h \cdot w \cdot \left(z_{NA.d.pre} - \frac{h}{2} \right)^2 \right] \ldots + \left(\alpha_d - 1 \right) \cdot \left[\begin{array}{l} \left(\frac{n_{c.RF.p} \cdot w_{RF.p} \cdot h_{RF.p}^3}{12} \right) + A_{c.RF.p} \cdot \left(z_{NA.d.pre} - \frac{h_{RF.p}}{2} \right)^2 \ldots \\ + \frac{n_{t.RF.p} \cdot w_{RF.p} \cdot h_{RF.p}^3}{12} + A_{t.RF.p} \cdot \left(h - z_{NA.d.pre} - \frac{h_{RF.p}}{2} \right)^2 \end{array} \right]$$

$$I_{z.c.d.pre} := \begin{cases} \left(\alpha_d - 1 \right) \cdot \frac{h_{RF.p} \cdot w_{RF.p}^3}{12} & \text{if } n_{c.RF.p} = 1 \\ \left(\alpha_d - 1 \right) \left[\sum_{n=1}^{\frac{n_{c.RF.p}}{2}} \left[2 \left[\left(\frac{h_{RF.p} \cdot w_{RF.p}^3}{12} \right) \ldots + h_{RF.p} \cdot w_{RF.p} \left[\frac{w}{2 \cdot \left(n_{c.RF.p} + 1 \right)} \cdot (2n - 1) \right]^2 \right] \right] & \text{if } \left(\frac{n_{c.RF.p}}{2} \right) \in Z \\ \left(\alpha_d - 1 \right) \left[\begin{array}{l} \frac{h_{RF.p} \cdot w_{RF.p}^3}{12} \ldots \\ + \sum_{n=2}^{\frac{n_{c.RF.p}+1}{2}} \left[2 \left[\left(\frac{h_{RF.p} \cdot w_{RF.p}^3}{12} \right) + h_{RF.p} \cdot w_{RF.p} \left[\frac{w}{\left(n_{c.RF.p} + 1 \right)} \cdot (n - 1) \right]^2 \right] \right] \end{array} \right] & \text{otherwise} \end{cases}$$

$$I_{z.t.d.pre} := \begin{cases} (\alpha_d - 1)\cdot\frac{h_{RF.p}\cdot w_{RF.p}^{3}}{12} & \text{if } n_{t.RF.p} = 1 \\ (\alpha_d - 1)\left[\sum_{n=1}^{\frac{n_{t.RF.p}}{2}}\left[2\left[\left(\frac{h_{RF.p}\cdot w_{RF.p}^{3}}{12}\right)\ldots + h_{RF.p}\cdot w_{RF.p}\cdot\left[\frac{w}{2\cdot(n_{t.RF.p}+1)}\cdot(2n-1)\right]^2\right]\right]\right] & \text{if } \left(\frac{n_{t.RF.p}}{2}\right) \in Z \\ (\alpha_d - 1)\left[\frac{h_{RF.p}\cdot w_{RF.p}^{3}}{12}\ldots + \sum_{n=2}^{\frac{n_{t.RF.p}+1}{2}}\left[2\left[\left(\frac{h_{RF.p}\cdot w_{RF.p}^{3}}{12}\right) + h_{RF.p}\cdot w_{RF.p}\cdot\left[\frac{w}{(n_{t.RF.p}+1)}\cdot(n-1)\right]^2\right]\right]\right] & \text{otherwise} \end{cases}$$

$$I_{z.d.pre} := \frac{h\cdot w^{3}}{12} + I_{z.c.d.pre} + I_{z.t.d.pre} = 6.06\times 10^{-4}\,m^4$$

Calculating the bending resistance

$$z_{max.d.pre} := \max\left[z_{NA.d.pre}, (h - z_{NA.d.pre})\right] = 0.369m \qquad W_{y.d.pre} := \frac{I_{y.d.pre}}{z_{max.d.pre}} = 0.025\cdot m^3$$

$$S_{top.d.pre} := z_{NA.d.pre}\cdot w\cdot\frac{z_{NA.d.pre}}{2} = 0.015\,m^3$$

$$S_{bot.d.pre} := (h - z_{NA.d.pre})\cdot w\cdot\frac{h - z_{NA.d.pre}}{2} = 0.012\,m^3$$

$$S_{d.pre} := \max(S_{top.d.pre}, S_{bot.d.pre}) = 0.015\,m^3$$

$I_{y.d.pre} = 9.115\times 10^{-3}\cdot m^4$ $I_{z.d.pre} = 6.06\times 10^{-4}\,m^4$ $W_{y.d.pre} = 0.025\,m^3$

$S_{d.pre} = 0.015\,m^3$

2.4 Self-weights and other load considered as permanent load

Self-weight - regular beam

$$G_{reg} := A_{reg}\cdot\rho_{GL}\cdot g + G_{perm} = 560.842\frac{N}{m}$$

Self-weight - slack-reinforced beam

$$G_{slack} := g\cdot(A_{slack.GL}\cdot\rho_{GL} + A_{slack.RF}\cdot\rho_{RF}) + G_{perm} = 581.848\frac{N}{m}$$

Self-weight - pre-stressed beam

$$G_{pre} := g \cdot \left(A_{pre.GL} \cdot \rho_{GL} + A_{pre.RF} \cdot \rho_{RF}\right) + G_{perm} = 581.848 \frac{N}{m}$$

2.5 Calculated material parameters

Regular glulam beam

$$EI_{d.ef.reg} := E_{0.d.GL.mean} \cdot I_{y.reg} = 5.703 \times 10^{7} \cdot N \cdot m^{2}$$

Slack-reinforced glulam beam

$$EI_{d.ef.slack} := E_{0.d.GL.mean} \cdot \left[\frac{w \cdot h^{3}}{12} + h \cdot w \cdot \left(z_{NA.d.slack} - \frac{h}{2}\right)^{2}\right] \ldots + \left[E_{0.d.GL.mean} \cdot \left(\alpha_{d} - 1\right)\right] \cdot \left[\begin{array}{l} \left(\frac{n_{c.RF.s} \cdot w_{RF.s} \cdot h_{RF.s}^{3}}{12}\right) \ldots \\ + A_{c.RF.s} \cdot \left(z_{NA.d.slack} - \frac{h_{RF.s}}{2}\right)^{2} \ldots \\ + \left(\frac{n_{t.RF.s} \cdot w_{RF.s} \cdot h_{RF.s}^{3}}{12}\right) \ldots \\ + A_{t.RF.s} \cdot \left(h - z_{NA.d.slack} - \frac{h_{RF.s}}{2}\right)^{2} \end{array}\right]$$

$$EI_{d.ef.slack} = 8.459 \times 10^{7} \cdot N \cdot m^{2}$$

Pre-stressed glulam beam

$$EI_{d.ef.pre} := E_{0.d.GL.mean} \cdot \left[\frac{w \cdot h^{3}}{12} + h \cdot w \cdot \left(z_{NA.d.pre} - \frac{h}{2}\right)^{2}\right] \ldots + \left[E_{0.d.GL.mean} \cdot \left(\alpha_{d} - 1\right)\right] \cdot \left[\begin{array}{l} \left(\frac{n_{c.RF.p} \cdot w_{RF.p} \cdot h_{RF.p}^{3}}{12}\right) \ldots \\ + A_{c.RF.p} \cdot \left(z_{NA.d.pre} - \frac{h_{RF.p}}{2}\right)^{2} \ldots \\ + \left(\frac{n_{t.RF.p} \cdot w_{RF.p} \cdot h_{RF.p}^{3}}{12}\right) \ldots \\ + A_{t.RF.p} \cdot \left(h - z_{NA.d.pre} - \frac{h_{RF.p}}{2}\right)^{2} \end{array}\right]$$

$$EI_{d.ef.pre} = 8.459 \times 10^{7} \cdot N \cdot m^{2}$$

3. Capacity

3.1 Capacity of regular glulam beam

3.1.1 Bending

The beam is fully suported against lateral movements

$f_{m.d.reg} := f_{m.d.GL} = 1.792\times 10^{7}\ Pa$ $M_{cap.EC5.d.reg} := f_{m.d.reg}\cdot W_{y.reg} = 3.146\times 10^{5}\cdot N\cdot m$

3.1.2 Bending with consideration to lateral torsional stability

The beam is restrained against torsional rotation at ends, prevented from moving laterally at ends

$$I_{tor} := \frac{w^3\cdot h}{3}\cdot\left[1 - 0.63\cdot\left(\frac{w}{h}\right)\right] = 1.87\times 10^{-3}\ m^4$$

$$L_{ef} := \begin{cases} 0.9\cdot L_s + 2\cdot h & \text{if Loadcase} = 1 \quad = 10.4m \\ 0.8\cdot L_s + 2\cdot h & \text{if Loadcase} = 2 \\ 0.53\cdot L_s + 2\cdot h & \text{if Loadcase} = 3 \end{cases}$$

$$M_{y.crit} := \frac{\pi\cdot\sqrt{E_{0.k.GL.0.05}I_{z.reg}\cdot G_{0.k.GL.0.05}I_{tor}}}{L_{ef}} = 7.392\times 10^{5}\cdot N\cdot m$$

$$\sigma_{m.crit} := \frac{M_{y.crit}}{W_{y.reg}} = 4.21\times 10^{7}\ Pa$$

$$\lambda_{rel.m} := \sqrt{\frac{f_{m.k.GL}}{\sigma_{m.crit}}} = 0.816$$

$$k_{crit} := \begin{cases} 1 & \text{if } \lambda_{rel.m} \le 0.75 \quad = 0.948 \\ 1.56 - 0.75\cdot\lambda_{rel.m} & \text{if } 0.75 < \lambda_{rel.m} \le 1.4 \\ \frac{1}{\lambda_{rel.m}^{2}} & \text{if } 1.4 < \lambda_{rel.m} \end{cases}$$

$f_{m.buck.d.reg} := f_{m.d.GL}\cdot k_{crit}$

$M_{cap.buck.d.reg} := f_{m.buck.d.reg}\cdot W_{y.reg}$

$f_{m.buck.d.reg} = 1.699\times 10^{7}\ Pa$ $M_{cap.buck.d.reg} = 2.984\times 10^{5}\cdot N\cdot m$

3.1.2 Bending using our model

Elastic phase

$$\varepsilon_{c.limit.e.r} := \frac{f_{c.0.d.GL}}{E_{0.d.GL.mean}} = 1.655\times 10^{-3}$$

$$\varepsilon_{t.limit.r} := \frac{f_{t.0.d.GL}}{E_{0.d.GL.mean}} = 2.517\times 10^{-3}$$

$$\varepsilon_{c.init.e.r} := 10^{-9}$$

$$\varepsilon_{add.r} := \frac{\varepsilon_{c.limit.e.r}}{100} = 1.655\times 10^{-5}$$

$$\begin{pmatrix} M_{cap.re.e} \\ \varepsilon_{c.GL.reg.e} \\ \varepsilon_{t.GL.reg.e} \\ Failure\_mode_{reg.e} \end{pmatrix} := \left| \begin{array}{l} i \leftarrow 0 \\ \varepsilon_c \leftarrow \varepsilon_{c.init.e.r} \\ \text{while } \varepsilon_c < \varepsilon_{c.limit.e.r} \\ \quad \left| \begin{array}{l} \varepsilon_t \leftarrow \left(\frac{h}{z_{NA.d.reg}} - 1\right)\cdot\varepsilon_c \\ M \leftarrow \frac{\varepsilon_c \cdot E_{0.d.GL.mean} \cdot w \cdot z_{NA.d.reg}^{2}}{3} \ldots \\ \qquad + \frac{\varepsilon_t \cdot E_{0.d.GL.mean} \cdot w \cdot \left(h - z_{NA.d.reg}\right)^2}{3} \\ b_i \leftarrow \varepsilon_c \\ c_i \leftarrow \varepsilon_t \\ \text{break if } \varepsilon_t > \varepsilon_{t.limit.r} \\ a_i \leftarrow M \cdot \frac{1}{J} \\ i \leftarrow i + 1 \\ \varepsilon_c \leftarrow \varepsilon_c + \varepsilon_{add.r} \end{array} \right. \\ d \leftarrow \left| \begin{array}{ll} \text{"Tension"} & \text{if } \varepsilon_t > \varepsilon_{t.limit.r} \\ \text{"Plastic phase"} & \text{otherwise} \end{array} \right. \\ \begin{pmatrix} a \\ b \\ c \\ d \end{pmatrix} \end{array} \right.$$

$$M_{cap.reg.e} := M_{cap.re.e} \cdot J$$

$Failure\_mode_{reg.e} = \text{"Plastic phase"}$

$$M_{cap.reg.el} := \max\left(M_{cap.reg.e}\right) = 266.999\,kN\cdot m$$

Plastic phase

$$\varepsilon_{c.limit.pl.r} := 3\varepsilon_{c.limit.e.r} = 4.966\times 10^{-3}$$

$$\varepsilon_{c.init.pl.r} := \max\left(\varepsilon_{c.GL.reg.e}\right) = 1.639\times 10^{-3}$$

$$\begin{pmatrix} M_{cap.re.pl} \\ \varepsilon_{c.GL.reg.pl} \\ \varepsilon_{t.GL.reg.pl} \\ Failure\_mode_{reg.pl} \end{pmatrix} := \left| \begin{array}{l} i \leftarrow 0 \\ \varepsilon_c \leftarrow \varepsilon_{c.init.pl.r} \\ \text{while } \varepsilon_c < \varepsilon_{c.limit.pl.r} \\ \quad \left| \begin{array}{l} x \leftarrow f_{c.0.d.GL} \cdot w \cdot \dfrac{\left(\varepsilon_c - \varepsilon_{c.limit.e.r}\right)}{\varepsilon_c} \ldots \\ \qquad + f_{c.0.d.GL} \cdot \dfrac{w}{2} \cdot \left(1 - \dfrac{\varepsilon_c - \varepsilon_{c.limit.e.r}}{\varepsilon_c}\right) \ldots \\ \qquad + -\left(\varepsilon_c \cdot \dfrac{w}{2} \cdot E_{0.d.GL.mean}\right) \\ y \leftarrow \varepsilon_c \cdot w \cdot h \cdot E_{0.d.GL.mean} \\ z \leftarrow \varepsilon_c \cdot -\left(\dfrac{w}{2} \cdot h^2 \cdot E_{0.d.GL.mean}\right) \\ z_{NA.pl} \leftarrow \dfrac{-y + \sqrt{y^2 - 4 \cdot x \cdot z}}{2 \cdot x} \\ z_{pl} \leftarrow \dfrac{\varepsilon_c - \varepsilon_{c.limit.e.r}}{\varepsilon_c} \cdot z_{NA.pl} \\ \varepsilon_t \leftarrow \left(\dfrac{h}{z_{NA.pl}} - 1\right) \cdot \varepsilon_c \\ M \leftarrow f_{c.0.d.GL} \cdot w \cdot z_{pl} \cdot \left(z_{NA.pl} - \dfrac{z_{pl}}{2}\right) \ldots \\ \qquad + f_{c.0.d.GL} \cdot \dfrac{z_{NA.pl} - z_{pl}}{2} \cdot w \cdot \dfrac{2\left(z_{NA.pl} - z_{pl}\right)}{3} \ldots \\ \qquad + \varepsilon_t \cdot E_{0.d.GL.mean} \cdot \dfrac{h - z_{NA.pl}}{2} \cdot w \cdot \dfrac{2\left(h - z_{NA.pl}\right)}{3} \\ b_i \leftarrow \varepsilon_c \\ c_i \leftarrow \varepsilon_t \\ \text{break if } \varepsilon_t > \varepsilon_{t.limit.r} \\ a_i \leftarrow M \cdot \dfrac{1}{J} \\ i \leftarrow i + 1 \\ \varepsilon_c \leftarrow \varepsilon_c + \varepsilon_{add.r} \end{array} \right. \\ d \leftarrow \left| \begin{array}{ll} \text{"Tension"} & \text{if } \varepsilon_t > \varepsilon_{t.limit.r} \\ \text{"Compression"} & \text{otherwise} \end{array} \right. \\ \begin{pmatrix} a \\ b \\ c \\ d \end{pmatrix} \end{array} \right.$$

$$M_{cap.reg.p} := M_{cap.re.pl} \cdot J$$

$$Failure\_mode_{reg.pl} = \text{"Tension"}$$

$$M_{cap.reg.pl} := \max\left(M_{cap.reg.p}\right) = 380.417\,kN\cdot m$$

$$M_{cap.d.reg} := \max\left(M_{cap.reg.el}, M_{cap.reg.pl}\right) = 380.417\,kN\cdot m$$

3.1.4 Shear

$$V_{cap.d.reg} := \frac{f_{v.0.d.GL} \cdot A_{beam}}{1.5} = 1.734\times 10^{5}\,N$$

$$f_{v.d.reg} := f_{v.0.d.GL} = 1.728\times 10^{6}\,Pa \qquad V_{cap.d.reg} = 1.734\times 10^{5}\,N$$

3.2 Capacity of slack-reinforced glulam beam

3.2.1 Bending

Elastic phase

$$\varepsilon_{c.limit.e.s} := \frac{f_{c.0.d.GL}}{E_{0.d.GL.mean}} = 1.655\times 10^{-3}$$

$$\varepsilon_{t.limit.s} := \frac{f_{t.0.d.GL}}{E_{0.d.GL.mean}} = 2.517\times 10^{-3}$$

$$\varepsilon_{c.init.e.s} := 10^{-9}$$

$$\varepsilon_{add.s} := \frac{\varepsilon_{c.limit.e.s}}{100} = 1.655\times 10^{-5}$$

$$\begin{pmatrix} M_{cap.slac.e} \\ \varepsilon_{c.GL.slack.e} \\ \varepsilon_{t.GL.slack.e} \\ \sigma_{c.RF.slac.e} \\ \sigma_{t.RF.slac.e} \\ Failure\_mode_{slack.e} \end{pmatrix} := \left| \begin{array}{l} i \leftarrow 0 \\ \varepsilon_c \leftarrow \varepsilon_{c.init.e.s} \\ \text{while } \varepsilon_c < \varepsilon_{c.limit.e.s} \\ \quad \left| \begin{array}{l} \varepsilon_t \leftarrow \left(\frac{h}{z_{NA.d.slack}} - 1 \right) \cdot \varepsilon_c \\ \varepsilon_{RF.c} \leftarrow \frac{z_{NA.d.slack} - Z_{c.s}}{z_{NA.d.slack}} \cdot \varepsilon_c \\ \varepsilon_{RF.t} \leftarrow \frac{h - z_{NA.d.slack} - Z_{t.s}}{z_{NA.d.slack}} \cdot \varepsilon_c \\ M \leftarrow \frac{\varepsilon_c \cdot E_{0.d.GL.mean} \cdot w \cdot z_{NA.d.slack}^2}{3} \ldots \\ \quad + \varepsilon_{RF.c} \cdot E_{0.d.RF} \cdot A_{c.RF.s} \cdot \left(z_{NA.d.slack} - Z_{c.s} \right) \ldots \\ \quad + \frac{\varepsilon_t \cdot E_{0.d.GL.mean} \cdot w \cdot \left(h - z_{NA.d.slack} \right)^2}{3} \ldots \\ \quad + \varepsilon_{RF.t} \cdot E_{0.d.RF} \cdot A_{t.RF.s} \cdot \left(h - z_{NA.d.slack} - Z_{t.s} \right) \\ b_i \leftarrow \varepsilon_c \\ c_i \leftarrow \varepsilon_t \\ d_i \leftarrow \varepsilon_{RF.c} \cdot E_{0.d.RF} \cdot \frac{1}{Pa} \\ e_i \leftarrow \varepsilon_{RF.t} \cdot E_{0.d.RF} \cdot \frac{1}{Pa} \\ \text{break if } \varepsilon_t > \varepsilon_{t.limit.s} \\ a_i \leftarrow M \cdot \frac{1}{J} \\ i \leftarrow i + 1 \\ \varepsilon_c \leftarrow \varepsilon_c + \varepsilon_{add.s} \end{array} \right. \\ f \leftarrow \left| \begin{array}{ll} \text{"Tension"} & \text{if } \varepsilon_t > \varepsilon_{t.limit.s} \\ \text{"Plastic phase"} & \text{otherwise} \end{array} \right. \\ \begin{pmatrix} a \\ b \\ c \\ d \\ e \\ f \end{pmatrix} \end{array} \right.$$

$M_{cap.slack.e} := M_{cap.slac.e} \cdot J$ $\sigma_{c.RF.slack.e} := \sigma_{c.RF.slac.e} \cdot Pa$ $\sigma_{t.RF.slack.e} := \sigma_{t.RF.slac.e} \cdot Pa$

$Failure\_mode_{slack.e} = \text{"Plastic phase"}$

$M_{cap.slack.el} := \max(M_{cap.slack.e}) = 383.779\,kN \cdot m$

Plastic phase

$\varepsilon_{c.limit.pl.s} := 3\varepsilon_{c.limit.e.s} = 4.966 \times 10^{-3}$

$\varepsilon_{c.init.pl.s} := \max(\varepsilon_{c.GL.slack.e}) = 1.639 \times 10^{-3}$

$\sigma_{RF.c.pl.init.s} := \max(\sigma_{c.RF.slack.e}) = 2.128 \times 10^{8}\,Pa$

$\sigma_{RF.t.pl.init.s} := \max(\sigma_{t.RF.slack.e}) = 1.89 \times 10^{8}\,Pa$

$$\begin{pmatrix} M_{cap.slac.pl} \\ \varepsilon_{c.GL.slack.pl} \\ \varepsilon_{t.GL.slack.pl} \\ \sigma_{c.RF.slac.pl} \\ \sigma_{t.RF.slac.pl} \\ Failure\_mode_{slack.pl} \end{pmatrix} := \left| \begin{array}{l} i \leftarrow 0 \\ \varepsilon_c \leftarrow \varepsilon_{c.init.pl.s} \\ \sigma_{RF.c} \leftarrow \sigma_{RF.c.pl.init.s} \\ \sigma_{RF.t} \leftarrow \sigma_{RF.t.pl.init.s} \\ \text{while } \varepsilon_c < \varepsilon_{c.limit.pl.s} \\ \quad x \leftarrow \left| \begin{array}{ll} f_{c.0.d.GL} \cdot w \cdot \left(1 - \frac{\varepsilon_{c.limit.e.s}}{\varepsilon_c}\right) \ldots & \text{if } \sigma_{RF.c} < f_{y.RF.d} \wedge \sigma_{RF.t} < f_{y.RF.d} \\ + f_{c.0.d.GL} \cdot \frac{w}{2} \cdot \left(\frac{\varepsilon_{c.limit.e.s}}{\varepsilon_c}\right) \ldots & \\ + -\left(\varepsilon_c \cdot \frac{w}{2} \cdot E_{0.d.GL.mean}\right) & \\ f_{c.0.d.GL} \cdot w \cdot \left(1 - \frac{\varepsilon_{c.limit.e.s}}{\varepsilon_c}\right) \ldots & \text{if } \sigma_{RF.c} \geq f_{y.RF.d} \wedge \sigma_{RF.t} < f_{y.RF.d} \\ + \frac{f_{c.0.d.GL} \cdot w}{2} \ldots & \\ + -\frac{f_{c.0.d.GL} \cdot w}{2} \cdot \frac{\varepsilon_c - \varepsilon_{c.limit.e.s}}{\varepsilon_c} \ldots & \\ + -\varepsilon_c \cdot \frac{w}{2} \cdot E_{0.d.GL.mean} & \\ f_{c.0.d.GL} \cdot w \cdot \left(1 - \frac{\varepsilon_{c.limit.e.s}}{\varepsilon_c}\right) \ldots & \text{if } \sigma_{RF.c} < f_{y.RF.d} \wedge \sigma_{RF.t} \geq f_{y.RF.d} \\ + \frac{f_{c.0.d.GL} \cdot w}{2} \ldots & \\ + -\frac{f_{c.0.d.GL} \cdot w}{2} \cdot \frac{\varepsilon_c - \varepsilon_{c.limit.e.s}}{\varepsilon_c} \ldots & \\ + -\varepsilon_c \cdot \frac{w}{2} \cdot E_{0.d.GL.mean} & \end{array} \right. \end{array} \right.$$

$$\left|\begin{array}{l}
\left|\begin{array}{ll}
\dfrac{f_{c.0.d.GL}\cdot w\cdot\left(\varepsilon_c-\varepsilon_{c.limit.e.s}\right)}{2\cdot\varepsilon_c}\ldots & \text{if } \sigma_{RF.c}\geq f_{y.RF.d}\wedge\sigma_{RF.t}\geq f_{y.RF.d}\\
+\dfrac{f_{c.0.d.GL}\cdot w}{2}-\dfrac{\varepsilon_c\cdot E_{0.d.GL.mean}\cdot w}{2} &
\end{array}\right.\\
y\leftarrow\left|\begin{array}{ll}
-E_{0.d.RF}\cdot A_{t.RF.s}\cdot\left(-\varepsilon_c\right)\ldots & \text{if } \sigma_{RF.c}<f_{y.RF.d}\wedge\sigma_{RF.t}<f_{y.RF.d}\\
+E_{0.d.GL.mean}\cdot w\cdot h\cdot\varepsilon_c\ldots & \\
+E_{0.d.RF}\cdot A_{c.RF.s}\cdot\varepsilon_c & \\
f_{y.RF.d}\cdot A_{c.RF.s}\ldots & \text{if } \sigma_{RF.c}\geq f_{y.RF.d}\wedge\sigma_{RF.t}<f_{y.RF.d}\\
+E_{0.d.GL.mean}\cdot\varepsilon_c\cdot w\cdot h\ldots & \\
+-E_{0.d.RF}\cdot A_{t.RF.s}\cdot\left(-\varepsilon_c\right) & \\
\varepsilon_c\cdot E_{0.d.RF}\cdot A_{c.RF.s}\ldots & \text{if } \sigma_{RF.c}<f_{y.RF.d}\wedge\sigma_{RF.t}\geq f_{y.RF.d}\\
+E_{0.d.GL.mean}\cdot\varepsilon_c\cdot w\cdot h\ldots & \\
+-f_{y.RF.d}\cdot A_{t.RF.s} & \\
f_{y.RF.d}\cdot A_{c.RF.s}-f_{y.RF.d}\cdot A_{t.RF.s}\ldots & \text{if } \sigma_{RF.c}\geq f_{y.RF.d}\wedge\sigma_{RF.t}\geq f_{y.RF.d}\\
+E_{0.d.GL.mean}\cdot\varepsilon_c\cdot w\cdot h &
\end{array}\right.\\
z\leftarrow\left|\begin{array}{ll}
\varepsilon_c\cdot\left[-E_{0.d.RF}\cdot A_{t.RF.s}\cdot\left(h-Z_{t.s}\right)\right]\ldots & \text{if } \sigma_{RF.c}<f_{y.RF.d}\wedge\sigma_{RF.t}<f_{y.RF.d}\\
+-\dfrac{\varepsilon_c\cdot E_{0.d.GL.mean}\cdot w\cdot h^2}{2}\ldots & \\
+-\varepsilon_c\cdot E_{0.d.RF}\cdot A_{c.RF.s}\cdot Z_{c.s} & \\
\left(-\varepsilon_c\right)\cdot\dfrac{w\cdot h^2}{2}\cdot E_{0.d.GL.mean}\ldots & \text{if } \sigma_{RF.c}\geq f_{y.RF.d}\wedge\sigma_{RF.t}<f_{y.RF.d}\\
+-\varepsilon_c\cdot E_{0.d.RF}\cdot A_{t.RF.s}\cdot\left(h-Z_{t.s}\right) & \\
-\varepsilon_c\cdot\dfrac{w\cdot h^2}{2}\cdot E_{0.d.GL.mean}\ldots & \text{if } \sigma_{RF.c}<f_{y.RF.d}\wedge\sigma_{RF.t}\geq f_{y.RF.d}\\
+-\varepsilon_c\cdot E_{0.d.RF}\cdot A_{c.RF.s}\cdot Z_{c.s} & \\
-\left(\dfrac{\varepsilon_c\cdot E_{0.d.GL.mean}\cdot w\cdot h^2}{2}\right) & \text{if } \sigma_{RF.c}\geq f_{y.RF.d}\wedge\sigma_{RF.t}\geq f_{y.RF.d}
\end{array}\right.\\
z_{NA.pl}\leftarrow\dfrac{-y+\sqrt{y^2-4\cdot x\cdot z}}{2\cdot x}\\
z_{pl}\leftarrow\dfrac{\varepsilon_c-\varepsilon_{c.limit.e.s}}{\varepsilon_c}\cdot z_{NA.pl}\\
\varepsilon_t\leftarrow\left(\dfrac{h}{z_{NA.pl}}-1\right)\cdot\varepsilon_c\\
\varepsilon_{RF.c}\leftarrow\left(\dfrac{z_{NA.pl}-Z_{c.s}}{z_{NA.pl}}\right)\cdot\varepsilon_c
\end{array}\right.$$

$$\varepsilon_{RF.t} \leftarrow \frac{h - z_{NA.pl} - Z_{t.s}}{z_{NA.pl}} \cdot \varepsilon_c$$

$$\sigma_{RF.c} \leftarrow \varepsilon_{RF.c} \cdot E_{0.d.RF}$$

$$\sigma_{RF.t} \leftarrow \varepsilon_{RF.t} \cdot E_{0.d.RF}$$

$$M \leftarrow \sigma_{RF.c} \cdot A_{c.RF.s} \cdot \left(z_{NA.pl} - Z_{c.s}\right) \ldots + f_{c.0.d.GL} \cdot w \cdot z_{pl} \cdot \left(z_{NA.pl} - \frac{z_{pl}}{2}\right) \ldots + f_{c.0.d.GL} \cdot \frac{z_{NA.pl} - z_{pl}}{2} \cdot w \cdot \frac{2\left(z_{NA.pl} - z_{pl}\right)}{3} \ldots + \sigma_{RF.t} \cdot A_{t.RF.s} \cdot \left(h - z_{NA.pl} - Z_{t.s}\right) \ldots + \varepsilon_t \cdot E_{0.d.GL.mean} \cdot \frac{h - z_{NA.pl}}{2} \cdot w \cdot \frac{2\left(h - z_{NA.pl}\right)}{3}$$

$$b_i \leftarrow \varepsilon_c$$

$$c_i \leftarrow \varepsilon_t$$

$$d_i \leftarrow \sigma_{RF.c} \cdot \frac{1}{Pa}$$

$$e_i \leftarrow \sigma_{RF.t} \cdot \frac{1}{Pa}$$

break if $\varepsilon_t > \varepsilon_{t.limit.s}$

$$a_i \leftarrow M \cdot \frac{1}{J}$$

$$i \leftarrow i + 1$$

$$\varepsilon_c \leftarrow \varepsilon_c + \varepsilon_{add.s}$$

$$f \leftarrow \begin{cases} \text{"Tension"} & \text{if } \varepsilon_t > \varepsilon_{t.limit.s} \\ \text{"Compression"} & \text{otherwise} \end{cases}$$

$$\begin{pmatrix} a \\ b \\ c \\ d \\ e \\ f \end{pmatrix}$$

$M_{cap.slack.p} := M_{cap.slac.pl} \cdot J$ $\sigma_{c.RF.slack.pl} := \sigma_{c.RF.slac.pl} \cdot Pa$ $\sigma_{t.RF.slack.pl} := \sigma_{t.RF.slac.pl} \cdot Pa$

$Failure\_mode_{slack.pl} = \text{"Tension"}$

$M_{cap.slack.pl} := \max\left(M_{cap.slack.p}\right) = 612.934\,kN \cdot m$

$M_{cap.d.slack} := \max\left(M_{cap.slack.el}, M_{cap.slack.pl}\right) = 612.934\,kN \cdot m$

Shear

$f_{v.d.slack} := f_{v.0.d.GL} = 1.728 \times 10^{6}\,Pa$

$V_{cap.d.slack} := \frac{f_{v.d.slack} \cdot I_{y.d.slack} \cdot w}{S_{d.slack}} = 2.318 \times 10^{5}\,N$

3.3 Capacity of pre-stressed glulam beam

3.3.1 Bending

Critical pre-tensioning force P.pre.d

Using linear elastic model

$\varepsilon_{bot.preload.d} := -\varepsilon_{c.d.ult}$

$\sigma_{bot.preload.d} := \varepsilon_{bot.preload.d} \cdot E_{0.d.GL.mean} = -15.36\,MPa$

$e_{N.d} := h - z_{NA.d.pre} - \frac{h_{RF.p}}{2} = 0.296m$

$z_{gc.d} := z_{NA.d.pre} = 0.369m$

$P_{pre.linear.d} := \sigma_{bot.preload.d} \cdot \left[\frac{A_{beam} \cdot I_{y.d.pre}}{e_{N.d} \cdot (h - z_{gc.d}) \cdot A_{beam} + I_{y.d.pre}} \right] = -8.818 \times 10^{5} \cdot N$

$\sigma_{top.preload.d} := \frac{P_{pre.linear.d}}{A_{beam}} + \frac{P_{pre.linear.d} \cdot e_{N.d}}{I_{y.d.pre}} \cdot -z_{gc.d} = 4.71 \cdot MPa$

$P_{pre1.d} := \begin{cases} P_{pre.linear.d} & \text{if } \sigma_{top.preload.d} < f_{t.0.d.GL} \\ -f_{t.0.d.GL} \left(\frac{A_{beam} \cdot I_{y.d.pre}}{e_{N.d} \cdot z_{gc.d} \cdot A_{beam} + I_{y.d.pre}} \right) & \text{otherwise} \end{cases}$

$P_{pre1.d} = -8.818 \times 10^{5}\,N$

Tension capacity in reinforcement

$f_{t.0.d.RF} = 2.435 \times 10^{9}\,Pa$

$P_{pre2.d} := -f_{t.0.d.RF} n_{t.RF.p} \cdot h_{RF.p} \cdot w_{RF.p}$

$P_{pre2.d} = -3.409 \times 10^{6}\,N$

Using EC5

$L_e := L_s \qquad \beta_c := 0.1 \qquad k_m := 0.7$

$i_{y.d} := \sqrt{\frac{I_{y.d.pre}}{A_{beam}}} = 0.246m$

$$i_{z.d} := \sqrt{\frac{I_{z.d.pre}}{A_{beam}}} = 0.063m$$

$$\lambda_{y.d} := \frac{L_e}{i_{y.d}} = 40.634$$

$$\lambda_{z.d} := \frac{L_e}{i_{z.d}} = 157.593$$

$$\lambda_{rel.y.d} := \frac{\lambda_{y.d}}{\pi} \cdot \sqrt{\frac{f_{c.0.k.GL}}{E_{0.k.GL.0.05}}} = 0.654$$

$$\lambda_{rel.z.d} := \frac{\lambda_{z.d}}{\pi} \cdot \sqrt{\frac{f_{c.0.k.GL}}{E_{0.k.GL.0.05}}} = 2.535$$

$$k_{y.d} := 0.5 \cdot \left[1 + \beta_c \cdot \left(\lambda_{rel.y.d} - 0.3\right) + \lambda_{rel.y.d}^{2}\right] = 0.731$$

$$k_{z.d} := 0.5 \cdot \left[1 + \beta_c \cdot \left(\lambda_{rel.z.d} - 0.3\right) + \lambda_{rel.z.d}^{2}\right] = 3.824$$

$$k_{c.y.d} := \frac{1}{k_{y.d} + \sqrt{k_{y.d}^{2} - \lambda_{rel.y.d}^{2}}} = 0.944$$

$$k_{c.z.d} := \frac{1}{k_{z.d} + \sqrt{k_{z.d}^{2} - \lambda_{rel.z.d}^{2}}} = 0.15$$

$$P_{d.cr.EC5.y} := \frac{1}{\frac{1}{k_{c.y.d} \cdot f_{c.0.d.GL} \cdot A_{beam}} + \frac{e_{N.d}}{f_{m.d.GL} \cdot W_{y.d.pre}}} = 8.873 \times 10^{5}\,N$$

$$P_{d.cr.EC5.z} := \frac{1}{\frac{1}{k_{c.z.d} \cdot f_{c.0.d.GL} \cdot A_{beam}} + k_m \cdot \frac{e_{N.d}}{f_{m.d.GL} \cdot W_{y.d.pre}}} = 2.975 \times 10^{5}\,N$$

$$P_{pre3.d} := \max\left(-P_{d.cr.EC5.y}, -P_{d.cr.EC5.z}\right)$$

$$P_{pre3.d} = -2.975 \times 10^{5}\,N$$

$$P_{pre.d} := \max\left(P_{pre1.d}, P_{pre2.d}, P_{pre3.d}\right)$$

$$P_{pre.d} = -2.975 \times 10^{5}\,N$$

Elastic phase

$$\sigma_{top.init} := \frac{P_{pre.d}}{A_{d.trans.p}} + \frac{P_{pre.d} \cdot e_{N.d}}{I_{y.d.pre}} \cdot \left(-z_{NA.d.pre}\right) = 1.921 \times 10^{6}\,\text{Pa}$$

$$\sigma_{bot.init} := \frac{P_{pre.d}}{A_{d.trans.p}} + \frac{P_{pre.d} \cdot e_{N.d}}{I_{y.d.pre}} \cdot \left(h - z_{NA.d.pre}\right) = -4.85 \times 10^{6}\,\text{Pa}$$

$$\varepsilon_{c.init.e.p} := \frac{\sigma_{top.init}}{E_{0.d.GL.mean}} = 2.07 \times 10^{-4}$$

$$\varepsilon_{t.init.p} := \frac{\sigma_{bot.init}}{E_{0.d.GL.mean}} = -5.227 \times 10^{-4}$$

$$\varepsilon_{c.limit.e.p} := -\frac{f_{c.0.d.GL}}{E_{0.d.GL.mean}} = -1.655 \times 10^{-3}$$

$$\varepsilon_{t.limit.p} := \frac{f_{t.0.d.GL}}{E_{0.d.GL.mean}} = 2.517 \times 10^{-3}$$

$$\varepsilon_{add.p} := \frac{\varepsilon_{c.limit.e.p}}{100} = -1.655 \times 10^{-5}$$

$$\begin{pmatrix} M_{cap.pr.e} \\ \varepsilon_{c.GL.pre.e} \\ \varepsilon_{t.GL.pre.e} \\ \sigma_{c.RF.pr.e} \\ \sigma_{t.RF.pr.e} \\ Failure\_mode_{pre.e} \end{pmatrix} :=$$

$i \leftarrow 0$

$\varepsilon_c \leftarrow \varepsilon_{c.init.e.p}$

while $\varepsilon_c > \varepsilon_{c.limit.e.p}$

$$M_{load} \leftarrow \frac{\left(E_{0.d.GL.mean} \cdot \varepsilon_c \cdot A_{d.trans.p} - P_{pre.d}\right) \cdot I_{y.d.pre}}{A_{d.trans.p} \cdot \left(-z_{NA.d.pre}\right)} \ldots + -\left(P_{pre.d} \cdot e_{N.d}\right)$$

$z_{GL.c} \leftarrow -z_{NA.d.pre}$

$z_{RF.c} \leftarrow Z_{c.p} - z_{NA.d.pre}$

$z_{RF.t} \leftarrow h - z_{NA.d.pre} - Z_{t.p}$

$z_{GL.t} \leftarrow h - z_{NA.d.pre}$

$$\varepsilon_{c.GL.M} \leftarrow (-1) \cdot \frac{M_{load}}{E_{0.d.GL.mean} \cdot I_{y.d.pre}} \cdot z_{GL.c}$$

$$\varepsilon_{c.RF.M} \leftarrow (-1) \cdot \frac{M_{load}}{E_{0.d.GL.mean} \cdot I_{y.d.pre}} \cdot z_{RF.c}$$

$$\varepsilon_{t.RF.M} \leftarrow \frac{M_{load}}{E_{0.d.GL.mean} \cdot I_{y.d.pre}} \cdot z_{RF.t}$$

$$\varepsilon_{t.GL.M} \leftarrow \frac{M_{load}}{E_{0.d.GL.mean} \cdot I_{y.d.pre}} \cdot z_{GL.t}$$

$$M \leftarrow \frac{1}{2} \cdot \varepsilon_{c.GL.M} \cdot E_{0.d.GL.mean} \cdot \frac{2}{3} \cdot w \cdot z_{NA.d.pre}^{2} \ldots + \varepsilon_{c.RF.M} \cdot E_{0.d.RF} \cdot A_{c.RF.p} \cdot \left(z_{NA.d.pre} - Z_{c.p}\right) \ldots + \frac{1}{2} \cdot \varepsilon_{t.GL.M} \cdot E_{0.d.GL.mean} \cdot \frac{2}{3} \cdot w \cdot \left(h - z_{NA.d.pre}\right)^{2} \ldots + \varepsilon_{t.RF.M} \cdot E_{0.d.RF} \cdot A_{t.RF.p} \cdot \left(h - z_{NA.d.pre} - Z_{t.p}\right)$$

$$\varepsilon_t \leftarrow \frac{P_{pre.d}}{E_{0.d.GL.mean} \cdot A_{d.trans.p}} + \frac{P_{pre.d} \cdot e_{N.d} + M_{load}}{E_{0.d.GL.mean} \cdot I_{y.d.pre}} \cdot z_{GL.t}$$

$$b_i \leftarrow \varepsilon_c$$

$$c_i \leftarrow \varepsilon_t$$

$$d_i \leftarrow E_{0.d.RF} \cdot \varepsilon_{c.RF.M} \cdot \frac{1}{Pa}$$

$$e_i \leftarrow E_{0.d.RF} \cdot \varepsilon_{t.RF.M} \cdot \frac{1}{Pa}$$

break if $\varepsilon_t > \varepsilon_{t.limit.p}$

$$a_i \leftarrow M \cdot \frac{1}{J}$$

$$i \leftarrow i + 1$$

$$\varepsilon_c \leftarrow \varepsilon_c + \varepsilon_{add.p}$$

$$f \leftarrow \begin{cases} \text{"Tension"} & \text{if } \varepsilon_t > \varepsilon_{t.limit.p} \\ \text{"Plastic phase"} & \text{otherwise} \end{cases}$$

$$\begin{pmatrix} a \\ b \\ c \\ d \\ e \\ f \end{pmatrix}$$

$$M_{cap.pre.e} := M_{cap.pr.e} \cdot J \qquad \sigma_{c.RF.pre.e} := \sigma_{c.RF.pr.e} \cdot Pa \qquad \sigma_{t.RF.pre.e} := \sigma_{t.RF.pr.e} \cdot Pa$$

$$Failure\_mode_{pre.e} = \text{"Plastic phase"}$$

$$M_{cap.pre.el} := \max\left(M_{cap.pre.e}\right) = 434.174\,kN \cdot m$$

Plastic phase

$$\varepsilon_{c.limit.pl.p} := -\left(3\varepsilon_{c.limit.e.p}\right) = 4.966 \times 10^{-3}$$

$$\varepsilon_{c.init.pl.p} := -\left(\min\left(\varepsilon_{c.GL.pre.e}\right)\right) = 1.647 \times 10^{-3}$$

$\varepsilon_{c.limit.e.p} := -\varepsilon_{c.limit.e.p} = 1.655\times 10^{-3}$

$\varepsilon_{add.pl.p} := \frac{\varepsilon_{c.limit.e.p}}{100} = 1.655\times 10^{-5}$

$\varepsilon_P := -\frac{P_{pre.d}}{E_{0.d.RF}\cdot A_{t.RF.p}} = 1.481\times 10^{-3}$

$\sigma_{RF.c.pl.init.p} := \max(\sigma_{c.RF.pre.e}) = 2.407\times 10^{8}\,Pa$

$\sigma_{RF.t.pl.init.p} := \max(\sigma_{t.RF.pre.e}) = 2.138\times 10^{8}\,Pa$

$z_{av} := \frac{\left(-\frac{P_{pre.d}}{A_{d.trans.p}}\right)\cdot I_{y.d.pre}}{\max(M_{cap.pre.e}) + P_{pre.d}\cdot e_{N.d}} = 0.043m$

$z_{NA.pl.init} := z_{NA.d.pre} + z_{av} = 0.412m$

$$\begin{pmatrix} M_{cap.pr.pl} \\ \varepsilon_{c.GL.pre.pl} \\ \varepsilon_{t.GL.pre.pl} \\ \sigma_{c.RF.pr.pl} \\ \sigma_{t.RF.pr.pl} \\ Failure\_mode_{pre.pl} \end{pmatrix} := \left| \begin{array}{l} i \leftarrow 0 \\ \varepsilon_c \leftarrow \varepsilon_{c.init.pl.p} \\ \sigma_{RF.c} \leftarrow \sigma_{RF.c.pl.init.p} \\ \sigma_{RF.t} \leftarrow \sigma_{RF.t.pl.init.p} \\ z_{NA.pl} \leftarrow z_{NA.pl.init} \\ \text{while } \varepsilon_c < \varepsilon_{c.limit.pl.p} \\ \quad \left| \begin{array}{ll} x \leftarrow & f_{c.0.d.GL}\cdot w\cdot\left(1-\frac{\varepsilon_{c.limit.e.p}}{\varepsilon_c}\right) \ldots \quad \text{if } \sigma_{RF.c} < f_{y.RF.d} \wedge \sigma_{RF.t} < f_{y.RF.d} \\ & +f_{c.0.d.GL}\cdot\frac{w}{2}\cdot\left(\frac{\varepsilon_{c.limit.e.p}}{\varepsilon_c}\right) \ldots \\ & +-\left(\varepsilon_c\cdot\frac{w}{2}\cdot E_{0.d.GL.mean}\right) \\ & f_{c.0.d.GL}\cdot w\cdot\left(1-\frac{\varepsilon_{c.limit.e.p}}{\varepsilon_c}\right) \ldots \quad \text{if } \sigma_{RF.c} \geq f_{y.RF.d} \wedge \sigma_{RF.t} < f_{y.RF.d} \\ & +\frac{f_{c.0.d.GL}\cdot w}{2} \ldots \\ & +-\frac{f_{c.0.d.GL}\cdot w}{2}\cdot\frac{\varepsilon_c-\varepsilon_{c.limit.e.p}}{\varepsilon_c} \ldots \\ & +-\varepsilon_c\cdot\frac{w}{2}\cdot E_{0.d.GL.mean} \\ & f_{c.0.d.GL}\cdot w\cdot\left(1-\frac{\varepsilon_{c.limit.e.p}}{\varepsilon_c}\right) \ldots \quad \text{if } \sigma_{RF.c} < f_{y.RF.d} \wedge \sigma_{RF.t} \geq f_{y.RF.d} \end{array} \right. \end{array} \right.$$

$$
\begin{aligned}
&\left|
\begin{array}{l}
+\dfrac{f_{c.0.d.GL}\cdot w}{2} \ldots \\
+-\dfrac{f_{c.0.d.GL}\cdot w}{2}\cdot\dfrac{\varepsilon_c-\varepsilon_{c.limit.e.p}}{\varepsilon_c} \ldots \\
+-\varepsilon_c\cdot\dfrac{w}{2}\cdot E_{0.d.GL.mean} \\
\dfrac{1}{2}\cdot f_{c.0.d.GL}\cdot w\cdot\dfrac{\varepsilon_c-\varepsilon_{c.limit.e.p}}{\varepsilon_c} \ldots \quad \text{if } \sigma_{RF.c}\geq f_{y.RF.d}\wedge\sigma_{RF.t}\geq f_{y.RF.d} \\
+\dfrac{1}{2}f_{c.0.d.GL}\cdot w-\dfrac{1}{2}\varepsilon_c\cdot E_{0.d.GL.mean}\cdot w
\end{array}
\right. \\
y\leftarrow &\left|
\begin{array}{l}
-E_{0.d.RF}\cdot A_{t.RF.p}\cdot\left(-\varepsilon_c+\varepsilon_p\right) \ldots \quad \text{if } \sigma_{RF.c}<f_{y.RF.d}\wedge\sigma_{RF.t}<f_{y.RF.d} \\
+E_{0.d.GL.mean}\cdot w\cdot h\cdot\varepsilon_c \ldots \\
+E_{0.d.RF}\cdot A_{c.RF.p}\cdot\varepsilon_c \\
f_{y.RF.d}\cdot A_{c.RF.p} \ldots \quad \text{if } \sigma_{RF.c}\geq f_{y.RF.d}\wedge\sigma_{RF.t}<f_{y.RF.d} \\
+E_{0.d.GL.mean}\cdot\varepsilon_c\cdot w\cdot h \ldots \\
+-E_{0.d.RF}\cdot A_{t.RF.p}\cdot\left(-\varepsilon_c+\varepsilon_p\right) \\
\varepsilon_c\cdot E_{0.d.RF}\cdot A_{c.RF.p} \ldots \quad \text{if } \sigma_{RF.c}<f_{y.RF.d}\wedge\sigma_{RF.t}\geq f_{y.RF.d} \\
+E_{0.d.GL.mean}\cdot\varepsilon_c\cdot w\cdot h \ldots \\
+-f_{y.RF.d}\cdot A_{t.RF.p} \\
f_{y.RF.d}\cdot A_{c.RF.p}-f_{y.RF.d}\cdot A_{t.RF.p} \ldots \quad \text{if } \sigma_{RF.c}\geq f_{y.RF.d}\wedge\sigma_{RF.t}\geq f_{y.RF.d} \\
+E_{0.d.GL.mean}\cdot\varepsilon_c\cdot w\cdot h
\end{array}
\right. \\
z\leftarrow &\left|
\begin{array}{l}
\varepsilon_c\cdot\left[-E_{0.d.RF}\cdot A_{t.RF.p}\cdot\left(h-Z_{t.p}\right)\right] \ldots \quad \text{if } \sigma_{RF.c}<f_{y.RF.d}\wedge\sigma_{RF.t}<f_{y.RF.d} \\
+-\dfrac{\varepsilon_c\cdot E_{0.d.GL.mean}\cdot w\cdot h^2}{2} \ldots \\
+-\varepsilon_c\cdot E_{0.d.RF}\cdot A_{c.RF.p}\cdot\left(Z_{c.p}\right) \\
\left(-\varepsilon_c\right)\cdot\dfrac{w\cdot h^2}{2}\cdot E_{0.d.GL.mean} \ldots \quad \text{if } \sigma_{RF.c}\geq f_{y.RF.d}\wedge\sigma_{RF.t}<f_{y.RF.d} \\
+-\varepsilon_c\cdot E_{0.d.RF}\cdot A_{t.RF.p}\cdot\left(h-Z_{t.p}\right) \\
-\varepsilon_c\cdot\dfrac{w\cdot h^2}{2}\cdot E_{0.d.GL.mean} \ldots \quad \text{if } \sigma_{RF.c}<f_{y.RF.d}\wedge\sigma_{RF.t}\geq f_{y.RF.d} \\
+-\varepsilon_c\cdot E_{0.d.RF}\cdot A_{c.RF.p}\cdot Z_{c.p} \\
-\left(\dfrac{\varepsilon_c\cdot E_{0.d.GL.mean}\cdot w\cdot h^2}{2}\right) \quad \text{if } \sigma_{RF.c}\geq f_{y.RF.d}\wedge\sigma_{RF.t}\geq f_{y.RF.d}
\end{array}
\right. \\
z_{NA.pl}&\leftarrow\frac{-y+\sqrt{y^2-4\cdot x\cdot z}}{2\cdot x} \\
z_{pl}&\leftarrow\frac{\varepsilon_c-\varepsilon_{c.limit.e.p}}{\varepsilon_c}\cdot z_{NA.pl}
\end{aligned}
$$

$$\varepsilon_t \leftarrow \left(\frac{h}{z_{NA.pl}} - 1\right)\cdot\varepsilon_c$$

$$\varepsilon_{RF.c} \leftarrow \left(1 - \frac{Z_{c.p}}{z_{NA.pl}}\right)\cdot\varepsilon_c$$

$$\varepsilon_{RF.t} \leftarrow \frac{h - z_{NA.pl} - Z_{t.p}}{z_{NA.pl}}\cdot\varepsilon_c + \varepsilon_p$$

$$\sigma_{RF.c} \leftarrow \varepsilon_{RF.c}\cdot E_{0.d.RF}$$

$$\sigma_{RF.t} \leftarrow \varepsilon_{RF.t}\cdot E_{0.d.RF}$$

$$M \leftarrow \sigma_{RF.c}\cdot A_{c.RF.p}\cdot\left(z_{NA.pl} - Z_{c.p}\right) \ldots + f_{c.0.d.GL}\cdot w\cdot z_{pl}\cdot\left(z_{NA.pl} - \frac{z_{pl}}{2}\right) \ldots + f_{c.0.d.GL}\cdot\frac{z_{NA.pl} - z_{pl}}{2}\cdot w\cdot\frac{2\left(z_{NA.pl} - z_{pl}\right)}{3} \ldots + \sigma_{RF.t}\cdot A_{t.RF.p}\cdot\left(h - z_{NA.pl} - Z_{t.p}\right) \ldots + \varepsilon_t\cdot E_{0.d.GL.mean}\cdot\frac{h - z_{NA.pl}}{2}\cdot w\cdot\frac{2\left(h - z_{NA.pl}\right)}{3}$$

$$b_i \leftarrow \varepsilon_c$$

$$c_i \leftarrow \varepsilon_t$$

$$d_i \leftarrow \sigma_{RF.c}\cdot\frac{1}{Pa}$$

$$e_i \leftarrow \sigma_{RF.t}\cdot\frac{1}{Pa}$$

break if $\varepsilon_t > \varepsilon_{t.limit.p}$

$$a_i \leftarrow M\cdot\frac{1}{J}$$

$$i \leftarrow i + 1$$

$$\varepsilon_c \leftarrow \varepsilon_c + \varepsilon_{add.pl.p}$$

$$f \leftarrow \begin{cases} \text{"Tension"} & \text{if } \varepsilon_t > \varepsilon_{t.limit.p} \\ \text{"Compression"} & \text{otherwise} \end{cases}$$

$$\begin{pmatrix} a \\ b \\ c \\ d \\ e \\ f \end{pmatrix}$$

$M_{cap.pre.p} := M_{cap.pr.pl}\cdot J$ $\sigma_{c.RF.pre.pl} := \sigma_{c.RF.pr.pl}\cdot Pa$ $\sigma_{t.RF.pre.pl} := \sigma_{t.RF.pr.pl}\cdot Pa$

$Failure\_mode_{pre.pl} = \text{"Tension"}$

$M_{cap.pre.pl} := \max\left(M_{cap.pre.p}\right) = 715.173\,kN\cdot m$

$$M_{cap.d.pre} := \max\left(M_{cap.pre.el}, M_{cap.pre.pl}\right) = 715.173\,kN\cdot m$$

Camber

$$\delta_{camb.pre.d}(x) := \left(P_{pre.d}\cdot e_{N.d}\right)\cdot\frac{\left(L_s - x\right)\cdot L_s}{6\cdot EI_{d.ef.pre}}\cdot\left[1 - \frac{\left(L_s - x\right)^2}{L_s^{\,2}}\right] \ldots$$

$$+\left(P_{pre.d}\cdot e_{N.d}\right)\cdot\frac{x\cdot L_s}{6\cdot EI_{d.ef.pre}}\cdot\left(1 - \frac{x^2}{L_s^{\,2}}\right) + \frac{G_{pre}\cdot x\cdot L_s^{\,3}}{24\cdot EI_{d.ef.pre}}\cdot\left(1 - \frac{2\cdot x^2}{L_s^{\,2}} + \frac{x^3}{L_s^{\,3}}\right)$$

$$\delta_{camb.mid.pre.d} := \delta_{camb.pre.d}\left(\frac{L_s}{2}\right) = -0.012\,m$$

Camber - at midspan

$\delta_{camb.mid.pre.d} = -0.012\,m$ (Negative value gives a positive camber - upwards)

Shear

$$f_{v.d.pre} := f_{v.0.d.GL} = 1.728\times 10^6\,Pa$$

$$V_{cap.d.pre} := \frac{f_{v.d.pre}\cdot I_{y.d.pre}\cdot w}{S_{d.pre}} = 2.318\times 10^5\,N$$

4. Maximum load capacity

$\gamma_{Q.ULS} := 1.5$ $\quad$ $\gamma_{Q.SLS} := 1$ $\qquad$ $\gamma_{G.ULS} := 1.35$ $\quad$ $\gamma_{G.SLS} := 1$

Functions and values needed for analysis

$$L_{sq} := L_s\cdot\frac{1}{m} = 10 \qquad x_{init} := 0.4\,L_{sq} \qquad Q_{init} := 1$$

$$M_{Q.tri}\left(x, Q_q\right) := \frac{\gamma_{Q.ULS}\cdot Q_q\cdot L_{sq}\cdot x}{6}\cdot\left(1 - \frac{x^2}{L_{sq}^{\,2}}\right)$$

4.1 Regular glulam beam - ULS

Functions and values needed for analysis

$$G_{regq} := G_{reg}\cdot\frac{m}{N} = 560.842$$

$$M_{self.regq}(x) := \frac{\gamma_{G.ULS}\,G_{regq}\cdot L_{sq}\cdot x}{2} - \frac{\gamma_{G.ULS}\,G_{regq}\cdot x^2}{2}$$

4.1.1 Bending - EC5

$$Q_{m.d.reg.uni.EC5} := \frac{8}{\gamma_{Q.ULS} \cdot L_s^{\,2}} \cdot \left(M_{cap.EC5.d.reg} - \frac{\gamma_{G.ULS} G_{reg} \cdot L_s^{\,2}}{8} \right) = 1.628 \times 10^4 \, \frac{kg}{s^2}$$

$$P_{m.d.reg.EC5} := \frac{4}{\gamma_{Q.ULS} \cdot L_s} \cdot \left(M_{cap.EC5.d.reg} - \frac{\gamma_{Q.ULS} G_{reg} \cdot L_s^{\,2}}{8} \right) = 8.11 \times 10^4 \, N$$

$$M_{tot}(x, Q_q) := M_{self.regq}(x) + M_{Q.tri}(x, Q_q)$$

$$M_{test}(x, Q_{q.}) := M_{cap.EC5.d.reg} \cdot \frac{1}{J}$$

Given

$$0.49 L_{sq} < x_{init} < 0.578 L_{sq}$$

$$M_{tot}(x_{init}, Q_{init}) = M_{test}(x_{init}, Q_{init})$$

$$\begin{pmatrix} x_{max} \\ Q_{max} \end{pmatrix} := \text{Find}(x_{init}, Q_{init}) = \begin{pmatrix} 4.9 \\ 3.278 \times 10^4 \end{pmatrix}$$

$$Q_{m.d.reg.tri.EC5} := Q_{max} \cdot \frac{N}{m} = 3.278 \times 10^4 \, \frac{kg}{s^2}$$

$$Q_{m.d.reg.uni.EC5} = 1.628 \times 10^4 \cdot \frac{N}{m} \qquad P_{m.d.reg.EC5} = 8.11 \times 10^4 \, N$$

$$Q_{m.d.reg.tri.EC5} = 3.278 \times 10^4 \cdot \frac{N}{m}$$

4.1.2 Bending with consideration to lateral torsional stability

$$Q_{m.d.reg.uni.buck} := \frac{8}{\gamma_{Q.ULS} \cdot L_s^{\,2}} \cdot \left(M_{cap.buck.d.reg} - \frac{\gamma_{G.ULS} G_{reg} \cdot L_s^{\,2}}{8} \right) = 1.541 \times 10^4 \cdot \frac{N}{m}$$

$$P_{m.d.reg.buck} := \frac{4}{\gamma_{Q.ULS} \cdot L_s} \cdot \left(M_{cap.buck.d.reg} - \frac{\gamma_{G.ULS} G_{reg} \cdot L_s^{\,2}}{8} \right) = 7.705 \times 10^4 \, N$$

$$M_{tot}(x, Q_q) := M_{self.regq}(x) + M_{Q.tri}(x, Q_q)$$

$$M_{test}(x, Q_{q.}) := M_{cap.buck.d.reg} \cdot \frac{1}{J}$$

Given

$$0.49 L_{sq} < x_{init} < 0.578 L_{sq}$$

$$M_{tot}(x_{init}, Q_{init}) = M_{test}(x_{init}, Q_{init})$$

$$\begin{pmatrix} x_{max} \\ Q_{max} \end{pmatrix} := \text{Find}(x_{init}, Q_{init}) = \begin{pmatrix} 4.9 \\ 3.104\times 10^{4} \end{pmatrix}$$

$$Q_{m.d.reg.tri.buck} := Q_{max} \cdot \frac{N}{m} = 3.104\times 10^{4} \frac{kg}{s^2}$$

$Q_{m.d.reg.uni.buck} = 1.541\times 10^{4} \cdot \frac{N}{m}$ $P_{m.d.reg.buck} = 7.705\times 10^{4}\,N$

$Q_{m.d.reg.tri.buck} = 3.104\times 10^{4} \cdot \frac{N}{m}$

4.1.3 Bending using our model

$$Q_{m.d.reg.uni} := \frac{8}{\gamma_{Q.ULS} \cdot L_s^{2}} \cdot \left(M_{cap.d.reg} - \frac{\gamma_{G.ULS} G_{reg} \cdot L_s^{2}}{8} \right) = \blacksquare \cdot \frac{N}{m}$$

$$P_{m.d.reg} := \frac{4}{\gamma_{Q.ULS} \cdot L_s} \cdot \left(M_{cap.d.reg} - \frac{\gamma_{G.ULS} G_{reg} \cdot L_s^{2}}{8} \right) = \blacksquare$$

$$M_{tot}(x, Q_q) := M_{self.regq}(x) + M_{Q.tri}(x, Q_q)$$

$$M_{test}(x, Q_q) := M_{cap.d.reg} \cdot \frac{1}{J}$$

Given

$0.49 L_{sq} < x_{init} < 0.578 L_{sq}$

$M_{tot}(x_{init}, Q_{init}) = M_{test}(x_{init}, Q_{init})$

$$\begin{pmatrix} x_{max} \\ Q_{max} \end{pmatrix} := \text{Find}(x_{init}, Q_{init}) = \begin{pmatrix} 5.78 \\ 3.857\times 10^{4} \end{pmatrix}$$

$$Q_{m.d.reg.tri} := Q_{max} \cdot \frac{N}{m} = 3.857\times 10^{4} \frac{kg}{s^2}$$

$Q_{m.d.reg.uni} = 1.978\times 10^{4} \cdot \frac{N}{m}$ $P_{m.d.reg} = 9.892\times 10^{4}\,N$

$Q_{m.d.reg.tri} = 3.857\times 10^{4} \cdot \frac{N}{m}$

4.1.4 Shear force

$$Q_{v.d.reg.uni} := \frac{2}{\gamma_{Q.ULS} \cdot L_s} \cdot \left(V_{cap.d.reg} - \frac{\gamma_{G.ULS} G_{reg} \cdot L_s}{2} \right) = 2.261\times 10^{4} \cdot \frac{N}{m}$$

$$P_{v.d.reg} := \frac{2}{\gamma_{Q.ULS}} \cdot \left(V_{cap.d.reg} - \frac{\gamma_{G.ULS} G_{reg} \cdot L_s}{2} \right) = 2.261\times 10^{5}\,N$$

$$Q_{v.d.reg.tri} := \frac{3}{\gamma_{Q.ULS} L_s} \cdot \left(V_{cap.d.reg} - \frac{\gamma_{G.ULS} G_{reg} \cdot L_s}{2} \right) = 3.392 \times 10^4 \cdot \frac{N}{m}$$

$Q_{v.d.reg.uni} = 2.261 \times 10^4 \cdot \frac{N}{m}$ $\quad P_{v.d.reg} = 2.261 \times 10^5 \, N$ $\quad Q_{v.d.reg.tri} = 3.392 \times 10^4 \cdot \frac{N}{m}$

4.2 Slack-reinforced glulam beam - ULS

Functions and values needed for analysis

$$G_{slackq} := G_{slack} \cdot \frac{m}{N} = 581.848$$

$$M_{self.slackq}(x) := \frac{\gamma_{G.ULS} G_{slackq} \cdot L_{sq} \cdot x}{2} - \frac{\gamma_{G.ULS} G_{slackq} \cdot x^2}{2}$$

4.2.1 Bending using our model

$$Q_{m.d.slack.uni} := \frac{8}{\gamma_{Q.ULS} L_s^2} \cdot \left(M_{cap.d.slack} - \frac{\gamma_{G.ULS} G_{slack} \cdot L_s^2}{8} \right) = 3.217 \times 10^4 \cdot \frac{N}{m}$$

$$P_{m.d.slack} := \frac{4}{\gamma_{Q.ULS} L_s} \cdot \left(M_{cap.d.slack} - \frac{\gamma_{G.ULS} G_{slack} \cdot L_s^2}{8} \right) = 1.608 \times 10^5 \, N$$

$$M_{tot}(x, Q_q) := M_{self.slackq}(x) + M_{Q.tri}(x, Q_q)$$

$$M_{test}(x, Q_{q.}) := M_{cap.d.slack} \cdot \frac{1}{J}$$

Given

$0.49 L_{sq} < x_{init} < 0.578 L_{sq}$

$$M_{tot}(x_{init}, Q_{init}) = M_{test}(x_{init}, Q_{init})$$

$$\begin{pmatrix} x_{max} \\ Q_{max} \end{pmatrix} := Find(x_{init}, Q_{init}) = \begin{pmatrix} 5.78 \\ 6.27 \times 10^4 \end{pmatrix}$$

$$Q_{m.d.slack.tri} := Q_{max} \cdot \frac{N}{m} = 6.27 \times 10^4 \, \frac{kg}{s^2}$$

$Q_{m.d.slack.uni} = 3.217 \times 10^4 \cdot \frac{N}{m}$ $\quad P_{m.d.slack} = 1.608 \times 10^5 \, N$ $\quad Q_{m.d.slack.tri} = 6.27 \times 10^4 \cdot \frac{N}{m}$

4.2.2 Shear force

$$Q_{v.d.slack.uni} := \frac{2}{\gamma_{Q.ULS} L_s} \cdot \left(V_{cap.d.slack} - \frac{\gamma_{G.ULS} G_{slack} \cdot L_s}{2} \right) = 3.039 \times 10^4 \cdot \frac{N}{m}$$

$$P_{v.d.slack} := \frac{2}{\gamma_{Q.ULS}} \cdot \left(V_{cap.d.slack} - \frac{\gamma_{G.ULS} G_{slack} \cdot L_s}{2} \right) = 3.039 \times 10^5 \, N$$

$$Q_{v.d.slack.tri} := \frac{3}{\gamma_{Q.ULS} \cdot L_s} \cdot \left(V_{cap.d.slack} - \frac{\gamma_{G.ULS} G_{slack} \cdot L_s}{2} \right) = 4.558 \times 10^4 \cdot \frac{N}{m}$$

$Q_{v.d.slack.uni} = 3.039 \times 10^4 \cdot \frac{N}{m}$ $P_{v.d.slack} = 3.039 \times 10^5 \, N$ $Q_{v.d.slack.tri} = 4.558 \times 10^4 \cdot \frac{N}{m}$

4.3 Pre-stressed glulam beam - ULS

Functions and values needed for analysis

$$G_{preq} := G_{pre} \cdot \frac{m}{N} = 581.848$$

$$M_{self.preq}(x) := \frac{\gamma_{G.ULS} G_{preq} \cdot L_{sq} \cdot x}{2} - \frac{\gamma_{G.ULS} G_{preq} \cdot x^2}{2}$$

4.3.1 Bending using our model

$$Q_{m.d.pre.uni} := \frac{8}{\gamma_{Q.ULS} \cdot L_s^2} \cdot \left(M_{cap.d.pre} - \frac{\gamma_{G.ULS} G_{pre} \cdot L_s^2}{8} \right) = 3.762 \times 10^4 \cdot \frac{N}{m}$$

$$P_{m.d.pre} := \frac{4}{\gamma_{Q.ULS} \cdot L_s} \cdot \left(M_{cap.d.pre} - \frac{\gamma_{G.ULS} G_{pre} \cdot L_s^2}{8} \right) = 1.881 \times 10^5 \, N$$

$$M_{tot}(x, Q_q) := M_{self.preq}(x) + M_{Q.tri}(x, Q_q)$$

$$M_{test}(x, Q_{q.}) := M_{cap.d.pre} \cdot \frac{1}{J}$$

Given

$0.48 \cdot L_{sq} < x_{init} < 0.578 L_{sq}$

$M_{tot}(x_{init}, Q_{init}) = M_{test}(x_{init}, Q_{init})$

$$\begin{pmatrix} x_{max} \\ Q_{max} \end{pmatrix} := Find(x_{init}, Q_{init}) = \begin{pmatrix} 5.78 \\ 7.333 \times 10^4 \end{pmatrix}$$

$$Q_{m.d.pre.tri} := Q_{max} \cdot \frac{N}{m} = 7.333 \times 10^4 \, \frac{kg}{s^2}$$

$Q_{m.d.pre.uni} = 3.762 \times 10^4 \cdot \frac{N}{m}$ $P_{m.d.pre} = 1.881 \times 10^5 \, N$ $Q_{m.d.pre.tri} = 7.333 \times 10^4 \cdot \frac{N}{m}$

4.3.2 Shear force

$$Q_{v.d.pre.uni} := \frac{2}{\gamma_{Q.ULS} \cdot L_s} \cdot \left(V_{cap.d.pre} - \frac{\gamma_{G.ULS} G_{pre} \cdot L_s}{2} \right) = 3.039 \times 10^4 \cdot \frac{N}{m}$$

$$P_{v.d.pre} := \frac{2}{\gamma_{Q.ULS}} \cdot \left(V_{cap.d.pre} - \frac{\gamma_{G.ULS} G_{pre} \cdot L_s}{2} \right) = 3.039 \times 10^5 \, N$$

$$Q_{v.d.pre.tri} := \frac{3}{\gamma_{Q.ULS} \cdot L_s} \cdot \left(V_{cap.d.pre} - \frac{\gamma_{G.ULS} G_{pre} \cdot L_s}{2} \right) = 4.558 \times 10^4 \cdot \frac{N}{m}$$

$Q_{v.d.pre.uni} = 3.039 \times 10^4 \cdot \frac{N}{m}$ $\quad$ $P_{v.d.pre} = 3.039 \times 10^5 \, N$ $\quad$ $Q_{v.d.pre.tri} = 4.558 \times 10^4 \cdot \frac{N}{m}$

4.4 Regular glulam beam - SLS

Functions and values needed for analysis

$$E_{0.d.GL.meanq} := E_{0.d.GL.mean} \cdot \frac{1}{Pa} = 9.28 \times 10^9 \qquad E_{0.k.GL.meanq} := E_{0.k.GL.mean} \cdot \frac{1}{Pa} = 1.16 \times 10^{10}$$

$$I_{y.regq} := I_{y.reg} \cdot \frac{1}{m^4} = 6.145 \times 10^{-3}$$

Instantaneous

Uniformly distributed load

$$Q_{\delta.d.reg.uni.inst} := \frac{384 E_{0.d.GL.mean} \cdot I_{y.reg}}{5 \cdot L_s^4} \cdot \left(\delta_{lim.inst} - \frac{5 \cdot G_{reg} \cdot L_s^4}{384 E_{0.d.GL.mean} \cdot I_{y.reg}} \right) = 1.039 \times 10^4 \cdot \frac{N}{m}$$

Point load

$$P_{\delta.d.reg.inst} := \frac{48 \cdot E_{0.d.GL.mean} \cdot I_{y.reg}}{L_s^3} \cdot \left(\delta_{lim.inst} - \frac{5 \cdot G_{reg} \cdot L_s^4}{384 E_{0.d.GL.mean} \cdot I_{y.reg}} \right) = 6.493 \times 10^4 \, N$$

Triangular distributed load

$$\delta_{inst.perm.tri.reg.d}(x) := \frac{G_{regq} \cdot x \cdot L_{sq}^3}{24 \cdot E_{0.d.GL.meanq} \cdot I_{y.regq}} \cdot \left(1 - \frac{2 \cdot x^2}{L_{sq}^2} + \frac{x^3}{L_{sq}^3} \right)$$

$$\delta_{inst.var.tri.reg.d}(x, Q_q) := \frac{Q_q \cdot x \cdot L_{sq}^3}{360 \cdot E_{0.d.GL.meanq} \cdot I_{y.regq}} \cdot \left(7 - \frac{10 \cdot x^2}{L_{sq}^2} + \frac{3 \cdot x^4}{L_{sq}^4} \right)$$

$$\delta_{inst.reg.d}(x, Q_q) := \delta_{inst.perm.tri.reg.d}(x) + \delta_{inst.var.tri.reg.d}(x, Q_q)$$

$$\delta_{test}(x, Q_q) := \delta_{lim.inst} \cdot \frac{1}{m}$$

Given

$$0.49 \cdot L_{sq} < x_{init} < 0.578 \cdot L_{sq}$$

$$\delta_{inst.reg.d}(x_{init}, Q_{init}) = \delta_{test}(x_{init}, Q_{init})$$

$$\begin{pmatrix} x_{max} \\ Q_{max} \end{pmatrix} := \text{Find}(x_{init}, Q_{init})$$

$$Q_{\delta.d.reg.tri.inst} := Q_{max} \cdot \frac{N}{m} = 2.083 \times 10^4 \cdot \frac{N}{m}$$

Final

Uniformly distributed load

$$Q_{\delta.d.reg.uni.fin} := \frac{384 E_{0.d.GL.mean} \cdot I_{y.reg}}{\left(1 + \psi_2 \cdot k_{def}\right) \cdot 5 \cdot L_s^{\,4}} \cdot \left[\delta_{lim.fin} - \left(\frac{5 \cdot G_{reg} \cdot L_s^{\,4}}{384 E_{0.d.GL.mean} \cdot I_{y.reg}} \right) \cdot \left(1 + k_{def}\right) \right]$$

$$Q_{\delta.d.reg.uni.fin} = 1.423 \times 10^4 \frac{N}{m}$$

Point load

$$P_{\delta.d.reg.fin} := \frac{48 \cdot E_{0.d.GL.mean} \cdot I_{y.reg}}{\left(1 + \psi_2 \cdot k_{def}\right) \cdot L_s^{\,3}} \cdot \left[\delta_{lim.fin} - \left(\frac{5 \cdot G_{reg} \cdot L_s^{\,4}}{384 E_{0.d.GL.mean} \cdot I_{y.reg}} \right) \cdot \left(1 + k_{def}\right) \right]$$

$$P_{\delta.d.reg.fin} = 8.895 \times 10^4 \, N$$

Triangular distributed load

$$\delta_{fin.reg.d}\left(x, Q_q\right) := \left(1 + k_{def}\right) \cdot \delta_{inst.perm.tri.reg.d}(x) + \left(1 + \psi_2 \cdot k_{def}\right) \cdot \delta_{inst.var.tri.reg.d}\left(x, Q_q\right)$$

$$\delta_{test}\left(x, Q_q\right) := \delta_{lim.fin} \cdot \frac{1}{m}$$

Given

$$0.49 \cdot L_{sq} < x_{init} < 0.578 \cdot L_{sq}$$

$$\delta_{fin.reg.d}\left(x_{init}, Q_{init}\right) = \delta_{test}\left(x_{init}, Q_{init}\right)$$

$$\begin{pmatrix} x_{max} \\ Q_{max} \end{pmatrix} := Find\left(x_{init}, Q_{init}\right)$$

$$Q_{\delta.d.reg.tri.fin} := Q_{max} \cdot \frac{N}{m} = 2.853 \times 10^4 \cdot \frac{N}{m}$$

Max load

$$Q_{\delta.d.reg.uni} := \min\left(Q_{\delta.d.reg.uni.inst}, Q_{\delta.d.reg.uni.fin}\right)$$

$$P_{\delta.d.reg} := \min\left(P_{\delta.d.reg.inst}, P_{\delta.d.reg.fin}\right)$$

$$Q_{\delta.d.reg.tri} := \min\left(Q_{\delta.d.reg.tri.inst}, Q_{\delta.d.reg.tri.fin}\right)$$

$Q_{\delta.d.reg.uni} = 1.039 \times 10^4 \cdot \frac{N}{m}$ $P_{\delta.d.reg} = 6.493 \times 10^4 \, N$ $Q_{\delta.d.reg.tri} = 2.083 \times 10^4 \cdot \frac{N}{m}$

4.5 Slack-reinforced glulam beam - SLS

Functions and values needed for analysis

$$EI_{d.ef.slackq} := EI_{d.ef.slack} \cdot \frac{1}{N \cdot m^2} = 8.459 \times 10^7$$

Instantaneous

Uniformly distributed load

$$Q_{\delta.d.slack.uni.inst} := \frac{384 EI_{d.ef.slack}}{5 \cdot L_s^4} \cdot \left(\delta_{lim.inst} - \frac{5 \cdot G_{slack} \cdot L_s^4}{384 EI_{d.ef.slack}} \right) = 1.566 \times 10^4 \cdot \frac{N}{m}$$

Point load

$$P_{\delta.d.slack.inst} := \frac{48 \cdot EI_{d.ef.slack}}{L_s^3} \cdot \left(\delta_{lim.inst} - \frac{5 \cdot G_{slack} \cdot L_s^4}{384 EI_{d.ef.slack}} \right) = 9.787 \times 10^4 \, N$$

Triangular distributed load

$$\delta_{inst.perm.tri.slack.d}(x) := \frac{G_{slackq} \cdot x \cdot L_{sq}^3}{24 \cdot EI_{d.ef.slackq}} \cdot \left(1 - \frac{2 \cdot x^2}{L_{sq}^2} + \frac{x^3}{L_{sq}^3} \right)$$

$$\delta_{inst.var.tri.slack.d}(x, Q_q) := \frac{Q_q \cdot x \cdot L_{sq}^3}{360 \cdot EI_{d.ef.slackq}} \cdot \left(7 - \frac{10 \cdot x^2}{L_{sq}^2} + \frac{3 \cdot x^4}{L_{sq}^4} \right)$$

$$\delta_{inst.slack.d}(x, Q_q) := \delta_{inst.perm.tri.slack.d}(x) + \delta_{inst.var.tri.slack.d}(x, Q_q)$$

$$\delta_{test}(x, Q_q) := \delta_{lim.inst} \cdot \frac{1}{m}$$

Given

$$0.49 \cdot L_{sq} < x_{init} < 0.578 L_{sq}$$

$$\delta_{inst.slack.d}(x_{init}, Q_{init}) = \delta_{test}(x_{init}, Q_{init})$$

$$\begin{pmatrix} x_{max} \\ Q_{max} \end{pmatrix} := Find(x_{init}, Q_{init})$$

$$Q_{\delta.d.slack.tri.inst} := Q_{max} \cdot \frac{N}{m} = 3.139 \times 10^4 \cdot \frac{N}{m}$$

Final

Uniformly distributed load

$$Q_{\delta.d.slack.uni.fin} := \frac{384 EI_{d.ef.slack}}{(1 + \psi_2 \cdot k_{def}) \cdot 5 \cdot L_s^4} \cdot \left[\delta_{lim.fin} - \left(\frac{5 \cdot G_{slack} \cdot L_s^4}{384 EI_{d.ef.slack}} \right) \cdot (1 + k_{def}) \right] = 2.15 \times 10^4 \cdot \frac{N}{m}$$

Point load

$$P_{\delta.d.slack.fin} := \frac{48 \cdot EI_{d.ef.slack}}{(1 + \psi_2 \cdot k_{def}) \cdot L_s^3} \cdot \left[\delta_{lim.fin} - \left(\frac{5 \cdot G_{slack} \cdot L_s^4}{384 EI_{d.ef.slack}} \right) \cdot (1 + k_{def}) \right] = 1.344 \times 10^5 \, N$$

Triangular distributed load

$$\delta_{fin.slack.d}(x, Q_q) := (1 + k_{def}) \cdot \delta_{inst.perm.tri.slack.d}(x) + (1 + \psi_2 \cdot k_{def}) \cdot \delta_{inst.var.tri.slack.d}(x, Q_q)$$

$$\delta_{test}(x, Q_q) := \delta_{lim.fin} \cdot \frac{1}{m}$$

Given

$$0.49 \cdot L_{sq} < x_{init} < 0.578 \cdot L_{sq}$$

$$\delta_{fin.slack.d}(x_{init}, Q_{init}) = \delta_{test}(x_{init}, Q_{init})$$

$$\begin{pmatrix} x_{max} \\ Q_{max} \end{pmatrix} := \text{Find}(x_{init}, Q_{init})$$

$$Q_{\delta.d.slack.tri.fin} := Q_{max} \cdot \frac{N}{m} = 4.31 \times 10^4 \cdot \frac{N}{m}$$

Max load

$$Q_{\delta.d.slack.uni} := \min(Q_{\delta.d.slack.uni.inst}, Q_{\delta.d.slack.uni.fin})$$

$$P_{\delta.d.slack} := \min(P_{\delta.d.slack.inst}, P_{\delta.d.slack.fin})$$

$$Q_{\delta.d.slack.tri} := \min(Q_{\delta.d.slack.tri.inst}, Q_{\delta.d.slack.tri.fin})$$

$$Q_{\delta.d.slack.uni} = 1.566 \times 10^4 \cdot \frac{N}{m} \qquad P_{\delta.d.slack} = 9.787 \times 10^4 \, N \qquad Q_{\delta.d.slack.tri} = 3.139 \times 10^4 \cdot \frac{N}{m}$$

4.6 Pre-stressed glulam beam - SLS

Functions and values needed for analysis

$$EI_{d.ef.preq} := EI_{d.ef.pre} \cdot \frac{1}{N \cdot m^2} = 8.459 \times 10^7$$

Functions and values needed for analysis

$$P_{pre.dq} := P_{pre.d} \cdot \frac{1}{N} = -2.975 \times 10^5$$

$$e_{N.dq} := e_{N.d} \cdot \frac{1}{m}$$

$$\delta_{camb.pre.dq}(x) := (P_{pre.dq} \cdot e_{N.dq}) \cdot \frac{(L_{sq} - x) \cdot L_{sq}}{6 \cdot EI_{d.ef.preq}} \cdot \left[1 - \frac{(L_{sq} - x)^2}{L_{sq}^2} \right] \ldots + (P_{pre.dq} \cdot e_{N.dq}) \cdot \frac{x \cdot L_{sq}}{6 \cdot EI_{d.ef.preq}} \cdot \left(1 - \frac{x^2}{L_{sq}^2} \right) \ldots + \frac{G_{preq} \cdot x \cdot L_{sq}^3}{24 \cdot EI_{d.ef.preq}} \cdot \left(1 - \frac{2 \cdot x^2}{L_{sq}^2} + \frac{x^3}{L_{sq}^3} \right)$$

Instantaneous

Uniformly distributed load

$$Q_{\delta.d.pre.uni.inst} := \frac{384 EI_{d.ef.pre}}{5 \cdot L_s^{\,4}} \cdot \left(\delta_{lim.inst} - \frac{5 \cdot G_{pre} \cdot L_s^{\,4}}{384 EI_{d.ef.pre}} \right) = 1.566 \times 10^4 \cdot \frac{N}{m}$$

Point load

$$P_{\delta.d.pre.inst} := \frac{48 \cdot EI_{d.ef.pre}}{L_s^{\,3}} \cdot \left(\delta_{lim.inst} - \frac{5 \cdot G_{pre} \cdot L_s^{\,4}}{384 EI_{d.ef.pre}} \right) = 9.787 \times 10^4 \, N$$

Triangular distributed load

$$\delta_{inst.perm.tri.pre.d}(x) := \frac{G_{preq} \cdot x \cdot L_{sq}^{\,3}}{24 \cdot EI_{d.ef.preq}} \cdot \left(1 - \frac{2 \cdot x^2}{L_{sq}^{\,2}} + \frac{x^3}{L_{sq}^{\,3}} \right)$$

$$\delta_{inst.var.tri.pre.d}(x, Q_q) := \frac{Q_q \cdot x \cdot L_{sq}^{\,3}}{360 \cdot EI_{d.ef.preq}} \cdot \left(7 - \frac{10 \cdot x^2}{L_{sq}^{\,2}} + \frac{3 \cdot x^4}{L_{sq}^{\,4}} \right)$$

$$\delta_{inst.pre.d}(x, Q_q) := \delta_{inst.perm.tri.pre.d}(x) + \delta_{inst.var.tri.pre.d}(x, Q_q)$$

$$\delta_{test}(x, Q_q) := \delta_{lim.inst} \cdot \frac{1}{m}$$

Given

$$0.49 \cdot L_{sq} < x_{init} < 0.578 \, L_{sq}$$

$$\delta_{inst.pre.d}(x_{init}, Q_{init}) = \delta_{test}(x_{init}, Q_{init})$$

$$\begin{pmatrix} x_{max} \\ Q_{max} \end{pmatrix} := Find(x_{init}, Q_{init})$$

$$Q_{\delta.d.pre.tri.inst} := Q_{max} \cdot \frac{N}{m} = 3.139 \times 10^4 \cdot \frac{N}{m}$$

Final

Uniformly distributed load

$$Q_{\delta.d.pre.uni.fin} := \frac{384 EI_{d.ef.pre}}{(1 + \psi_2 \cdot k_{def}) \cdot 5 \cdot L_s^{\,4}} \cdot \left[\delta_{lim.fin} - \left(\frac{5 \cdot G_{pre} \cdot L_s^{\,4}}{384 EI_{d.ef.pre}} \right) \cdot (1 + k_{def}) \right] = 2.15 \times 10^4 \cdot \frac{N}{m}$$

Point load

$$P_{\delta.d.pre.fin} := \frac{48 \cdot EI_{d.ef.pre}}{(1 + \psi_2 \cdot k_{def}) \cdot L_s^{\,3}} \cdot \left[\delta_{lim.fin} - \left(\frac{5 \cdot G_{pre} \cdot L_s^{\,4}}{384 EI_{d.ef.pre}} \right) \cdot (1 + k_{def}) \right] = 1.344 \times 10^5 \, N$$

Triangular distributed load

$$\delta_{fin.pre.d}(x, Q_q) := (1 + k_{def}) \cdot \delta_{inst.perm.tri.pre.d}(x) + (1 + \psi_2 \cdot k_{def}) \cdot \delta_{inst.var.tri.pre.d}(x, Q_q)$$

$$\delta_{test}(x, Q_q) := \delta_{lim.fin} \cdot \frac{1}{m}$$

Given

Given

$0.49 \cdot L_{sq} < x_{init} < 0.578 L_{sq}$

$\delta_{fin.pre.d}(x_{init}, Q_{init}) = \delta_{test}(x_{init}, Q_{init})$

$\begin{pmatrix} x_{max} \\ Q_{max} \end{pmatrix} := \text{Find}(x_{init}, Q_{init})$

$Q_{\delta.d.pre.tri.fin} := Q_{max} \cdot \frac{N}{m} = 4.31 \times 10^4 \cdot \frac{N}{m}$

Net deflection - final

Uniformly distributed load

$$Q_{\delta.d.pre.uni.net.fin} := \frac{384 EI_{d.ef.pre}}{\left(1 + \psi_2 \cdot k_{def}\right) \cdot 5 \cdot L_s^{\,4}} \cdot \left[\delta_{lim.net.fin} - \left(\frac{5 \cdot G_{pre} \cdot L_s^{\,4}}{384 EI_{d.ef.pre}} \right) \cdot \left(1 + k_{def}\right) \ldots + \left(-\delta_{camb.mid.pre.d}\right) \right]$$

$Q_{\delta.d.pre.uni.net.fin} = 2.829 \times 10^4 \frac{N}{m}$

Point load

$$P_{\delta.d.pre.net.fin} := \frac{48 \cdot EI_{d.ef.pre}}{\left(1 + \psi_2 \cdot k_{def}\right) \cdot L_s^{\,3}} \cdot \left[\delta_{lim.net.fin} - \left(\frac{5 \cdot G_{pre} \cdot L_s^{\,4}}{384 EI_{d.ef.pre}} \right) \cdot \left(1 + k_{def}\right) \ldots + -\delta_{camb.mid.pre.d} \right] = 1.768 \times 10^5 \, N$$

Triangular distributed load

$$\delta_{net.fin.pre.d}(x, Q_q) := \left(1 + k_{def}\right) \cdot \delta_{inst.perm.tri.pre.d}(x) \ldots + \left(1 + \psi_2 \cdot k_{def}\right) \cdot \delta_{inst.var.tri.pre.d}(x, Q_q) + \delta_{camb.pre.dq}(x)$$

$\delta_{test}(x, Q_q) := \delta_{lim.net.fin} \cdot \frac{1}{m}$

Given

$0.49 \cdot L_{sq} < x_{init} < 0.578 L_{sq}$

$\delta_{net.fin.pre.d}(x_{init}, Q_{init}) = \delta_{test}(x_{init}, Q_{init})$

$\begin{pmatrix} x_{max} \\ Q_{max} \end{pmatrix} := \text{Find}(x_{init}, Q_{init})$

$Q_{\delta.d.pre.tri.net.fin} := Q_{max} \cdot \frac{N}{m} = 5.672 \times 10^4 \cdot \frac{N}{m}$

Max load

$Q_{\delta.d.pre.uni} := \min(Q_{\delta.d.pre.uni.inst}, Q_{\delta.d.pre.uni.fin}, Q_{\delta.d.pre.uni.net.fin})$

$P_{\delta.d.pre} := \min(P_{\delta.d.pre.inst}, P_{\delta.d.pre.fin}, P_{\delta.d.pre.net.fin})$

$Q_{\delta.d.pre.tri} := \min(Q_{\delta.d.pre.tri.inst}, Q_{\delta.d.pre.tri.fin}, Q_{\delta.d.pre.tri.net.fin})$

$Q_{\delta.d.pre.uni} = 1.566\times 10^4 \cdot \frac{N}{m}$ $P_{\delta.d.pre} = 9.787\times 10^4 N$ $Q_{\delta.d.pre.tri} = 3.139\times 10^4 \cdot \frac{N}{m}$

5. Results

5.1 Moment capacity

5.1.1 Unreinforced beam

According to EC5

Moment capacity

$M_{cap.EC5.d.reg} = 3.146\times 10^5 N\cdot m$

Maximum load

Uniformly distributed

$Q_{m.d.reg.uni.EC5} = 1.628\times 10^4 \frac{N}{m}$

Concentrated load at midspan

$P_{m.d.reg.EC5} = 8.11\times 10^4 N$

Triangular distributed

$Q_{m.d.reg.tri.EC5} = 3.278\times 10^4 \frac{N}{m}$

According to EC5 - consideration taken to lateral torsional buckling

Moment capacity

$M_{cap.buck.d.reg} = 2.984\times 10^5 N\cdot m$

Maximum load

Uniformly distributed

$Q_{m.d.reg.uni.buck} = 1.541\times 10^4 \frac{N}{m}$

Concentrated load at midspan

$P_{m.d.reg.buck} = 7.705\times 10^4 N$

Triangular distributed

$Q_{m.d.reg.tri.buck} = 3.104\times 10^4 \frac{N}{m}$

Our calculation model

Moment capacity

$M_{cap.EC5.d.reg} = 3.146\times 10^5 N\cdot m$

Maximum load

Uniformly distributed

$Q_{m.d.reg.uni} = 1.978\times 10^4 \frac{N}{m}$

Concentrated load at midspan

$P_{m.d.reg} = 9.892\times 10^4 N$

Triangular distributed

$$Q_{m.d.reg.tri} = 3.857\times 10^{4}\ \frac{N}{m}$$

5.1.2 Rerinforced beam

Our calculation model

Moment capacity

$$M_{cap.d.slack} = 6.129\times 10^{5}\ N\cdot m$$

Maximum load

Uniformly distributed

$$Q_{m.d.slack.uni} = 3.217\times 10^{4}\ \frac{N}{m}$$

Concentrated load at midspan

$$P_{m.d.slack} = 1.608\times 10^{5}\ N$$

Triangular distributed

$$Q_{m.d.slack.tri} = 6.27\times 10^{4}\ \frac{N}{m}$$

5.1.3 Pre-stressed beam

Our calculation model

Moment capacity

$$M_{cap.d.pre} = 7.152\times 10^{5}\ N\cdot m$$

Maximum load

Uniformly distributed

$$Q_{m.d.pre.uni} = 3.762\times 10^{4}\ \frac{N}{m}$$

Concentrated load at midspan

$$P_{m.d.pre} = 1.881\times 10^{5}\ N$$

Triangular distributed

$$Q_{m.d.pre.tri} = 7.333\times 10^{4}\ \frac{N}{m}$$

5.2 Shear capacity

5.2.1 Unreinforced beam

Shear capacity

$$V_{cap.d.reg} = 1.734\times 10^{5}\ N$$

Maximum load

Uniformly distributed

$$Q_{v.d.reg.uni} = 2.261\times 10^{4}\ \frac{N}{m}$$

Concentrated load at midspan

$$P_{v.d.reg} = 2.261\times 10^{5}\ N$$

Triangular distributed

$$Q_{v.d.reg.tri} = 3.392\times 10^{4}\ \frac{N}{m}$$

5.2.2 Rerinforced beam

Shear capacity

$$V_{cap.d.slack} = 2.318\times 10^{5}\ N$$

Maximum load

Uniformly distributed

$$Q_{v.d.slack.uni} = 3.039\times 10^{4}\ \frac{N}{m}$$

Concentrated load at midspan

$$P_{v.d.slack} = 3.039\times 10^{5}\ N$$

Triangular distributed

$$Q_{v.d.slack.tri} = 4.558\times 10^{4}\ \frac{N}{m}$$

5.2.3 Pre-stressed beam

Shear capacity

$$V_{cap.d.pre} = 2.318\times 10^{5}\ N$$

Maximum load

Uniformly distributed

$$Q_{v.d.pre.uni} = 3.039\times 10^{4}\ \frac{N}{m}$$

Concentrated load at midspan

$$P_{v.d.pre} = 3.039\times 10^{5}\ N$$

Triangular distributed

$$Q_{v.d.pre.tri} = 4.558\times 10^{4}\ \frac{N}{m}$$

5.3 Maximum load due to deflection requirements

5.2.1 Unreinforced beam

Uniformly distributed

$$Q_{\delta.d.reg.uni} = 1.039\times 10^{4}\ \frac{N}{m}$$

Concentrated load at midspan

$$P_{\delta.d.reg} = 6.493\times 10^{4}\ N$$

Triangular distributed

$$Q_{\delta.d.reg.tri} = 2.083\times 10^{4}\ \frac{N}{m}$$

5.2.2 Rerinforced beam

Uniformly distributed

$$Q_{\delta.d.slack.uni} = 1.566\times 10^{4}\ \frac{N}{m}$$

Concentrated load at midspan

$$P_{\delta.d.slack} = 9.787\times 10^{4}\ N$$

Triangular distributed

$$Q_{\delta.d.slack.tri} = 3.139\times 10^{4}\ \frac{N}{m}$$

5.2.3 Pre-stressed beam

Uniformly distributed

$$Q_{\delta.d.pre.uni} = 1.566\times 10^{4}\ \frac{N}{m}$$

Concentrated load at midspan

$$P_{\delta.d.pre} = 9.787\times 10^{4}\ N$$

Triangular distributed

$$Q_{\delta.d.pre.tri} = 3.139\times 10^{4}\ \frac{N}{m}$$

10.2 Appendix B: The Matlab code for the model

The line break for the matlab code is set to matlab standards. A "Copy and Paste" to a clear m-file will create a more legible code. The line break was not change to the thesis size due to the errors that would occur when "Copy and Paste" will be attempted.

```
%%%%%%%%%%%%%%%%%%%%%%%%%%%%%%%%%%%%%%%%%%%%%%%%%%%%%%%%%%%%%%%%%%%%%%%
%%%%%%
%                                                     The  indata  file
%
%                                                  By  S.W  March  2011
%

%
%
%%%%%%%%%%%%%%%%%%%%%%%%%%%%%%%%%%%%%%%%%%%%%%%%%%%%%%%%%%%%%%%%%%%%%%%
%%%%%%
clear all
close all
clc


%% The new indata program
% This is the control program for the elastic and plastic analysis of
the
% reinforced glulam beams.


%The program differs on the main beam geometry and the settings of
each
%specific beam. e.i the diffrent beam type can be examned in an
optional
%amount of diffrent sizes.


%At the present the code can handle 8 diffrent beam configurations
and an
% enless amount of cross-sections, although a lot of cross-sections
% makes for very small plots.
%
%it is important to fill in all vectors !
%the code wont work otherwise!


%% Beams that are examined are;
```

```
% #1, Unreinforced glulam beam
%
% #2, Beam 9 from exjobb
%
% #3, New beam 1 unreinforced in compression side - heavily
reinforced in
%     tension side
% #4, Beam 9 from ex jobb, but Pre-stressed.
%
% #

%% The different beams that are to be tested

hg=[200 230 400];   %#ok<*NBRAK>            %[mm] Height
bg=[115 115 115];                           %[mm] width

L=[5000-400 5000-400 5000-400];             %[mm] Length

%% Glulam

Eg=[9490 9100 9000 9100];                     %[MPa] youngs modulus
Gg=[850 850 850 850];                        %[MPa] Shear modulus

ft=[40 45 40 45];                           %[MPa] tensile strength
fc=[35 35 40 35];                                  %[MPa] compressive
strength
to=[3 3 3 3];                               %[MPa] Shear strength

%  reinforcement is to be pre-stressed pre=2 normal re=1 otherwise =0
re=[0 1 1 2];
% increment number to plot the strain/stress curves in different
diagram
nr=[1 2 3 4];

%% Reinforcement

%Compresive reinforcement

Erc=[165000 165000 200000 165000];      %[MPa] Youngs modulus
bc=[1.4 1.4 1.4 1.4];                %[mm] width of laminate
```

```
hc=[30 30 30 30];                    %[mm] hight of laminate
nc=[0 3 0 3];                       %[-] number laminates
Arc=nc.*bc.*hc;                    %[mm2]area of reinforcement
Zc=hc./2;                         %[mm] dist. to GC

% tensile reinforcement

Ert=[165000 165000 165000 165000];
bt=[1.4 1.4 1.4 1.4];                 %[MPa] Youngs modulus
ht=[30 30 30 30];                    %[mm] width of laminate
nt=[0 6 10 6];                      %[mm] hight of laminate
Art=nt.*bt.*ht;                     %[mm2]area of reinforcement
Zt=ht./2;                          %[mm] dist. to GC

%ekvivalent tvärrsnitt
alfa=Ert/Eg;

%Zgv=(bg*hg*hg*Eg/2+Arc*Zc*Erc+Art*Ert*(hg-
Zt))/(bg*hg*Eg+Arc*Erc+Art*Ert);
%eN=hg-Zgv-Zc;
%% The sending of the data

dim=length(hg);   %nummer of dimentions to be tested
antal=length(nr);  %nummer of beams to be tested in each dimention.

for a=1:length(hg)

for f=1:length(nr)

if re(f)==2
            main_pre-
stressed(Eg(f),Gg(f),ft(f),fc(f),to(f),bc(f),hc(f),...

nc(f),bt(f),ht(f),nt(f),Ert(f),Erc(f),nr(f),hg(a),bg(a),...
                L(a),Arc(f),Art(f),Zc(f),Zt(f),re(f),dim,antal,a,f);

else

main_reinforced(Eg(f),Gg(f),ft(f),fc(f),to(f),bc(f),hc(f),...

nc(f),bt(f),ht(f),nt(f),Ert(f),Erc(f),nr(f),hg(a),bg(a),...
```

```
                L(a),Arc(f),Art(f),Zc(f),Zt(f),re(f),dim,antal,a,f);

end
end

end

%%%%%%%%%%%%%%%%%%%%%%%%%%%%%%%%%%%%%%%%%%%%%%%%%%%%%%%%%%%%%%%%%%%%%%%%
% %% inparametrar som kan användas när underfilerna skall skapas
eller kollas
% clear all
% close all
% clc
%
% %% The beams basic geometry
%
% hg=200 ;                  %[mm] Height
% bg=115 ;                  %[mm] width
%
% L=5000-400 ;              %[mm] Length
%
% %% Glulam
%
% Eg=9490 ;                          %[MPa] youngs modulus
% Gg=850 ;                           %[MPa] Shear modulus
%
% fm=30;
% ft=[25];                          %[MPa] tensile strength
% fc=[25] ;                         %[MPa] compressive strength
% to=[3];                           %[MPa] Shear strength
%
% %% Reinforcement
%
% %Compressive reinforcement
%
% Erc=[200000];                      %[MPa] Youngs modulus
% bc=[1.4];                          %[mm] width of laminate
% hc=[30];                           %[mm] hight of laminate
% nc=[2];                            %[-] number laminates
% Arc=nc.*bc.*hc;                    %[mm2]area of reinforcement
```

```
% Zc=hc./2;                          %[mm] dist. to GC
%
% % tensile reinforcement
%
% Ert=[200000];
% bt=[1.4];                          %[MPa] Youngs modulus
% ht=[30];                           %[mm] width of laminate
% nt=[6];                            %[mm] hight of laminate
% Art=nt.*bt.*ht;                    %[mm2]area of reinforcement
% Zt=ht./2;                          %[mm] dist. to GC
%
% fy=500;
% % increment number to plot the strain/stress curves in different
diagram
% nr=[1];
%
% %  reinforcement is to be pre-stressed pre=2 normal re=1 otherwise
=0
% re=[1];
% q=[1];
%
% %ekvivalent tvärsnitt
% alfa=Ert/Eg;
% Ag_ek=[hg*bg+(alfa-1)*(nt*bt*ht+nc*hc*bc)];
%                            Zgv=(bg*hg*hg*Eg/2+Arc*Zc*Erc+Art*Ert*(hg-
Zt))/(bg*hg*Eg+Arc*Erc+Art*Ert);
% eN=hg-Zgv-Zc;
%%%%%%%%%%%%%%%%%%%%%%%%%%%%%%%%%%%%%%%%%%%%%%%%%%%%%%%%%%%%%%%%%%%%%%%%
%%%%%%
%%%%%%%%%%%%%%%%%%%%%%%%%%%%%%%%%%%%%%%%%%%%%%%%%%%%%%%%%%%%%%%%%%%%%%%%%
%%%%%%


%%%%%%%%%%%%%%%%%%%%%%%%%%%%%%%%%%%%%%%%%%%%%%%%%%%%%%%%%%%%%%%%%%%%%%%%%
%%%%%%
%                                        The  main  calculations  file,
%
%                                             for  pre-stressed  beams
%
%                                                 By  S.W  April  2011
%
%
%
%%%%%%%%%%%%%%%%%%%%%%%%%%%%%%%%%%%%%%%%%%%%%%%%%%%%%%%%%%%%%%%%%%%%%%%%%
%%%%%%
```

```
% function main_pre-stressed(Eg,Gg,ft,fc,to,bc,hc,...
%             nc,bt,ht,nt,Ert,Erc,nr,hg,bg,...
%             L,Arc,Art,Zc,Zt,re,dim,antal,a,f);

%% inparametrar som kan användas när underfilerna skall skapas eller
kollas
clear all
close all
clc

%% The beams basic geometry

hg=200 ;                  %[mm] Height
bg=115 ;                  %[mm] width

L=5000-400 ;              %[mm] Length

%% Glulam
Eg=9490 ;                          %[MPa] youngs modulus
Gg=850 ;                           %[MPa] Shear modulus

fm=30;
ft=[25];                          %[MPa] tensile strength
fc=[25] ;                         %[MPa] compressive strength
to=[3];                           %[MPa] Shear strength

%% Reinforcement

%Compressive reinforcement

Erc=[200000];                      %[MPa] Youngs modulus
bc=[1.4];                          %[mm] width of laminate
hc=[30];                           %[mm] hight of laminate
nc=[0];                            %[-] number laminates
Arc=nc.*bc.*hc;                    %[mm2]area of reinforcement
Zc=hc./2;                          %[mm] dist. to GC

% tensile reinforcement
```

```
Ert=[200000];
bt=[1.4];                        %[MPa] Youngs modulus
ht=[30];                         %[mm] width of laminate
nt=[6];                          %[mm] hight of laminate
Art=nt.*bt.*ht;                  %[mm2]area of reinforcement
Zt=ht./2;                        %[mm] dist. to GC

fy=500;
% increment number to plot the strain/stress curves in different
diagram
nr=[1];

% reinforcement is to be pre-stressed pre=2 normal re=1 otherwise =0
re=[1];
q=[1];

%ekvivalent tvärsnitt
alfa=Ert/Eg;
Ag_ek=[hg*bg+(alfa-1)*(nt*bt*ht+nc*hc*bc)];
Zgv=(bg*hg*hg*Eg/2+Arc*Zc*Erc+Art*Ert*(hg-
Zt))/(bg*hg*Eg+Arc*Erc+Art*Ert);
eN=hg-Zgv-Zc;
Arc
procent=((Art+Arc)/(hg*bg))*100
%%%%%%%%%%%%%%%%%%%%%%%%%%%%%%%%%%%%%%%%%%%%%%%%%%%%%%%%%%%%%%%%%%%
%%%%%%
%%%%%%%%%%%%%%%%%%%%%%%%%%%%%%%%%%%%%%%%%%%%%%%%%%%%%%%%%%%%%%%%%%%
%%%%


%%%%%%%%%%%%%%%%%%%%%%%%%%%%%%%%%%%%%%%%%%%%%%%%%%%%%%%%%%%%%%%%%%%
%%%%%%
%% inparametrar
% saker som behövs innan själva lopparna skall starta upp

%ekvivalent tvärrsnitt


alfa=Ert/Eg;
Ag_ek=[hg*bg+(alfa-1)*(nt*bt*ht+nc*hc*bc)];


% elastiska tyngdpunkten
```

```
Zgv=(bg*hg*hg*Eg/2+Arc*Zc*Erc+Art*Ert*(hg-
Zt))/(bg*hg*Eg+Arc*Erc+Art*Ert);
eN=hg-Zgv-Zc;
%behöver ju P,I och alfa och den mostvarande startspänningen i
toppen.

[eps_top_preload,Nek_max]=Preload(L,Eg,ft,fc,fm,bc,hc,nc,bt,ht,nt,...
    Ert,hg,bg,Ag_ek,Arc,Art,Zc,Zt,Zgv);

P=Nek_max;
I=((bg*hg^3/12)+hg*bg*(Zgv-(hg/2))^2)+...
    (alfa-1)*(((nc*bc*hc^3)/(12))+Arc*(Zgv-Zc)^2+...
((nt*bt*ht^3)/(12))+Art*(hg-Zgv-Zt)^2);

%%%%%%%%%%%%%%%%%%%%%%%%%%%%%%%%%%%%%%%%%%%%%%%%%%%%%%%%%%%%%%%%%%%%%%%
%%%%%
%% Elastiska beräkingarna, här används teckenkonvertering

%räknevärden och annat intressant för loppen

% töjningar
eps_e_t=ft/Eg;      % elastic strain limit in tension
eps_e_c=-fc/Eg;      % elastic strain limit in compression

% eps_top_preload=0;
% Nek_max=0;
% P=0;

% välj stegstorlek,
delta_eps_c=(eps_e_c)/100

%fördefinerar kontrollvariabler.
shear_failure=0;
tension_failure=0;

%startar med ett steg så inget blir noll.
eps_c=eps_top_preload+delta_eps_c;
e(1)=eps_c;
i=2;
ner(1)=0;
```

```
bb=0;
%FIRE UP THE LOOP!
while abs(eps_c)<=abs(eps_e_c)

% Enligt beräkningarna i arbetet så;
    M_last=((Eg*eps_c)*Ag_ek*I-P*I)/(Ag_ek*(-Zgv))-P*eN;

%med denna M så kan vi räkna ut töjningsfördelningen
    z_c=(-Zgv);
    z_rc=(-Zgv+Zc);
    z_rt=(hg-Zgv-Zt);
z_t=(hg-Zgv);

    eps_c_3=(-1)*(M_last/(Eg*I))*z_c;
    eps_rc_3=(-1)*(M_last/(Eg*I))*z_rc;
    eps_rt_3=(M_last/(Eg*I))*z_rt;
    eps_t_3=(M_last/(Eg*I))*z_t;

    M(i)=1/2*eps_c_3*Eg*2/3*bg*Zgv^2+eps_rc_3*Erc*Arc*(Zgv-Zc)...
        +1/2*eps_t_3*Eg*2/3*bg*(hg-Zgv)^2+eps_rt_3*Ert*Art*(hg-Zgv-
Zt);

qq(i)=(M(i)*8)/L^2;
    V=(qq(i)*L/2);

%för tensile kollen
    eps_t=((P/(Eg*Ag_ek))+(((P*eN)+M_last)/(Eg*I))*z_t);

% för nerböjningen
%plockar ut en fiktiv last för P*e

    M_pre=P*eN;

    eps_c_fik=(-1)*(M_pre/(Eg*I))*z_c;
    eps_rc_fik=(-1)*(M_pre/(Eg*I))*z_rc;
    eps_rt_fik=(M_pre/(Eg*I))*z_rt;
    eps_t_fik=(M_pre/(Eg*I))*z_t;
```

```
    M_fik=1/2*eps_c_fik*Eg*2/3*bg*Zgv^2+eps_rc_fik*Erc*Arc*(Zgv-
Zc)...
        +1/2*eps_t_fik*Eg*2/3*bg*(hg-Zgv)^2+eps_rt_fik*Ert*Art*(hg-
Zgv-Zt);

    q_fik=(M_fik*8)/L^2;

% EI, kanske inte helt nödvändigt här.
%z_av(i)=(((-(P/Ag_ek))*I)/(M(i)+P*eN)) %fungerar inte helt okey
%z_0=(Zgv)+z_av(i)
%phi(i)=(-1)*eps_c/z_0;
%EI(i)=M(i)/phi(i);

    ner(i)=(5*(qq(i)+q_fik)*L^4)/(384*Eg*I);

%för tvärkraften
    shear(i)=3*V/(hg*bg*2);

if(eps_t>=eps_e_t);
        disp('tensile failure')
        tension_failure=1;
break;
end

if(shear(i)>=to);
        disp('shear failure');
        shear_failure=1;
        tension_failure=1;
break;
end

    e(i)=eps_c+delta_eps_c;
eps_c=eps_c+delta_eps_c ;

    i=i+1;

end
% trix för att fixa till saker
M_el=M(i-1)/1e6;
```

```
tension_failure;
shear_failure;
 z_av=(((-(P/Ag_ek))*I)/(M(i-1)+P*eN)); %fungerar inte helt okey
 z_0=(Zgv)+z_av;

%fixa nerböjningen vektor då den inte börjar på nollan.
ner(1)=(5*(qq(1)+q_fik)*L^4)/(384*Eg*I);

%% kopiera in plot commandon!!

%% Plastiska beräkningar, här avänds ingen teckenkonvertering

% töjningar
eps_e_t=ft/Eg;      % elastic strain limit in tension
eps_e_c=fc/Eg;      % elastic strain limit in compression
% plastisk töjning
eps_p_c=3*eps_e_c;  % ultimate plastic strain

%  varibaler som först måste defineras.
eps_p_0=(-1)*P/(Ert*Art)
%eps_p_0=0;

%0/0 är inte så trevligt, däeför görs eps_c positiv och lägger på en
liten
%spänning
eps_c=(eps_c*(-1))+(1*10^(-12));

% välj stegstorlek,
delta_eps_c=(eps_e_c)/100

%då kör vi
% start neutral axeln blir den sista neutralaxeln i elastiska.
x_pl_prev=z_0;

if tension_failure ~= 1
while eps_c<=eps_p_c

        x_pl=plast_x(fc,eps_c,eps_e_c,eps_p_0,hg,...
            bg,Arc,Art,Zt,Zc,Eg,Erc,Ert,x_pl_prev,fy);
```

```
%plastiseringsgraden
        x=((eps_c-eps_e_c)/eps_c)*x_pl;

% lite räknevektorer för att kolla fel
        pl(i)=x_pl;
        xx(i)=x;

%spänningar, för momentet
        sig_e_c=Eg*eps_c*((x_pl-x)/(x_pl));
        sig_rc=Erc*eps_c*((x_pl-Zc)/(x_pl));
        sig_P=Ert*(((eps_c*(hg-x_pl-Zt))/(x_pl))+eps_p_0);
        sig_t=Eg*eps_c*((hg-x_pl)/(x_pl));

Ac1=bg*x;
        Ac2=(1/2)*(x_pl-x)*bg;
        At=(1/2)*(hg-x_pl)*bg;

        M(i)=sig_t*At*(((2/3)*(hg-x_pl)))...
+sig_e_c*Ac1*(x_pl-x/2)...
            + sig_e_c*Ac2*((2/3)*(x_pl-x))...
            +(sig_rc*Arc*(x_pl-Zc))...
            +sig_P*Art*(hg-x_pl-Zt);

        qq(i)=(M(i)*8)/L^2;
        V=(qq(i)*L/2);

%nerböjningen
        phi(i)=eps_c/x_pl;
        EI(i)=M(i)/phi(i);
        ner(i)=(5*(qq(i)+q_fik)*L^4)/(384*EI(i));

% kollarna, för tensil
        eps_t=((hg-x_pl)/(x_pl))*eps_c;

if(eps_t>=eps_e_t);
            disp('tensile failure')
break;
end
```

```
%för shear
        shear(i)=3*V/(hg*bg*2);
if(shear(i)>=to);
            disp('shear failure');
            shear_failure=1;
            tension_failure=1;
break;
end

%räkna upp räkneverken
        e(i)=eps_c+delta_eps_c;
        eps_c=eps_c+delta_eps_c;
         xpl_prev=x_pl;
        i=i+1;
%          bb=bb+1;
%
%          if bb == 8
%              break
%          end
end
end

M_pl=M(i-1)/1e6;
Q=qq.*L;
figure(1)
plot(M)

%figure(2)
%plot(ner)

%%%%%%%%%%%%%%%%%%%%%%%%%%%%%%%%%%%%%%%%%%%%%%%%%%%%%%%%%%%%%%%%%%%%%%
%%%%%%
%                                        The  main  calculations  file,
%
%                                    for reinforced an un-reinforced beam
%
%                                                    By  S.W  April  2011
%
%
%
```

```
%%%%%%%%%%%%%%%%%%%%%%%%%%%%%%%%%%%%%%%%%%%%%%%%%%%%%%%%%%%%%%%%%%%%%%%%
%%%%%%
%
% function main_reinforced(Eg,Gg,ft,fc,to,bc,hc,...
%                  nc,bt,ht,nt,Ert,Erc,nr,hg,bg,...
%                  L,Arc,Art,Zc,Zt,re,dim,antal,a,f);

%% inparametrar som kan användas när underfilerna skall skapas eller
kollas
clear all
close all
clc
%% The beams basic geometry

hg=200 ;                  %[mm] Height
bg=115 ;                  %[mm] width

L=10000-400 ;              %[mm] Length
%% Glulam

Eg=9490 ;                          %[MPa] youngs modulus
Gg=850 ;                           %[MPa] Shear modulus

ft=[40];                          %[MPa] tensile strength
fc=[35] ;                         %[MPa] compressive strength
to=[3];                           %[MPa] Shear strength

%% Reinforcement

%Compressive reinforcement
Erc=[165000];                      %[MPa] Youngs modulus
bc=[1.4];                          %[mm] width of laminate
hc=[30];                           %[mm] hight of laminate
nc=[2];                            %[-] number laminates
Arc=nc.*bc.*hc;                    %[mm2]area of reinforcement
Zc=hc./2;                          %[mm] dist. to GC

% tensile reinforcement
Ert=[165000];
bt=[1.4];                         %[MPa] Youngs modulus
```

```
ht=[30];                          %[mm] width of laminate
nt=[6];                           %[mm] hight of laminate
Art=nt.*bt.*ht;                   %[mm2]area of reinforcement
Zt=ht./2;                         %[mm] dist. to GC

% increment number to plot the strain/stress curves in different
diagram
nr=[1];

%  reinforcement is to be pre-stressed pre=2 normal re=1 otherwise =0
re=[1];
q=[1];

%ekvivalent tvärsnitt
alfa=Ert/Eg;
Ag_ek=[hg*bg+(alfa-1)*(nt*bt*ht+nc*hc*bc)];
Zgv=(bg*hg*hg*Eg/2+Arc*Zc*Erc+Art*Ert*(hg-
Zt))/(bg*hg*Eg+Arc*Erc+Art*Ert);
eN=hg-Zgv-Zc;
%%%%%%%%%%%%%%%%%%%%%%%%%%%%%%%%%%%%%%%%%%%%%%%%%%%%%%%%%%%%%%%%%%%%%%%
%%%%%%
%%%%%%%%%%%%%%%%%%%%%%%%%%%%%%%%%%%%%%%%%%%%%%%%%%%%%%%%%%%%%%%%%%%%%%%
%%%%

%%%%%%%%%%%%%%%%%%%%%%%%%%%%%%%%%%%%%%%%%%%%%%%%%%%%%%%%%%%%%%%%%%%%%%%
%%%%%%
%% inparametrar

% saker som behövs innan själva lopparna skall starta upp

%ekvivalent tvärrsnitt
alfa=Ert/Eg;
Ag_ek=[hg*bg+(alfa-1)*(nt*bt*ht+nc*hc*bc)]

% neutral axeln för det elastiska fallet.
x_el=(bg*hg*hg*Eg/2+Arc*Zc*Erc+Art*Ert*(hg-
Zt))/(bg*hg*Eg+Arc*Erc+Art*Ert);
y_tp=x_el;

% töjningar
eps_e_t=ft/Eg;      % elastic strain limit in tension
```

```
eps_e_c=fc/Eg;      % elastic strain limit in compression

% plastisk töjning
eps_c_p=3*eps_e_c;  % ultimate plastic strain 1

%gör valet av start pkt för top spänningen
eps_c0=eps_e_c/100;

% välj stegstorlek, osäker på att jag behöver denna.
delta_eps_c=eps_e_c/100;

%%%%%%%%%%%%%%%%%%%%%%%%%%%%%%%%%%%%%%%%%%%%%%%%%%%%%%%%%%%%%%%%%%%%%%%%
%%%%%%
%% Elastiska modellen

%fördefinerar kontrollvariabler.
shear_failure=0;
tension_failure=0;
eps_c=eps_c0;
e(1)=eps_c;
i=2;

% dåså, då kör vi, elastiska loopen defineras som
while eps_c<=eps_e_c

%räknar ut motsvarande botten töjning
    eps_t=((hg/x_el)-1)*eps_c;

%tar fram töjningarna i armeringslagrerna
    eps_rc=((x_el-Zc)/x_el)*eps_c;
    eps_rt=((hg-x_el-Zt)/x_el)*eps_c;

%kontrollerar så botten töjning ligger innin gränserna
if(eps_t>=eps_e_t);
        display('tensile failure');
        tension_failure=1;
break;
end
```

```
%beräknar krökningen
    phi(i)=eps_c/x_el

%beräknar resisterande momentet
    M(i)=1/2*eps_c*Eg*2/3*bg*x_el^2+eps_rc*Erc*Arc*(x_el-Zc)...
        +1/2*eps_t*Eg*2/3*bg*(hg-x_el)^2+eps_rt*Ert*Art*(hg-x_el-Zt);

    EI(i)=M(i)/phi(i);
     q(i)=(M(i)*8)/L^2;
    EI(i)=M(i)/phi(i);
    u(i)=(5*q(i)*L^4)/(384*EI(i));
    V=(q(i)*L/2);
shear(i)=3*V/(hg*bg*2);
if(shear(i)>=to);
                display('shear failure');
                shear_failure=1;
                tension_failure=1;
break;
end


e(i)=eps_c+delta_eps_c;
    eps_c=eps_c+delta_eps_c;
    i=i+1;
end
%fixar till vektorerna

phi_el=phi(i-1)*1000;
M_el=M(i-1)/1e6;
q_el=q(i-1)/1000;
u_el=u(i-1);

%% elastiska ploter
set(0,'DefaultFigureWindowStyle','docked')
%för att få töjningsdigrammet
eps_h(1)=eps_c;
h_sec(1)=0;

eps_h(2)=-((hg-x_el)./x_el)*eps_c;
```

```
h_sec(2)=hg;

figure(nr+2)
subplot(2,1,1)
plot(eps_h,h_sec,'b-');
grid on
set(gca,'YDir','reverse');
xlabel('Strains')
ylabel('Depth [mm]')
hold on
plot([0 0],[0 hg],'k-');
%plotar spännings diagrammet för elstiska fasen

sigma_h(1)=eps_c*Eg;
sigma_h(2)=eps_h(2)*Eg;

figure(nr+2)
subplot(2,1,2)
plot([sigma_h(1) sigma_h(2)],[h_sec(1) h_sec(2)],'b-');
set(gca,'YDir','reverse');
xlabel('Stress[N/mm2]')
ylabel('Depth [mm]')
grid on
hold on
plot([0 0],[0 hg],'k-');
%%%%%%%%%%%%%%%%%%%%%%%%%%%%%%%%%%%%%%%%%%%%%%%%%%%%%%%%%%%%%%%%%%%%%%
%%%%%%
%% plastisk model

%anser start för den plastiska modellen
x_pl=0;

%0/0 är inte så trevligt
eps_c=eps_c+0.00000001;

%då kör vi
if tension_failure ~= 1

while eps_c<=eps_c_p
```

```
    a=fc*bg*(eps_c-eps_e_c)/eps_c+...
        fc*bg/2*(1-(eps_c-eps_e_c)/eps_c)-...
        eps_c*bg/2*Eg;
    b=eps_c*(Erc*Arc+bg*hg*Eg+Art*Ert);
    c=eps_c*(Zt*Art*Ert-Zc*Erc*Arc-(bg/2)*Eg*hg^2-hg*Art*Ert);

    x_pl=(-b+sqrt(b^2-4*a*c))/(2*a);
    x_test(i)=x_pl;
% ypl_prev=x_pl;

    eps_t=((hg/x_pl)-1)*eps_c;

if(eps_t>=eps_e_t);
        display('tensile failure')
break;
end

    eps_rc=(1-Zc/x_pl)*eps_c;
    eps_rt=((hg-x_pl-Zt)/x_pl)*eps_c;

sigma_c_lam=eps_rc*Erc;
    sigma_t_lam=eps_rt*Ert;

Zp=(((eps_c-eps_e_c)/eps_c))*x_pl;
    phi(i)=eps_c/x_pl;

%beräknar restisterande moment

    M(i)=sigma_c_lam*Arc*(x_pl-Zc)+fc*bg*Zp*(x_pl-Zp/2)+...
1/2*fc*(x_pl-Zp)*bg*2/3*(x_pl-Zp)+...
        sigma_t_lam*Art*(hg-x_pl-Zt)+...
        1/2*(eps_t*Eg)*(hg-x_pl)*bg*2/3*(hg-x_pl);

q(i)=(M(i)*8)/L^2;
    EI(i)=M(i)/phi(i);
    u(i)=(5*q(i)*L^4)/(384*EI(i));
   V=(q(i)*L/2);

shear(i)=3*V/(hg*bg*2);
```

```
if(shear(i)>=to);
                display('shear failure');
                shear_failure=1;
                tension_failure=1;
break;
end

    e(i)=eps_c;
i=i+1;
eps_c=eps_c+delta_eps_c;

end
end

phi_pl=phi(i-1)*1000;
M_pl=M(i-1)/1e6;
q_pl=q(i-1)/1000;
u_pl=u(i-1);

%% plota den plastiska töjning och spänningen.

%för töjningen blir det samma som den elastiska
eps_h(1)=eps_c;
h_sec(1)=0;

eps_h(2)=-((hg-x_el)./x_el)*eps_c;
h_sec(2)=hg;

figure(nr+2)
subplot(2,1,1)
plot(eps_h,h_sec,'r-');
set(gca,'YDir','reverse');
xlabel('Strains')
ylabel('Depth [mm]')
hold on
plot([0 0],[0 hg],'k-');

%för spännningen så behövs det 3 pkt för att beskriva kurvan.
```

```
sigma_h(1)=eps_c*Eg;
sigma_h(2)=eps_h(2)*Eg;
h_sec(2)=Zp;
h_sec(3)=hg;

figure(nr+2)
subplot(2,1,2)
plot([sigma_h(1) sigma_h(1)],[h_sec(1) h_sec(2)],'r-');
hold on
plot([sigma_h(1) sigma_h(2)],[h_sec(2) h_sec(3)],'r-');

set(gca,'YDir','reverse');
xlabel('Stress[N/mm2]')
ylabel('Depth [mm]')
grid on
hold on
plot([0 0],[0 hg],'k-');
%% resultat

%%%%%%%%%%%%%%%%%%%%%%%%%%%%%%%%%%%%%%%%
% huvudplotar
%%%%%%%%%%%%%%%%%%%%%%%%%%%%%%%%%%%%%%%%

 figure(1)
% M(1)=0;
% phi(1)=0;
% q(1)=0;

plot(phi,M,'--')
 title('Moment Curvature Relation');
  grid on;
  xlabel('\phi')
  Ylabel('Moment [kNm]')

figure(2)

plot(u,q,'-.')
  title('Load Displacement Relation');
grid on;
```

```
    xlabel('\delta')
ylabel('Load [kN]')

%%%%%%%%%%%%%%%%%%%%%%%%%%%%%%%%%%%%%%%%%%%%%%%%%%%%%%%%%%%%%%%%%%%%%%
%%%%%%
%                                                  Pre-stressed  Beam,
%
%                                    plastic yielding, neutral axies
%
%                                                By;  S.W,  March  2011
%
%%%%%%%%%%%%%%%%%%%%%%%%%%%%%%%%%%%%%%%%%%%%%%%%%%%%%%%%%%%%%%%%%%%%%%
%%%%%%


function x_pl=plast_x(fc,eps_c,eps_e_c,eps_p_0,hg,...
                      bg,Arc,Art,Zt,Zc,Eg,Erc,Ert,x_pl_prev,fy,nc,M);

%% för de olika flytkriterierna

eps_rc=((x_pl_prev-Zc)/x_pl_prev)*eps_c;
eps_rt=(((hg-x_pl_prev-Zt)/x_pl_prev)*eps_c)+eps_p_0;



sig_rc=eps_rc*Erc;
sig_rt=eps_rt*Ert;

if sig_rc >= fy
    sig_rc = fy;
end

if Arc == 0
    sig_rc=0;
end

if sig_rt >= fy
    sig_rt = fy;
end
sig_rc;
sig_rt;
test=0;
```

```
%% om inget flyter

if sig_rc<fy && sig_rt<fy

%a1=(Eg*eps_c*bg*((eps_c-eps_e_c)/(eps_c))*(1-((eps_c-
eps_e_c)/(eps_c)))+...
%     (1/2)*Eg*bg*eps_c*(1-((eps_c-eps_e_c)/(eps_c)))^2-...
%     (1/2)*Eg*bg*eps_c);

    a1=(fc*bg*(1-((eps_e_c)/(eps_c)))...
        +((fc*bg)/(2))*((eps_e_c)/(eps_c))...
-(eps_c*bg/2)*Eg);

    b1=(-Ert*Art*(-eps_c+eps_p_0)+...
        Eg*bg*hg*eps_c+...
        Erc*Arc*eps_c);

    c1=eps_c*(-Ert*Art*(hg-Zt)-...
        (1/2)*Eg*bg*(hg^2)+...
        Erc*Arc*(-Zc));
%  length(M)
    x_pl=(-b1+sqrt(b1^2-4*a1*c1))/(2*a1);
    test=test+1;
    disp('inget flyter')
end

%% Om topp armeringen flyter

if sig_rc == fy && sig_rt < fy

a1=(fc*bg*(1-((eps_e_c)/(eps_c)))...
        +(fc*bg)/(2)...
-(((fc*bg)/(2))*((eps_c-eps_e_c)/(eps_c)))...
-(eps_c*bg/2)*Eg);

    b1=(sig_rc*Arc...
+Eg*eps_c*bg*hg...
-Ert*Art*(-eps_c+eps_p_0));
```

```
    c1=((-eps_c*((bg*hg^2)/(2))*Eg)...
-(eps_c*Ert*Art*(hg-Zt)));

    x_pl=(-b1+sqrt(b1^2-4*a1*c1))/(2*a1);
    test=test+1;
% length(M)
    disp('top flyter')

end

%% Om bottenarmeringen flyter

if sig_rc < fy && sig_rt == fy

%a1=1/2*fc*bg*(eps_c-eps_e_c)/eps_c+1/2*fc*bg-1/2*eps_c*Eg*bg;
% b1=eps_c*Erc*Arc-sig_rt*Art+1/2*eps_c*Eg*bg*2*hg;
%
% c1=-1/2*eps_c*Eg*bg*hg*hg-eps_c*Erc*Arc*Zc;

    a1=(fc*bg*(1-((eps_e_c)/(eps_c)))...
        +((fc*bg)/(2))...
-(((fc*bg)/(2))*((eps_c-eps_e_c)/(eps_c)))...
-((eps_c*bg)/(2))*Eg);

    b1=(+eps_c*Erc*Arc...
+Eg*eps_c*bg*hg...
-(sig_rt)*Art);

c1=(-eps_c*((bg*hg^2)/(2))*Eg...
-eps_c*Erc*Arc*Zc);

% length(M)
    x_pl=(-b1+sqrt(b1^2-4*a1*c1))/(2*a1);
    test=test+1;
    disp('botten flyter')
end

%% om båda flyter
```

```
if sig_rc == fy && sig_rt == fy
a1=1/2*fc*bg*(eps_c-eps_e_c)/eps_c+1/2*fc*bg-1/2*eps_c*Eg*bg;

b1=(sig_rc*Arc...
        +Eg*eps_c*bg*hg...
-sig_rt*Art);

    c1=-1/2*eps_c*Eg*bg*hg*hg;

x_pl=(-b1+sqrt(b1^2-4*a1*c1))/(2*a1);
% length(M)
    test=test+1;
    disp('dubbel flyt')
end

%% loop koll

if test>1
disp('mer än en plastiskmöjlighet har räknats')
end

%%%%%%%%%%%%%%%%%%%%%%%%%%%%%%%%%%%%%%%%%%%%%%%%%%%%%%%%%%%%%%%%%%%%%%%%%%%%%%%%%%%%
%%%%%%
%                                                  Pre-stressed  Beam,
%
%                                                Preload  calcualtions
%
%                                                By;  S.W,  March  2011
%
%%%%%%%%%%%%%%%%%%%%%%%%%%%%%%%%%%%%%%%%%%%%%%%%%%%%%%%%%%%%%%%%%%%%%%%%%%%%%%%%%%%%
%%%%%%

function
[eps_top_preload,Nek_max]=Preload(L,Eg,ft,fc,fm,bc,hc,nc,bt,...
ht,nt,Ert,hg,bg,Ag_ek,...
Arc,Art,Zc,Zt,Zgv)

% Function file for the Alann André file to be able to calculate
% pre-stressed beams too.

%The  sign  rules  given  in  "bärande  konstruktioner",del2  s.B231.  has
been
```

```
%applied.

%The same approch as in the MathCAD file has been applied here.
%For further information look in the MathCAD file or the Thesis.

%%%%%%%%%%%%%%%%%%%%%%%%%%%%%%%%%%%%%%%%%%%%%%%%%%%%%%%%%%%%%%%%%%%%%%%%%%%%
%%%%%%
%% finding the strain diffrence casused by the pre-stressing force.

%following the MathCAD file.
eN=hg-Zgv-Zc;

% Need a I and alfa
alfa=Ert/Eg;

I=((bg*hg^3/12)+hg*bg*(Zgv-(hg/2))^2)+...
    (alfa-1)*(((nc*bc*hc^3)/(12))+Arc*(Zgv-Zc)^2+...
((nt*bt*ht^3)/(12))+Art*(hg-Zgv-Zt)^2);

%there, now we will follow the MathCAD file again.
eps_bot_preload=-(fc/Eg)/10;

Nek_max=(eps_bot_preload*Eg)*((Ag_ek*I)/(eN*(hg-Zgv)*Ag_ek+I));
sigma_ek=Nek_max/Art;

eps_top_preload=((Nek_max/Ag_ek)+((Nek_max*eN)/(I))*-Zgv)/Eg;

% eps_top_diff=abs(eps_top_preload-(-fc/Eg));
% eps_bot_diff=abs(eps_bot_preload-(ft/Eg));

%% vippningskravet

%geezus, jag är glad att det inte var jag som behövde defineria den.

%I_z för toparmeringen
if nc == 0
I_z_c=0;

elseif nc == 1
```

```
   I_z_c=(alfa-1)*((hc*bc^3)/12);

elseif nc/2 == round(nc/2)
for i=1:1:nc/2
    PP(i)=(2*((hc*bc^3/12)+hc*bc*((((bc)/(2*(nc+1)))*(2*(i-1)))^2)));
end
    I_z_c=(alfa-1)*sum(PP);

else
for j=2:1:(nc/2)
    PPP(j-1)=(2*(((hc*bc^3)/(12))+hc*bc(((bc)/(nc+1))*(j-1))^2));
end
 I_z_c=(alfa-1)*((hc*bc^3/12)+sum(PPP));

end

%samma för bottenarmeringen
if nt == 0
I_z_t=0;
elseif nt == 1
    I_z_t=(alfa-1)*((ht*bt^3)/12);

elseif nt/2 == round(nt/2)
for k=1:1:nt/2
    PP(k)=(2*((ht*bt^3/12)+ht*bt*((((bt)/(2*(nt+1)))*(2*(k-1)))^2)));
end
    I_z_t=(alfa-1)*sum(PP);

else
for m=2:1:(nt/2)
    PPP(m-1)=(2*(((ht*bt^3)/(12))+ht*bt(((bt)/(nt+1))*(m-1))^2));
end
 I_z_t=(alfa-1)*((ht*bt^3/12)+sum(PPP));

end

I_z=((hg*bg^3)/(12)+I_z_c+I_z_t);

zmax=max(Zgv,hg-Zgv);
```

```
Wy=I/zmax;

%dåsså, då kör vi EC vippnings formel jox.
beta_c=0.1;
km=0.7;

iz=sqrt(I_z/(hg*bg));
lam_z=(L/iz);
lam_rel_z=(lam_z/pi)*sqrt(fc/Eg);
k_z=(1/2)*(1+beta_c*(lam_rel_z-0.3)+lam_rel_z^2);
k_c_z=1/((k_z)+(sqrt(k_z^2+lam_rel_z^2)));

P=1/((1/(k_c_z*fc*(hg*bg)))+(km*(eN/(fm*Wy))));

Nek_max=max(Nek_max,-P);%*(1.4);
sigma_ek=Nek_max/Art
eps_top_preload=((Nek_max/Ag_ek)+((Nek_max*eN)/(I))*-Zgv)/Eg;
```

10.3 Appendix C: Calculation sheet – economy

Input

General	
Beam length L [m]	18
Width w [m]	0,215
Height h [m] (without RF)	1,62
Glulam	
Density [kg/m3]	400
Reinforcement - Steel	
Density [kg/m3]	7850
Glue	
Density [kg/m3]	1650
% of RF C-S area [%]	28%

Reduced heitght due to RF [m]				
% RF	Reinforced	Gain	Prestressed	Gain
0.5%	1,391	0,229	1,305	0,315
1.0%	1,244	0,376	1,183	0,437
1.5%	1,146	0,474	1,095	0,525
2.0%	1,078	0,542	1,038	0,582
2.5%	1,030	0,590	1,000	0,620
3.0%	0,997	0,623	0,973	0,647

Reduced width due to RF [m]				
% RF	Reinforced	Gain	Prestressed	Gain
0.5%	0,215	0,000	0,215	0,000
1.0%	0,215	0,000	0,215	0,000
1.5%	0,215	0,000	0,215	0,000
2.0%	0,215	0,000	0,215	0,000
2.5%	0,215	0,000	0,215	0,000
3.0%	0,215	0,000	0,215	0,000

Costs

Material		
Glulam (GL28)	3000	SEK/m3
	4000	SEK/m3
	5000	SEK/m3
Steel (460)	9	SEK/kg
Glue	34	SEK/kg
Production		
Unreinforced	(Included in material)	
Pre-stressed	185	SEK/m3
Reinforced (estimated)	93	SEK/m3
Other costs		
Factory - loans etc.	105	SEK/m3
Maintenance and operation	34	SEK/m3

Material and volume calculations

	C-S-A	Tot mass	Volume				
Unreinforced	0,3483	2507,76	6,2694				
	Tot C-S-A	Tot mass	RF C-S-A	GL C-S-A	Glue	RF	GL
Reinforced	[m2]	[kg]	[m2]	[m2]	[kg]	[kg]	[m3]
0,50%	0,2991	2401,3	0,00174	0,2973	14,48	246,07	5,35
1,00%	0,2675	2421,7	0,00348	0,2640	28,96	492,15	4,75
1,50%	0,2464	2518,1	0,00522	0,2412	43,45	738,22	4,34
2,00%	0,2318	2660,8	0,00697	0,2248	57,93	984,30	4,05
2,50%	0,2215	2834,5	0,00871	0,2127	72,41	1230,37	3,83
3,00%	0,2144	3031,5	0,01045	0,2039	86,89	1476,44	3,67
Prestressed							
0,50%	0,2806	2268,2	0,00174	0,2788	14,48	246,07	5,02
1,00%	0,2543	2327,3	0,00348	0,2509	28,96	492,15	4,52
1,50%	0,2354	2439,1	0,00522	0,2302	43,45	738,22	4,14
2,00%	0,2232	2598,9	0,00697	0,2162	57,93	984,30	3,89
2,50%	0,2150	2788,1	0,00871	0,2063	72,41	1230,37	3,71
3,00%	0,2092	2994,3	0,01045	0,1987	86,89	1476,44	3,58

Cost calculations

	GL-3000	GL-4000	GL-5000	RF	Glue	Production	Other
Unreinforced	18808	25078	31347	0	0	0	871
Reinforced							
0,50%	16055	21407	26759	2215	492	501	748
1,00%	14255	19006	23758	4429	985	448	669
1,50%	13023	17364	21705	6644	1477	412	616
2,00%	12139	16186	20232	8859	1970	388	580
2,50%	11488	15317	19147	11073	2462	371	554
3,00%	11011	14681	18352	13288	2954	359	536
Prestressed							
0,50%	15057	20076	25095	2215	492	934	702
1,00%	13547	18062	22578	4429	985	847	636
1,50%	12431	16574	20718	6644	1477	784	589
2,00%	11675	15567	19458	8859	1970	743	558
2,50%	11140	14853	18566	11073	2462	716	538
3,00%	10732	14310	17887	13288	2954	697	523

Beam costs and savings						
	Total cost per beam			Savings per beam		
	GL-3000	GL-4000	GL-5000	GL-3000	GL-4000	GL-5000
Unreinforced	19680	25949	32218			
Reinforced						
0,50%	20011	25363	30715	332	-586	-1503
1,00%	20786	25537	30289	1106	-412	-1929
1,50%	22173	26514	30855	2493	565	-1363
2,00%	23936	27982	32028	4256	2033	-190
2,50%	25948	29778	33607	6269	3829	1388
3,00%	28148	31819	35489	8469	5870	3271
Prestressed						
0,50%	19400	24419	29438	-279	-1530	-2780
1,00%	20444	24960	29475	764	-990	-2743
1,50%	21925	26069	30212	2245	120	-2006
2,00%	23805	27696	31588	4125	1747	-630
2,50%	25929	29642	33356	6249	3693	1137
3,00%	28195	31772	35350	8515	5823	3131

Input - Project	
Building	
Width [m]	18
Length [m]	30
Nr. of beams	4

Savings - Project		
Structural		
Wall material	-750	SEK/m2
Transport		
Max load	28000	kg
Cost/transport	12000	SEK

Transport calculations		
	Beams/trans.	Cost/beam
Unreinforced	11	1091
Reinforced		
0,50%	11	1091
1,00%	11	1091
1,50%	11	1091
2,00%	10	1200
2,50%	9	1333
3,00%	9	1333
Prestressed		
0,50%	12	1000
1,00%	12	1000
1,50%	11	1091
2,00%	10	1200
2,50%	10	1200
3,00%	9	1333

Savings calculations								
	Beams			Structural	Transport	Saving		
Reinforced	GL-3000	GL-4000	GL-5000			GL-3000	GL-4000	GL-5000
0,50%	1327	-2343	-6013	-16488	0	-15161	-18831	-22501
1,00%	4425	-1647	-7718	-27072	0	-22647	-28719	-34790
1,50%	9974	2260	-5454	-34128	0	-24154	-31868	-39582
2,00%	17024	8132	-760	-39024	436	-21564	-30456	-39347
2,50%	25074	15314	5554	-42480	970	-16436	-26196	-35956
3,00%	33875	23479	13083	-44856	970	-10011	-20407	-30804
Prestressed								
0,50%	-1117	-6119	-11120	-22680	-364	-24161	-29162	-34164
1,00%	3057	-3958	-10974	-31464	-364	-28770	-35786	-42801
1,50%	8981	478	-8025	-37800	0	-28819	-37322	-45825
2,00%	16501	6990	-2521	-41904	436	-24967	-34478	-43989
2,50%	24997	14773	4548	-44640	436	-19206	-29431	-39655
3,00%	34060	23292	12524	-46584	970	-11554	-22322	-33090

Input						
Beam			Building			Costs
Length	Width	Height	Width	Length	Nr. of beams	Reinforced
18	0,215	1,62	18	30	4	93

Results													
	Glulam	Reinforced						Prestressed					
		0,50%	1%	1,50%	2%	2,50%	3%	0,50%	1%	1,50%	2%	2,50%	3%
Height gain		**0,229**	**0,376**	**0,474**	**0,542**	**0,590**	**0,623**	**0,315**	**0,437**	**0,525**	**0,582**	**0,620**	**0,647**
Width gain		**0,000**	**0,000**	**0,000**	**0,000**	**0,000**	**0,000**	**0,000**	**0,000**	**0,000**	**0,000**	**0,000**	**0,000**
Beam cost													
GL-3000	**18808**	**16055**	**14255**	**13023**	**12139**	**11488**	**11011**	**15057**	**13547**	**12431**	**11675**	**11140**	**10732**
GL-4000	**25078**	**21407**	**21407**	**21407**	**21407**	**21407**	**21407**	**21407**	**21407**	**21407**	**21407**	**21407**	**21407**
GL-5000	**31347**	**26759**	**26759**	**26759**	**26759**	**26759**	**26759**	**26759**	**26759**	**26759**	**26759**	**26759**	**26759**
Beam saving													
GL-3000		332	1106	2493	4256	6269	8469	-279	764	2245	4125	6249	8515
GL-4000		-586	-412	565	2033	3829	5870	-1530	-990	120	1747	3693	5823
GL-5000		-1503	-1929	-1363	-190	1388	3271	-2780	-2743	-2006	-630	1137	3131
Project saving													
GL-3000		-15161	-22647	-24154	-21564	-16436	-10011	-24161	-28770	-28819	-24967	-19206	-11554
GL-4000		-18831	-28719	-31868	-30456	-26196	-20407	-29162	-35786	-37322	-34478	-29431	-22322
GL-5000		-22501	-34790	-39582	-39347	-35956	-30804	-34164	-42801	-45825	-43989	-39655	-33090

10.4 Appendix D: Economical diagrams

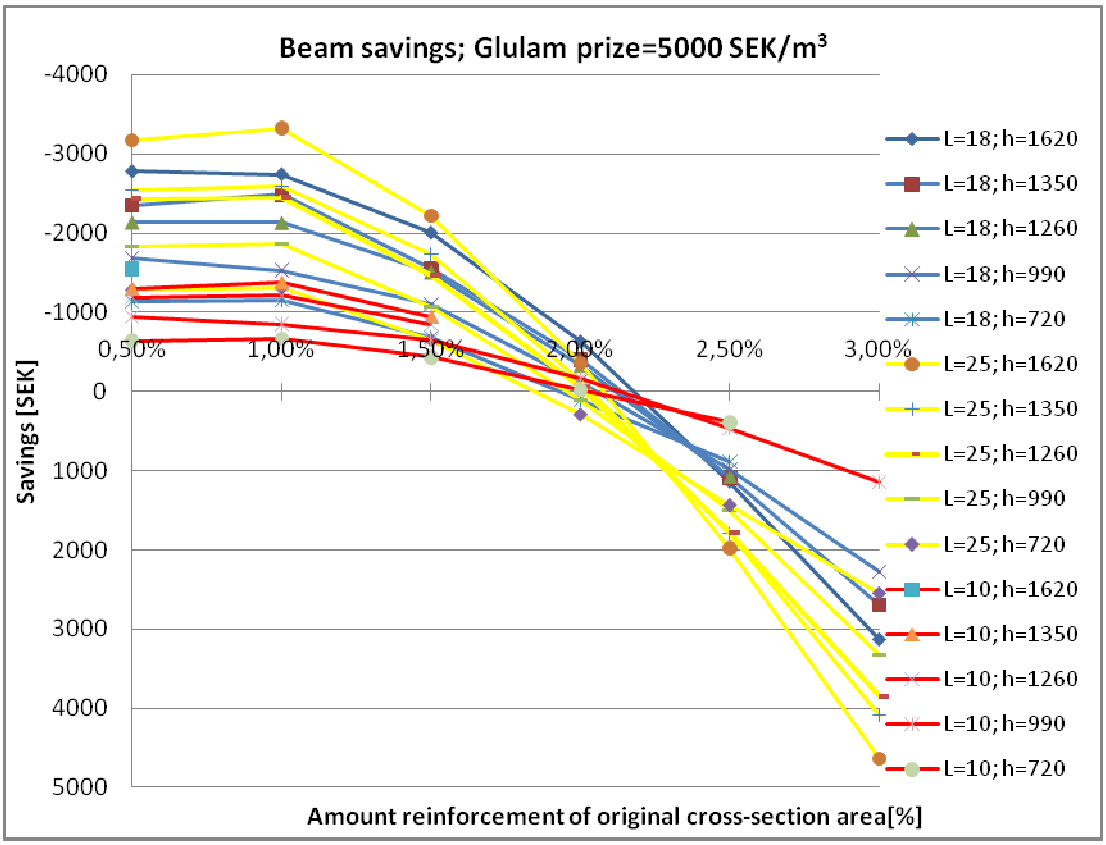

Figure 10.1 Beam length comparison; width = 215mm, L=length [m], h=height [mm]

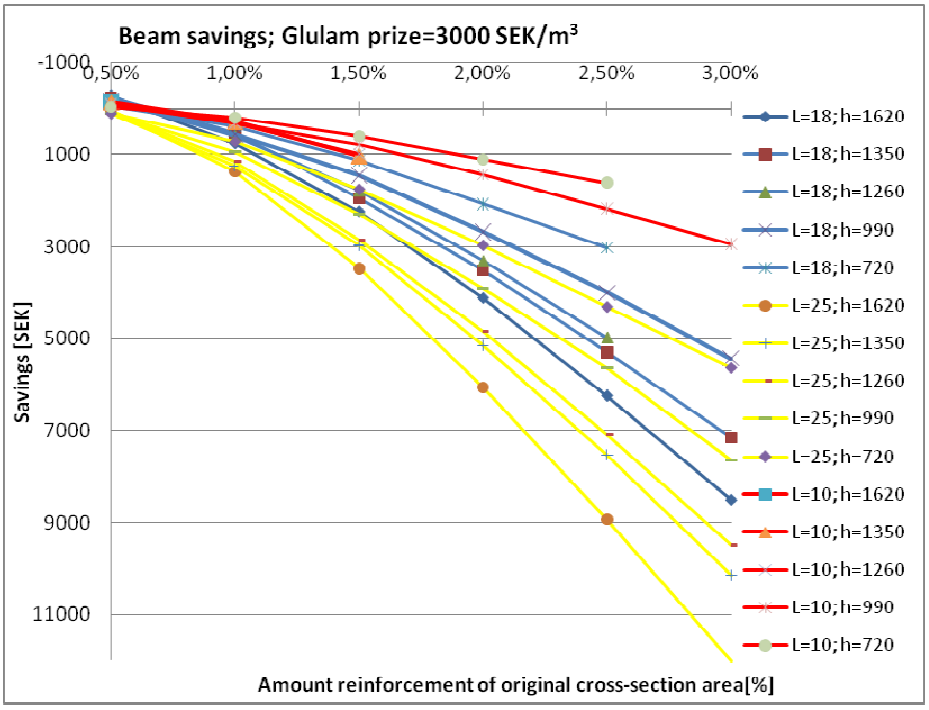

Figure 10.2 Beam length comparison; width = 215mm, L=length [m], h=height [mm]

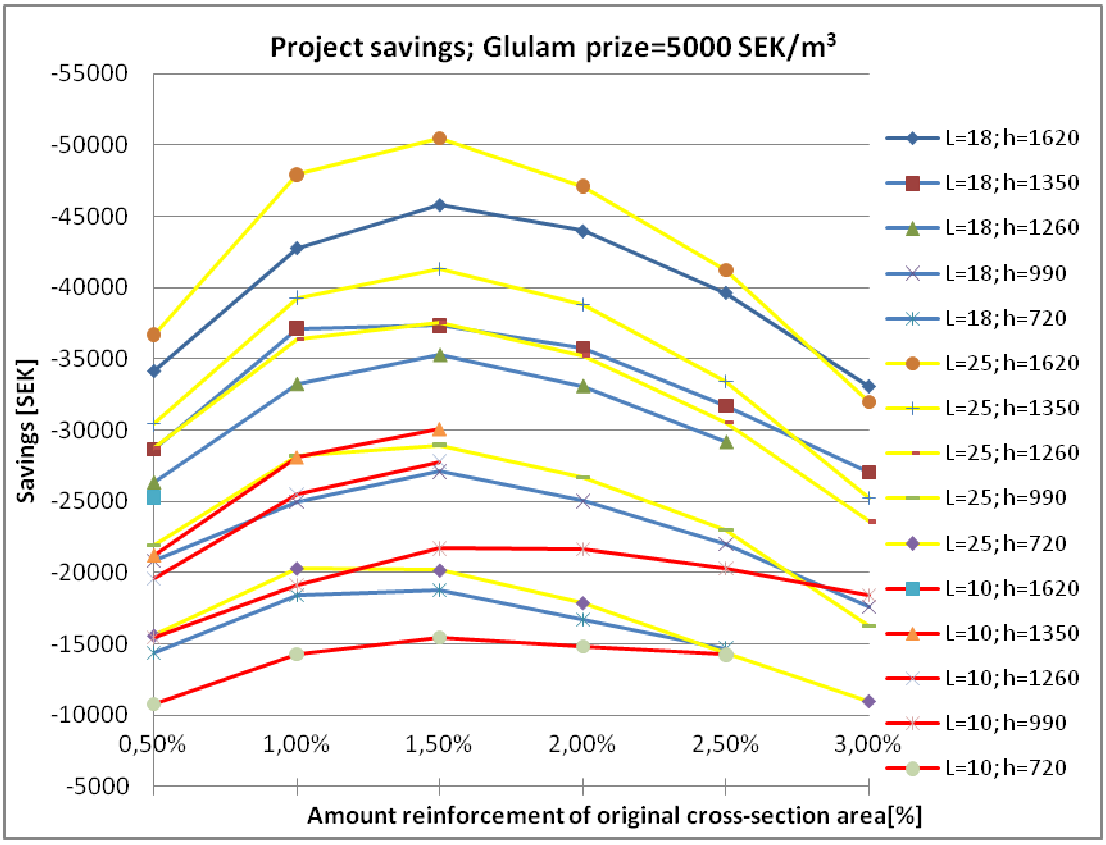

Figure 10.3 Beam length comparison; width = 215mm, L=length [m], h=height [mm]

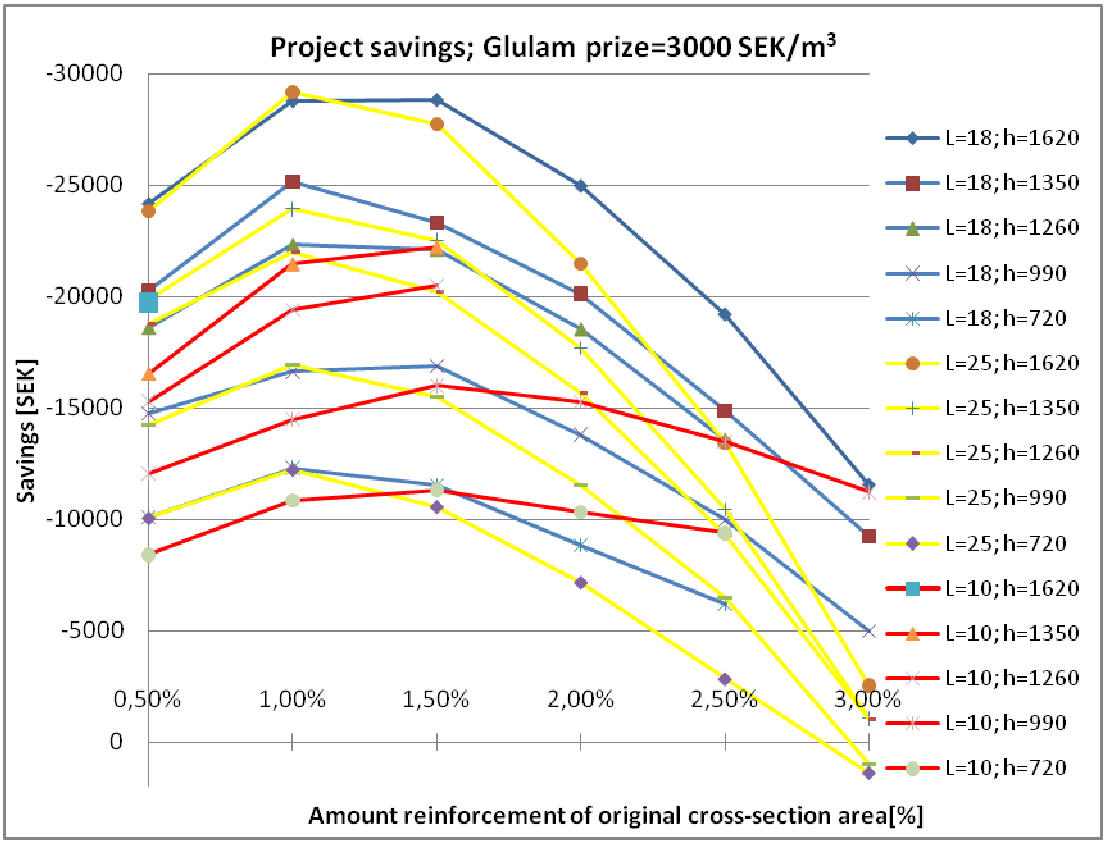

Figure 10.4 Beam length comparison; width = 215mm, L=length [m], h=height [mm]

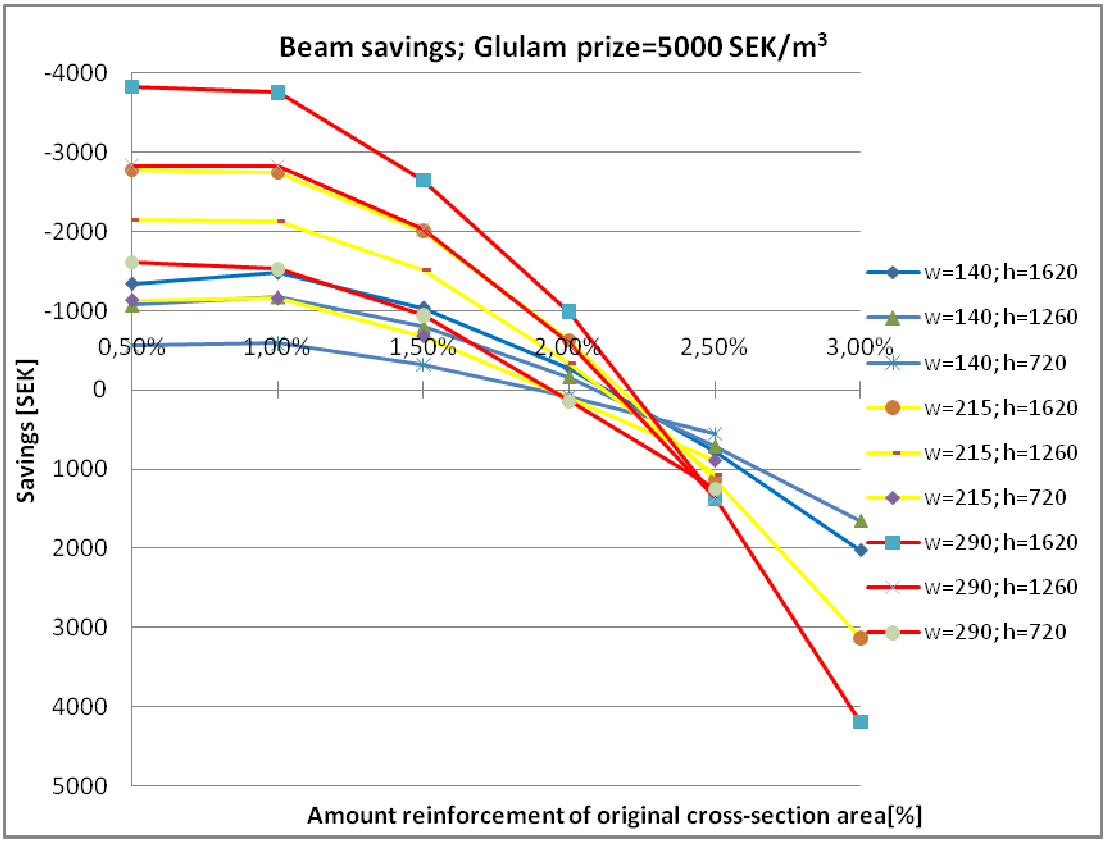

Figure 10.5 Beam width comparison; length = 18m, w=width [mm], h=height [mm]

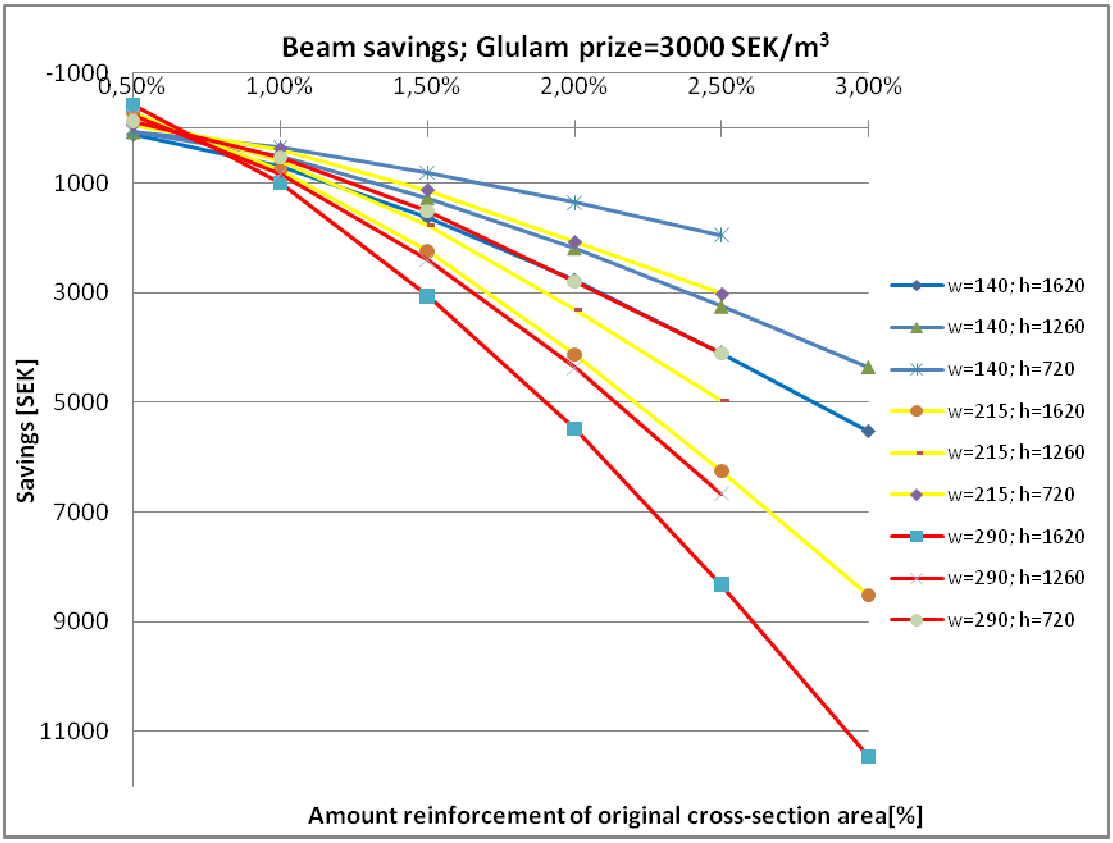

Figure 10.6 Beam width comparison; length = 18m, w=width [mm], h=height [mm]

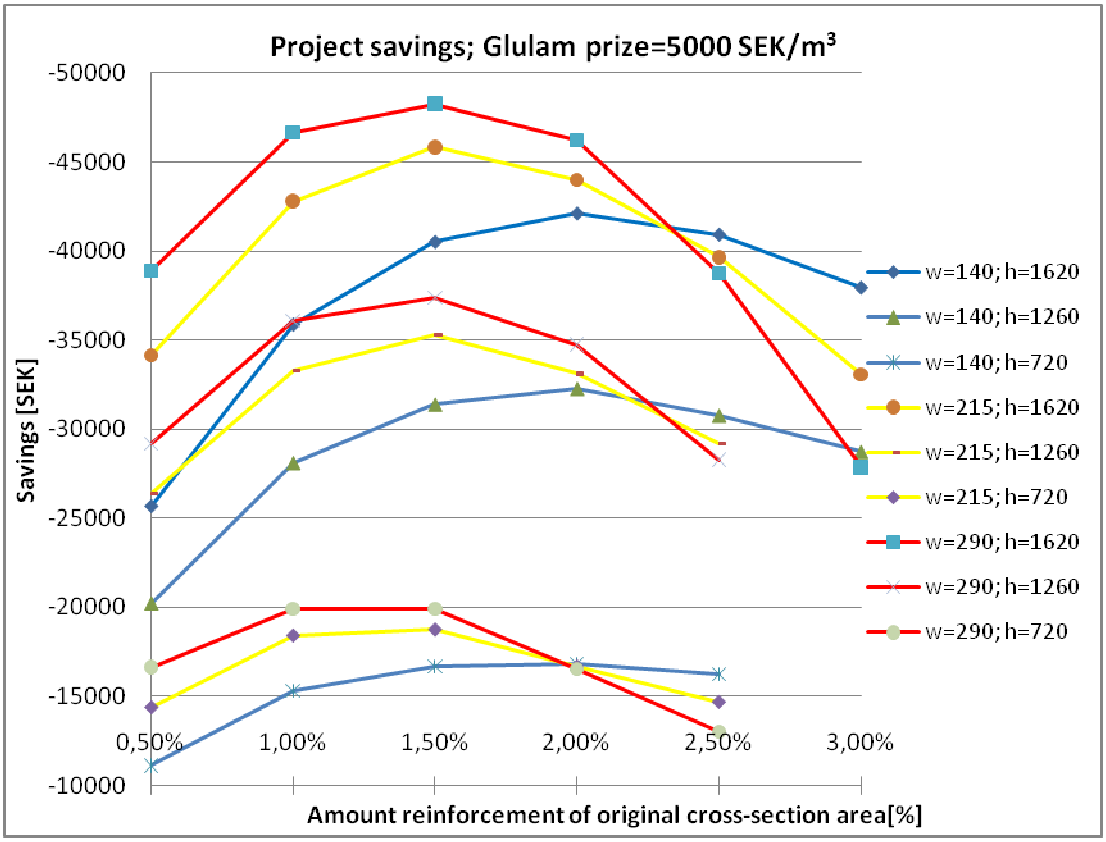

Figure 10.7 Beam width comparison; length = 18m, w=width [mm], h=height [mm]

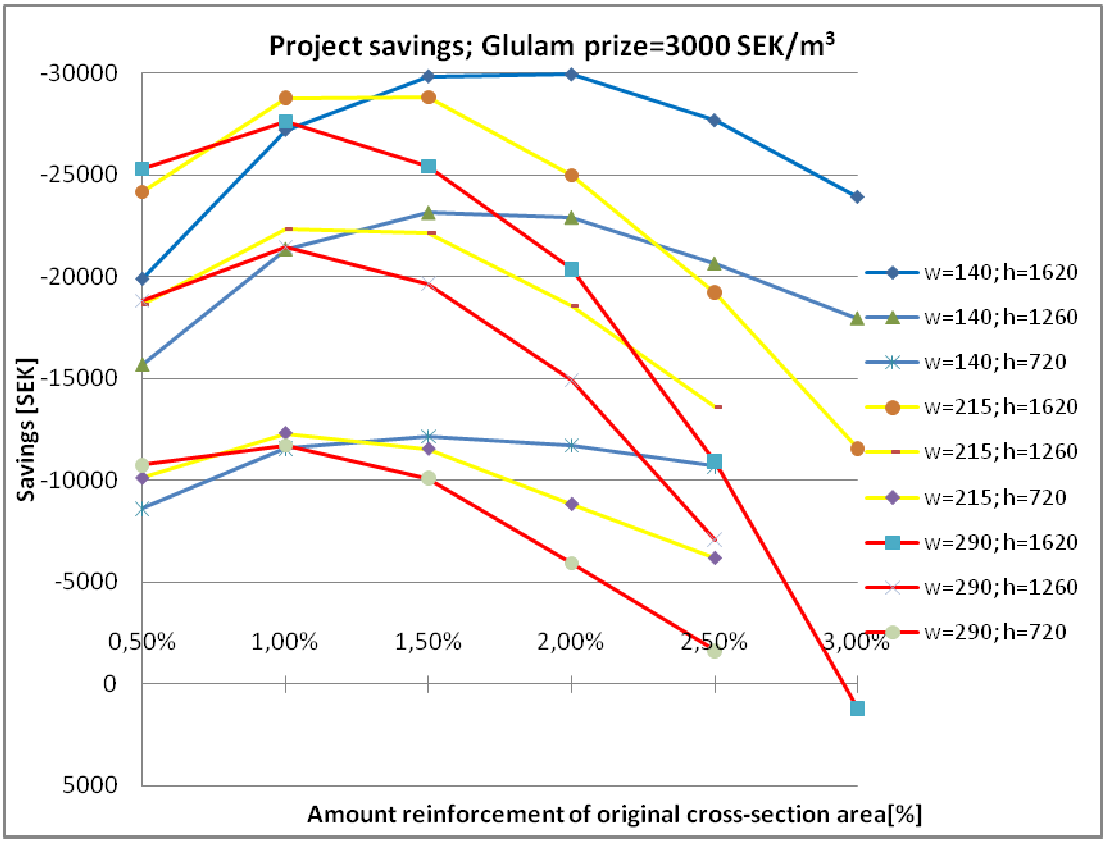

Figure 10.8 Beam width comparison; length = 18m, w=width [mm], h=height [mm]

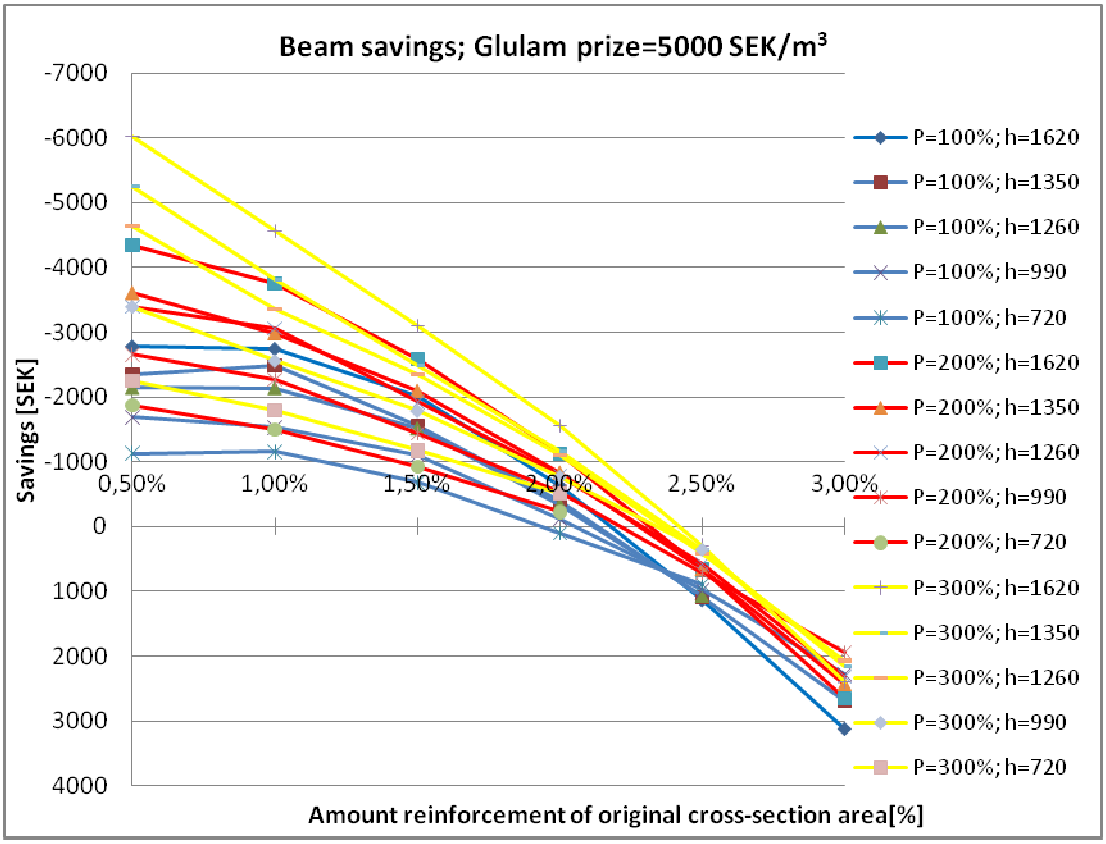

Figure 10.9 Various pre-stressing force; length=18 m, width=215 mm, P= amount of calculated acceptable pre-stressing force, h=height [mm]

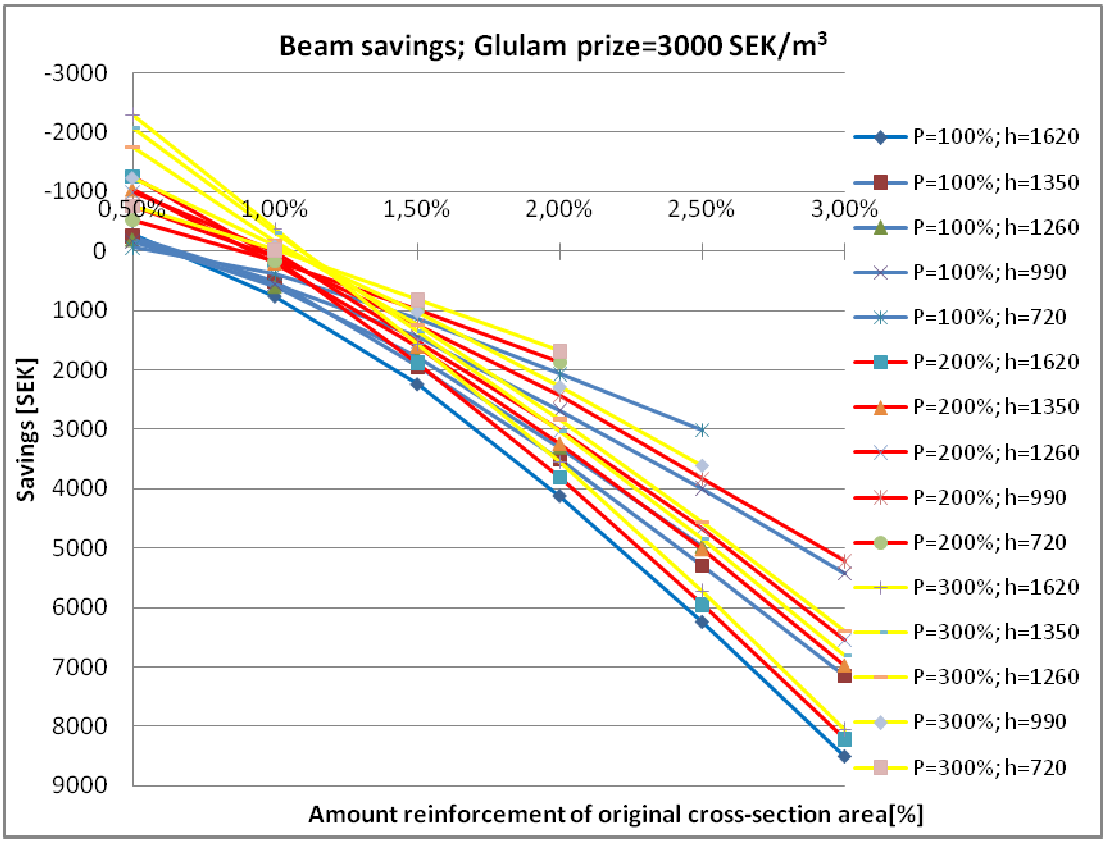

Figure 10.10 Various pre-stressing force; length=18 m, width=215 mm, P= amount of calculated acceptable pre-stressing force, h=height [mm]

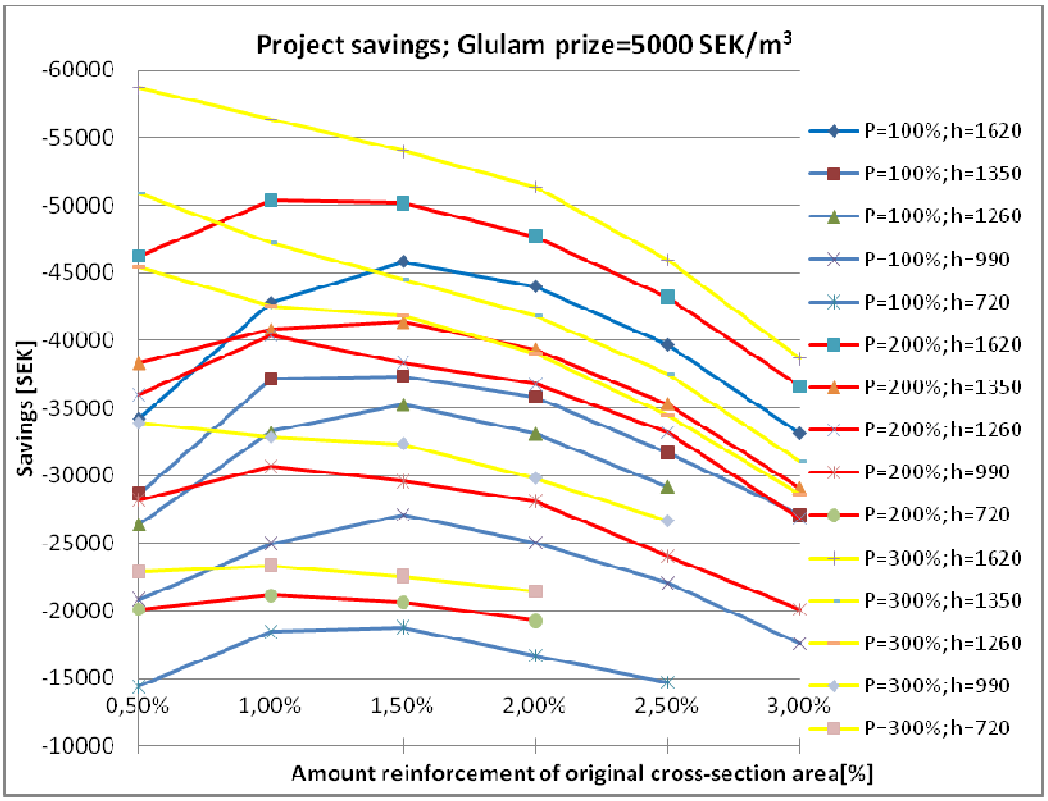

Figure 10.11 Various pre-stressing force; length=18 m, width=215 mm, P= amount of calculated acceptable pre-stressing force, h=height [mm]

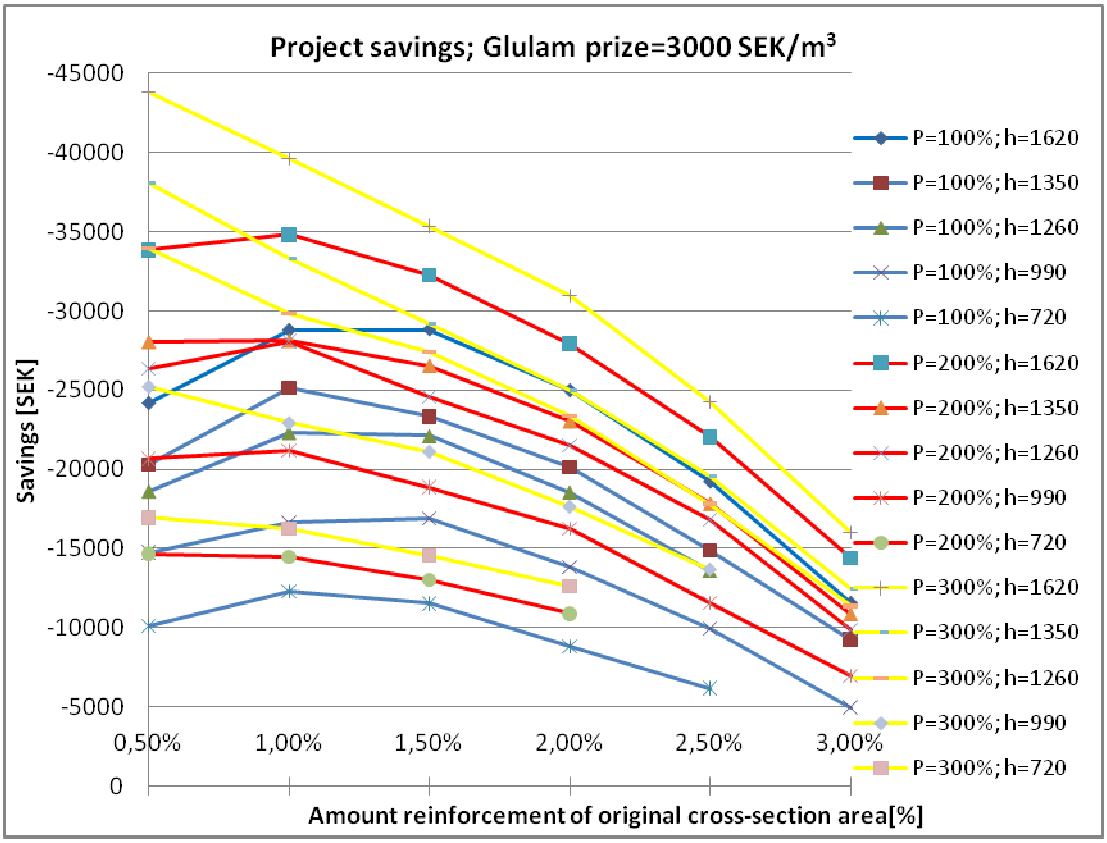

Figure 10.12 Various pre-stressing force; length=18 m, width=215 mm, P= amount of calculated acceptable pre-stressing force, h=height [mm]